BUOYANCY AND VERTICAL MOVEMENTS OF MARINE PLANKTONIC DIATOMS

by

Tammi Lee Richardson

Submitted in partial fulfillment of the requirements for the degree of
Doctor of Philosophy

at

Dalhousie University
Halifax, Nova Scotia
May, 1996

ISBN 0-612-15885-3

Name Tammi L. Richardson

Dissertation Abstracts International and *Masters Abstracts International* are arranged by broad general subject categories. Please select the one subject which most nearly describes the content of your dissertation or thesis. Enter the corresponding four-digit code in the spaces provided.

Biology - Oceanography
SUBJECT TERM

0416
SUBJECT CODE

UMI

Subject Categories

THE HUMANITIES AND SOCIAL SCIENCES

COMMUNICATIONS AND THE ARTS
- Architecture 0729
- Art History 0377
- Cinema 0900
- Dance 0378
- Fine Arts 0357
- Information Science 0723
- Journalism 0391
- Library Science 0399
- Mass Communications 0708
- Music 0413
- Speech Communication 0459
- Theater 0465

EDUCATION
- General 0515
- Administration 0514
- Adult and Continuing 0516
- Agricultural 0517
- Art 0273
- Bilingual and Multicultural 0282
- Business 0688
- Community College 0275
- Curriculum and Instruction 0727
- Early Childhood 0518
- Elementary 0524
- Finance 0277
- Guidance and Counseling 0519
- Health 0680
- Higher 0745
- History of 0520
- Home Economics 0278
- Industrial 0521
- Language and Literature 0279
- Mathematics 0280
- Music 0522
- Philosophy of 0998
- Physical 0523
- Psychology 0525
- Reading 0535
- Religious 0527
- Sciences 0714
- Secondary 0533
- Social Sciences 0534
- Sociology of 0340
- Special 0529
- Teacher Training 0530
- Technology 0710
- Tests and Measurements 0288
- Vocational 0747

LANGUAGE, LITERATURE AND LINGUISTICS
- Language
  - General 0679
  - Ancient 0289
  - Linguistics 0290
  - Modern 0291
- Literature
  - General 0401
  - Classical 0294
  - Comparative 0295
  - Medieval 0297
  - Modern 0298
  - African 0316
  - American 0591
  - Asian 0305
  - Canadian (English) 0352
  - Canadian (French) 0355
  - English 0593
  - Germanic 0311
  - Latin American 0312
  - Middle Eastern 0315
  - Romance 0313
  - Slavic and East European 0314

PHILOSOPHY, RELIGION AND THEOLOGY
- Philosophy 0422
- Religion
  - General 0318
  - Biblical Studies 0321
  - Clergy 0319
  - History of 0320
  - Philosophy of 0322
- Theology 0469

SOCIAL SCIENCES
- American Studies 0323
- Anthropology
  - Archaeology 0324
  - Cultural 0326
  - Physical 0327
- Business Administration
  - General 0310
  - Accounting 0272
  - Banking 0770
  - Management 0454
  - Marketing 0338
- Canadian Studies 0385
- Economics
  - General 0501
  - Agricultural 0503
  - Commerce-Business 0505
  - Finance 0508
  - History 0509
  - Labor 0510
  - Theory 0511
- Folklore 0358
- Geography 0366
- Gerontology 0351
- History
  - General 0578
  - Ancient 0579
  - Medieval 0581
  - Modern 0582
  - Black 0328
  - African 0331
  - Asia, Australia and Oceania 0332
  - Canadian 0334
  - European 0335
  - Latin American 0336
  - Middle Eastern 0333
  - United States 0337
- History of Science 0585
- Law 0398
- Political Science
  - General 0615
  - International Law and Relations 0616
  - Public Administration 0617
- Recreation 0814
- Social Work 0452
- Sociology
  - General 0626
  - Criminology and Penology 0627
  - Demography 0938
  - Ethnic and Racial Studies 0631
  - Individual and Family Studies 0628
  - Industrial and Labor Relations 0629
  - Public and Social Welfare 0630
  - Social Structure and Development 0700
  - Theory and Methods 0344
- Transportation 0709
- Urban and Regional Planning 0999
- Women's Studies 0453

THE SCIENCES AND ENGINEERING

BIOLOGICAL SCIENCES
- Agriculture
  - General 0473
  - Agronomy 0285
  - Animal Culture and Nutrition 0475
  - Animal Pathology 0476
  - Food Science and Technology 0359
  - Forestry and Wildlife 0478
  - Plant Culture 0479
  - Plant Pathology 0480
  - Plant Physiology 0817
  - Range Management 0777
  - Wood Technology 0746
- Biology
  - General 0306
  - Anatomy 0287
  - Biostatistics 0308
  - Botany 0309
  - Cell 0379
  - Ecology 0329
  - Entomology 0353
  - Genetics 0369
  - Limnology 0793
  - Microbiology 0410
  - Molecular 0307
  - Neuroscience 0317
  - Oceanography 0416
  - Physiology 0433
  - Radiation 0821
  - Veterinary Science 0778
  - Zoology 0472
- Biophysics
  - General 0786
  - Medical 0760

EARTH SCIENCES
- Biogeochemistry 0425
- Geochemistry 0996
- Geodesy 0370
- Geology 0372
- Geophysics 0373
- Hydrology 0388
- Mineralogy 0411
- Paleobotany 0345
- Paleoecology 0426
- Paleontology 0418
- Paleozoology 0985
- Palynology 0427
- Physical Geography 0368
- Physical Oceanography 0415

HEALTH AND ENVIRONMENTAL SCIENCES
- Environmental Sciences 0768
- Health Sciences
  - General 0566
  - Audiology 0300
  - Chemotherapy 0992
  - Dentistry 0567
  - Education 0350
  - Hospital Management 0769
  - Human Development 0758
  - Immunology 0982
  - Medicine and Surgery 0564
  - Mental Health 0347
  - Nursing 0569
  - Nutrition 0570
  - Obstetrics and Gynecology 0380
  - Occupational Health and Therapy 0354
  - Ophthalmology 0381
  - Pathology 0571
  - Pharmacology 0419
  - Pharmacy 0572
  - Physical Therapy 0382
  - Public Health 0573
  - Radiology 0574
  - Recreation 0575
  - Speech Pathology 0460
  - Toxicology 0383
- Home Economics 0386

PHYSICAL SCIENCES
Pure Sciences
- Chemistry
  - General 0485
  - Agricultural 0749
  - Analytical 0486
  - Biochemistry 0487
  - Inorganic 0488
  - Nuclear 0738
  - Organic 0490
  - Pharmaceutical 0491
  - Physical 0494
  - Polymer 0495
  - Radiation 0754
- Mathematics 0405
- Physics
  - General 0605
  - Acoustics 0986
  - Astronomy and Astrophysics 0606
  - Atmospheric Science 0608
  - Atomic 0748
  - Electronics and Electricity 0607
  - Elementary Particles and High Energy 0798
  - Fluid and Plasma 0759
  - Molecular 0609
  - Nuclear 0610
  - Optics 0752
  - Radiation 0756
  - Solid State 0611
- Statistics 0463

Applied Sciences
- Applied Mechanics 0346
- Computer Science 0984
- Engineering
  - General 0537
  - Aerospace 0538
  - Agricultural 0539
  - Automotive 0540
  - Biomedical 0541
  - Chemical 0542
  - Civil 0543
  - Electronics and Electrical 0544
  - Heat and Thermodynamics 0348
  - Hydraulic 0545
  - Industrial 0546
  - Marine 0547
  - Materials Science 0794
  - Mechanical 0548
  - Metallurgy 0743
  - Mining 0551
  - Nuclear 0552
  - Packaging 0549
  - Petroleum 0765
  - Sanitary and Municipal 0554
  - System Science 0790
- Geotechnology 0428
- Operations Research 0796
- Plastics Technology 0795
- Textile Technology 0994

PSYCHOLOGY
- General 0621
- Behavioral 0384
- Clinical 0622
- Developmental 0620
- Experimental 0623
- Industrial 0624
- Personality 0625
- Physiological 0989
- Psychobiology 0349
- Psychometrics 0632
- Social 0451

To Mum, Dad, and Tony, with love.

The Biology of Algae

The biology of algae is a duty, or a task,
That consumes the better portion of your time
In the sampling of waters from an ocean, or a flask,
Or a snow-field, or a gutter-full of slime.
You get cold, and wet, and grubby: you get dusty, hot, and dry;
You get dismal, and dejected, and defied;
But you'll find that, if you're lucky - if you're good - and if you try,
You can do a little science on the side.

R. A. Lewin (1971)
"The Biology of Algae" (Verse 1)
Phycol. Newsletter 7:1

Contents

List of Tables x

List of Figures xiv

Abstract xix

Acknowledgements xx

1 Introduction 1

2 Changes in buoyancy and chemical composition during growth of a coastal marine diatom 4

2.1 Introduction....4

2.2 Methods....8

2.2.1 Tank experiments....8

2.2.2 Batch culture experiments....13

2.3 Results....13
2.3.1 Nearly-neutral buoyancy in nitrate-replete *Thalassiosira weissflogii* grown in the experimental water column....13
2.3.2 Growth of cells and changes in carbohydrate and protein during batch culture experiments....14
2.4 Discussion....20
2.4.1 A model of nitrate-dependent sinking....20
2.4.2 Neutral buoyancy and sinking upon nitrate depletion....25
2.4.3 Increased intracellular density due to unbalanced growth....28
2.4.4 Ecological consequences and biogeochemical implications of buoyancy changes and changes in chemical composition during unbalanced growth....32

3 Physiological properties of *Rhizosolenia formosa* in the context of open-ocean vertical migration 36

3.1 Introduction....36
3.2 Methods....38
3.2.1 Culture conditions....38
3.2.2 Chemical composition time-course experiment....39
3.2.3 Buoyancy time-course experiment....40
3.2.4 Nitrate uptake measurements....42
3.2.5 Photosynthesis vs. irradiance measurements....43
3.3 Results....46
3.3.1 Chemical composition time-course experiment....46
3.3.2 Changes in buoyancy with N status....51
3.3.3 Nitrate uptake measurements....55

3.3.4 Photosynthesis vs. irradiance measurements.....55

3.4 Discussion.....55

3.4.1 Growth rate and chemical composition.....55

3.4.2 Nitrate uptake, changes in chemical composition and buoyancy...61

3.4.3 Photosynthetic physiology of *Rhizosolenia formosa*.....69

3.4.4 Potential role of *Rhizosolenia* in new production and biogeochemical cycling.....73

4 Potential contributions of vertically-migrating *Rhizosolenia* to nutrient cycling and new production in the open-ocean 76

4.1 Introduction.....76

4.2 Description of base model.....78

4.2.1 Physical structure.....78

4.2.2 Boundary conditions.....86

4.2.3 Initial conditions and other assumptions.....88

4.3 Variations in the base model.....89

4.3.1 Ascent and sinking velocities.....89

4.3.2 Critical values of C:N for sinking and floating.....89

4.3.3 Variations in the amplitude of the loss term with depth.....91

4.3.4 Calculations.....91

4.4 Results.....92

4.4.1 Base model predictions.....92

4.4.2 Variations in ascent and descent velocities.....93

4.4.3 Variations in critical C:N for sinking and floating.....97

4.4.4 Variations in the amplitude of the loss term with depth.....97

4.5 Discussion.....101
4.5.1 Potential sources of error.....101
4.5.2 Migration cycle times and specific rates of increase.....105
4.5.3 Vertical distributions of *Rhizosolenia* in steady state.....106
4.5.4 Fluxes of POC and PON.....107
4.5.5 Relative contributions of *Rhizosolenia* migrations to nutrient cycling and new production in the open ocean.....111

5 Conclusions **121**

6 Bibliography **125**

List of Tables

2.1 List of symbols for Chapter Two.....6

2.2 F-ratio comparison of fits of four versions of Equation (2.2) to observed surface chlorophyll distributions during growth of *Thalassiosira weissflogii* in the experimental tank.....24

3.1 Chemical composition of nitrate-replete (NR) and nitrate-depleted (ND) *Rhizosolenia formosa* used for P-I experiments. Values are averages ± standard errors.....45

3.2 List of symbols for Chapter Three.....47

3.3 Ambient nitrate concentrations and chemical composition of *Rhizosolenia formosa* before and after depletion of nitrate and after re-introduction of nitrate to culture medium. Nitrate-replete cells are those sampled at the pre-depletion point (Day 11) in the time-course experiment. Nitrate-depleted cells were sampled after 24 h (Cultures A and B), 53 h (Culture B and C), or 30 h (Cultures E and F) without ambient nitrate.....50

3.4 Calculation of minimum estimates of sinking velocities of negatively buoyant *Rhizosolenia formosa* with variations in N status.....53

3.5 Biomass concentrations, chemical composition, and rates of nitrate uptake in the light and the dark by nitrate-replete and nitrate-depleted *Rhizosolenia formosa.* NRLT and NDLT indicate N-replete and N-depleted triplicates, respectively, where measurements were done in the light. NRDK and NDDK indicate N-replete and N-depleted triplicates, respectively, where measurements were done in the dark....56

3.6 Summary of parameters determined from photosynthesis vs. irradiance experiments done with nitrate-replete (NR) and nitrate-depleted (ND) *Rhizosolenia formosa.* Values reported are averages of triplicate measurements from each culture ± standard error of the mean. Values for the overall averages of NR and ND parameters were compared using a Student's t-test for comparison of means. Calculated values of the t-statistic were compared with the critical value of *t* (2.1318) at the 0.05 significance level and 4 degrees of freedom.....59

4.1 Model variables and parameters. Multiple values in the Value column refer to rates for nitrate-replete and nitrate-depleted biomass and are used to define the range between which the actual value in the model varies (see equations 4.9, 4.10, and 4.11 in the text)..... 81

4.2 Variations of critical C:N ratios (mol:mol) for sinking and floating.....90

4.3 Predicted upward, downward, and net fluxes of POC and PON, specific rates of increase, and total migration cycle times with variations in ascent and descent velocities.....96

4.4 Predicted upward, downward, and net fluxes of POC and PON, specific rates of increase, and total migration cycle times for variations in critical C:N for sinking and floating.....99

4.5 Predicted upward, downward, and net fluxes of POC and PON, specific rates of increase, and migration cycle times with variations in the amplitude of the loss term with depth. For models where losses were not uniform with depth, the specific rate of increase has been calculated from the actual loss rate used in the model and the percentage of total cycle time that the loss was applied. See Table 4.6 for unadjusted loss rates and conversion factors and see text for details.....100

4.6 Calculation of adjusted loss rates for models where the amplitude of the loss term with depth was varied.....103

4.7 Calculated values of ϕ (d^{-1}) for variations of the *Rhizosolenia* migration model. The product of ϕ and the integrated water column abundance ($\mu mol\ m^{-2}$) of *Rhizosolenia* gives an estimate of net downward flux of POC or net upward flux of PON due to *Rhizosolenia* migrations.....111

4.8 Estimates of new production from turbulent fluxes of nitrate into the euphotic zone for comparison with vertical fluxes of N due to migrations of *Rhizosolenia* in the open ocean.....115

4.9 Estimates of nitrogen fixation used for comparison with estimates of new production resulting from vertical migrations of *Rhizosolenia* in the open ocean.....116

4.10 Estimates of new production as export production measured by sediment traps for comparison with vertical fluxes of N due to migrations of *Rhizosolenia* in the open ocean.....118

List of Figures

2.1. Schematic of tank experiment apparatus.....9

2.2 (A) Temperature profiles at three time points during the tank experiment, Day 1 (◆), Day 4 (◊), and Day 10 (x). (B) Irradiance profiles measured with distilled water in the tank (no cells) (◆, with exponential curve fit as solid line) and modeled curves for Day 5 (---) and Day 10 (···) of the experiment.....11

2.3. Time-course of (A) chlorophyll (◆) and nitrate (◊) in tank surface waters, (B) chlorophyll at mid-depth (110 cm) and (C) at the bottom (210 cm) during growth of *Thalassiosira weissflogii* in the tank. Error bars are ± SE of triplicate measurements. Symbols with error bars are true chlorophyll determinations, those without error bars are chlorophyll values converted from fluorescence profiles.....15

2.4. Representative chlorophyll profiles done at 20:00 daily during the tank experiment. (A) Profiles on Day 1 (initial), (B) Day 7, (C) Day 10, (D) Day 11, (E) Day 12, (F) Day 13, (G) Day 15, and (F) Day 16. Ambient nitrate was depleted after Day 10 of the experiment.....16

2.5. Time course of cell counts (◆) and chlorophyll per cell (◊) of *Thalassiosira weissflogii* taken from surface water of the experimental tank. Error bars are ± SE of triplicate measurements. Arrow indicates time at which nitrate was depleted from surface waters.....17

2.6. Diel series of chlorophyll profiles done on a representative day (Day 8) before depletion of nitrate from surface waters of the tank. Profiles were done at 01:00 ( ), 07:30 (◆),11:00 (Δ),14:00 (▼),17:00 (O), and 19:30 (x). The 07:30 profile is just before lights-on; 19:30 is just before lights-off. Error bars are ± SE of triplicate measurements.....18

2.7. Time-course of (A) chlorophyll, (B) nitrate, (C) protein, (D) carbohydrate, (E) carbohydrate:protein ratio during batch culture experiments with *Thalassiosira weissflogii*. Symbols represent triplicate cultures treated identically. Arrow indicates time at which nitrate was added back to the medium. Error bars are ± SE of triplicate measurements.....19

2.8. Fits of model equations (—) to observed chlorophyll (●) and nitrate (◊) data. (A) Fit of model equation with nitrate-dependent growth of cells but no sinking of biomass, (B) Fit of model equation with constant sinking rate, (C) Fit of model equation with no delay between depletion of ambient nitrate and initiation of sinking, (D) Fit of model equation with nitrate-dependent growth and nitrate-dependent sinking where cells reach 50% of their maximal sinking rate 115 h after depletion of ambient nitrate.....23

2.9. Model output of changes in sinking rate expected with concurrent changes in carbohydrate:protein ratio for a model cell of radius 7.5 μm (similar to the radius of *Thalassiosira weissflogii*). Solid line (—) shows expected sinking rate changes for a cell that keeps its total carbon content constant but shunts newly-acquired carbon into carbohydrate instead of protein (case 1). Dashed line (---) shows expected sinking rate changes if a cell increases its carbohydrate but keeps both

its protein and cell volume constant (case 2). Dotted line (···) shows expected sinking rate changes if a cell increases its carbohydrate, keeps its protein constant, but gradually increases its overall cell volume (case 3).....30

3.1. Time-course measurements of A) chlorophyll, B) cell numbers, C) nitrate, D) carbohydrate:protein, and E) C:N ratio for cultures of *Rhizosolenia formosa*. Different symbols represent replicate cultures. Error bars represent standard errors of triplicate measurements for each culture. Arrows indicates times at which nitrate was re-introduced into the medium.....48

3.2. The percentage of nitrate-replete, nitrate-depleted, and nitrate-resupplied cells found in the A) top, B) middle, and C) bottom fractions of settling columns. Note that the axes are scaled differently to reflect differences between treatments.....52

3.3 Calculated sinking velocities and C:N ratios of negatively buoyant *Rhizosolenia formosa* with variations in N status.....54

3.4. Photosynthesis vs. irradiance (P-I) curves for N-replete cultures of *Rhizosolenia formosa*. A), B), and C) are triplicate cultures of *R. formosa*, each of which had triplicate determinations of P-I as indicated by dotted, dashed, and solid lines (with the exception of B) which had only two P-I determinations).....57

3.5. Photosynthesis vs. irradiance (P-I) curves for N-depleted cultures of *Rhizosolenia formosa*. A), B), and C) are triplicate cultures of *R. formosa*, each of which had triplicate determinations of P-I as indicated by dotted, dashed, and solid lines..58

4.1 Schematic of a box model of a *Rhizosolenia* migration cycle. Numbered boxes 1,12, 13, and 24 correspond to boxes referred to in equations 4.15 to 4.22 (see text). Biomass ascends through boxes on the left hand side of the figure and sinks through boxes on the right hand side. Transfer of biomass from ascending to sinking paths (and vice-versa) occurs only at the top and bottom boundaries (boxes 12, 24, 1 and 13).....79

4.2 Predicted vertical distributions of POC and PON for the base model, and for models with ascent and descent velocities set to constant values of 3 m h^{-1}, 6 m h^{-1} and 8 m h^{-1}.....94

4.3 A) Net downward flux of POC and B) net upward flux of PON for the base model (solid symbols) and for models where ascent and descent velocities were set to constant values of 3 m h^{-1}, 6 m h^{-1} and 8 m h^{-1}. Although plotted for a rate of 4.5 m h^{-1} for convenience, the ascent and descent velocity used for flux calculations from the base model varied between 3.3 and 5.8 m h^{-1}.....95

4.4 Predicted vertical distributions of POC and PON for variations in critical C:N (all mol:mol) ratios for sinking and floating. A) base model, where sinking occurred when the C:N ratio reached 11.9 and floating occurred when the C:N ratio reached 8.3, B) sinking occurred when C:N reached 10.7 and floating occurred when C:N reached 7.1, C) sinking occurred when C:N ratio reached 15.0 and floating occurred when C:N reached 8.3.....98

4.5 Predicted vertical distributions of POC and PON for variations in the amplitude of the loss term with depth. A) base model, where losses occurred evenly with depth

at a specific loss rate of 0.12 d^{-1}, B) where losses occurred from the top layer of the model only, at a specific rate of 0.58 d^{-1}, C) where losses occurred only from the bottom layer of the model, at a rate of 0.46 d^{-1}, and D) where losses occurred at the top and bottom layers only, but not at mid-depths, at a rate of 0.26 d^{-1}..102

Abstract

The effects of light and nutrients on the buoyancy of marine planktonic diatoms and the potential biogeochemical consequences of vertical movements of diatoms in coastal and open-ocean ecosystems were examined. A study of a relatively small coastal diatom (*Thalassiosira weissflogii*) in an experimental water column showed that under nitrate-replete conditions, *T. weissflogii* grew rapidly and exhibited nearly-neutral buoyancy, but that cells sank after depletion of ambient nitrate. Experiments showed that increased carbohydrate ballast in nitrate-depleted cells may have caused the increased sinking of cells in the tank, and that reversion of chemical composition upon re-introduction of nitrate can result in detectable increases in cell buoyancy. The biogeochemical consequences of nutrient-dependent changes in sinking rates of small diatoms include increased residence time of cells in the mixed layer of the ocean and enhanced transport of deep nutrients to the euphotic zone uncoupled from inputs of inorganic carbon.

Time-course experiments involving the large, buoyant diatom, *Rhizosolenia formosa*, examined changes in chemical composition and buoyancy during nitrate-replete growth, N-starvation, and recovery. Cells could maintain unbalanced growth for at least 53 h after depletion of ambient nitrate. Increases in C:N and carbohydrate:protein ratios observed during N-depletion reversed upon re-introduction of nitrate to culture medium. Buoyancy was related to nutrition: upon N-depletion, the percentage of positively buoyant cells decreased, but increased within 12 h of nitrate re-addition. *Rhizosolenia formosa* took up nitrate in the dark at rates three times their N-specific growth rates, indicating the potential for luxury consumption of nitrate which can be stored for later use in N-depleted surface waters. These results are consistent with purported vertical migrations of *Rhizosolenia* in nature. Cells may survive fairly long periods in N-depleted surface waters and will continue to take up carbon, then can resume nitrate uptake and will become more buoyant upon returning to deep water sources of nitrate.

The potential contribution of migrations of *Rhizosolenia* to open-ocean new production was examined using a numerical model which predicted fluxes of carbon and nitrogen during a steady-state migration cycle, specific rates of increase of biomass, total migration cycle times, and vertical distributions. Modeled fluxes of POC and PON normalized to integrated water column abundance were used to derive a factor, ϕ (d^{-1}), which was then combined with literature estimates of *Rhizosolenia* abundance to predict fluxes of POC and PON. New production estimated by the model was on order of 5 μmoles N m^{-2} d^{-1}; this value represents up to 4% of new production that results from turbulent diffusive fluxes of N.

Acknowledgements

So many people have helped me over the past few years, it is difficult to know where to begin. First, thanks to my supervisor, John Cullen, for his guidance, his encouragement, his support, and most of all for his patience. It was a privilege and a pleasure to work with you, John. Thanks!

To my co-supervisor, Marlon Lewis, my thanks for his incredibly astute insights into many phases of my work, for the encouragement to be quantitative, and for the many scientific opportunities he gave me over the years. Thanks also to Landlord Marlon, Landlady Trudy, and Margaret (a.k.a. Pumpkin, Maggie May, or Sweetie Pie) who made Murray Place a wonderful place to come home to! I'll miss you all very much.

To the members of my supervisory committee, Glen Harrison, Jim Craigie, and Tony Bowen, many thanks for your support, encouragement, and for sharing your vast stores of knowledge.

Other members of the department contributed to my thesis in many ways. Thanks to Dan Kelley for great conversations (science and otherwise), for teaching me to model, for lunches at Wendy's and for making me go for a run, even when I didn't want to! (or, when he didn't want to!). Thanks to Áurea Ciotti (the Jacaré) for answering a million of my questions about trons, field work, computers, cooking, etc. and for feeding me proper meals, and to Betsy (Poo) Webb for relaxation sessions at Cosmos. To Geoff MacIntyre, thanks for just entertaining the heck out of me the last few years, and to Gary Maillet thanks for his technical expertise and for always being willing to lend a hand. Good luck with those Rhizo cultures! To all my friends in the second floor D-lab, past and present, thanks for making life fun. Thanks to Carl Boyd for encouragement and for support of this work in its early stages, and for giving me the freedom to go where I had to go. Finally, thanks go to Pierre Clement, Les Harris, and Peter Cranford at BIO for help with nutrient analyses, mass spec measurements, and CHN analyses, respectively.

The support of friends and family were critical to the successful completion of this thesis. Thanks to Claudio DiBacco for his encouragement, support, and understanding, and for keeping me sane even when I really started to lose it. Thanks to Mary-Elena Carr for encouraging phone calls and e-mails, and for stays at Spa Mary-Elena. To my housemates at 1824 Robie St. (Terri, Pierre, Barbara, and Conrad), thanks for keeping me company during the last year, for watching a thousand movies with me, and for Friday night viewings of The X-Files. My non-academic life was enhanced greatly by my membership in the All Saint's Cathedral Choir. Thanks to all of you!

Finally, thanks to Mum, Dad, and Tony for their love and support, and for cat sitting, transportation, financial assistance, and car repair. And to Spike, thanks for being such a cool cat.

Chapter 1

Introduction

The suspension and sinking of marine planktonic diatoms has been the subject of scientific research for over a century (e.g. Hensen 1887). Early studies were concerned with how diatoms remain suspended in the euphotic zone (see Smayda 1970). Later work recognized that continuous residency in the euphotic zone is not necessarily advantageous, and that sinking to nutrient-rich deep waters is a strategy crucial to the survival of diatoms in some oceanic regions (Smetacek 1985). Buoyancy regulation allows diatoms to achieve both suspended and sinking modes of existence, and it is now generally accepted that, to varying degrees, diatoms can regulate their buoyancy independent of movements of the surrounding water (Smayda 1970, Bienfang and Szyper 1982).

The extent to which a diatom can control its buoyancy is partly determined by its ratio of total cell volume (including contributions from the silica cell wall) to its internal cell volume (Smayda 1970, Villareal 1988). Physiological regulation of buoyancy involves changes in the internal density of the cell. Assuming equal thickness of cell walls, cells with larger internal volumes have higher capacities for changing internal density, thus higher capacities for buoyancy regulation. Large cells (>100 μm) may achieve positive buoyancy (Villareal 1988, 1992); small cells (<50 μm) may be near-neutrally buoyant (Strickland et al. 1968, Takahashi and Bienfang 1983, Richardson and Cullen 1995). In all size classes, control of buoyancy may be manifested as increases or decreases in cell

sinking velocities which are often the result of changes in the light and nutrient status of the organism (Steele and Yentsch 1960, Bienfang et al. 1982, 1983, Waite et al. 1992 a, b).

In this thesis, I examine the effects of light and nutrients on the chemical composition and buoyancy of marine planktonic diatoms and I investigate the potential ecological and biogeochemical consequences of vertical movements of diatoms in coastal and open-ocean regions. Vertical movements of diatoms, for the purpose of this thesis, include both the sinking and resuspension of small cells by advection, upwelling, or turbulence, as well as vertical movements in the form of migrations by large diatoms such as *Rhizosolenia* and *Ethmodiscus*, this ability is made possible by their large capacity for buoyancy change (Villareal et al. 1993, Villareal and Carpenter 1994). This thesis is essentially three scientific publications linked together by a general Introduction (Ch. 1) and overall Conclusions (Ch. 5). The nature of the thesis, therefore, has produced some degree of repetition of background information in the Introduction and Discussion sections of the various chapters.

Chapter 2 presents results which show the importance of nutrients to the maintenance of buoyancy in a coastal diatom, *Thalassiosira weissflogii*. Vertical distributions of this diatom in a 2.1 m tall laboratory water column were determined under nitrate-replete and nitrate-depleted conditions. Batch culture experiments and modeling exercises were used to determine possible causes of the observed changes in vertical distribution, and results were discussed in terms of the biogeochemical consequences of nutrient-dependent changes in sinking rates of small diatoms.

Chapter 3 presents results of experiments with the large, sometimes positively buoyant diatom *Rhizosolenia formosa*. This organism was used to examine further the relationship between chemical composition and cell buoyancy, and to assess whether physiological characteristics of *R. formosa* were consistent with the ability to migrate vertically in the open-ocean. The potential biogeochemical consequences of migrations of *Rhizosolenia* are discussed, and are investigated more fully in Chapter 4, where a

numerical model is used to estimate the potential contributions of migrations of *Rhizosolenia* to nutrient cycling and new production in the open-ocean. The model also predicts the vertical distribution of biomass, specific rates of increase and total migration cycle times.

Finally, I conclude by summarizing the major findings of this research, namely, that reversible changes in the chemical composition of *Thalassiosira weissflogii* and *Rhizosolenia formosa* with variations in light and nutrient regimes affect cell buoyancy. Buoyancy changes lead to increases or decreases in cell sinking rate, and, for the case of *Rhizosolenia*, reversions in buoyancy state allow vertical migrations of these cells through the water column. The upward transport of nitrogen during migrations of *Rhizosolenia* is a form of new production (*sensu* Dugdale and Goering 1967), and may represent at most 4% of new production that results from the turbulent diffusion of nitrate into the euphotic zone.

Chapter 2

Changes in buoyancy and chemical composition during growth of a coastal marine diatom

2.1 Introduction

Suspension and sinking of marine phytoplankton have received considerable attention in recent years due to increased interest in the flux of organic material to the deep sea (Michaels and Silver 1988, Jahnke 1990). Since an organism's vertical position in the water column will ultimately determine its overall primary productivity and growth, an understanding of mechanisms of suspension and sinking is critical to accurate descriptions of marine ecosystems (Smayda 1970, Walsby and Reynolds 1980).

Stokes' law is usually used to describe the sinking rate of phytoplankton cells (Smayda 1970, Vogel 1981, Oliver 1994):

$$V = \frac{2}{9} \frac{g r^2 (\rho - \rho')}{\mu \phi_r} \qquad (2.1)$$

where V is the sinking rate of the cell (m s^{-1}) (positive in the downwards direction), g is acceleration due to gravity (m s^{-2}), r is cell radius (m), ρ is intracellular density (kg m^{-3}), ρ' is the density of sea water (kg m^{-3}), μ is the dynamic viscosity of sea water (kg m^{-1} s^{-1}) and ϕ_r is a dimensionless coefficient of form resistance, which is the ratio of the velocity of

an equivalent sphere to that of cells of similar density and volume (Heaney and Butterwick 1985). The $(\rho - \rho')$ term is known as excess density. A list of symbols and definitions is found in Table 2.1.

Motile phytoplankton are capable of directed swimming and can control their position in the water column (e.g. Cullen 1985), while the vertical position of non-motile phytoplankton is determined by interactions between the buoyancy of a cell and its physical environment (Smayda 1970). Cell buoyancy is affected by changes in excess density. Physiological changes in excess density may include changes in internal ion concentration (Gross and Zeuthen 1948, Beklemishev et al. 1961, Anderson and Sweeney 1977, Anderson and Sweeney 1978, Kahn and Swift 1978), internal carbohydrate concentration (Villareal and Carpenter 1990, Romans et al. 1994), or the production of gas vesicles, an adaptation found in many species of freshwater and marine cyanobacteria (Walsby 1978, also reviewed by Oliver 1994). The most comprehensive studies of changes in excess density have concerned the buoyancy of cyanobacteria, where overall buoyancy conferred by gas vesicles can be modified by changes in cellular carbohydrate (e.g. van Rijn and Shilo 1985, Walsby et al. 1989, Ibelings et al. 1991, Romans et al. 1994). The density of carbohydrate (1600 kg m^{-3}) is greater than the density of cellular constituents like protein (1300 kg m^{-3}) and lipid (860 kg m^{-3}), thus increases in the proportion of carbohydrate will increase the excess density of the cell, resulting in increased sinking velocities (see Smayda 1970).

Physiological changes in buoyancy may be independent of changes in density of surrounding sea water (Bienfang and Szyper 1982), and of any morphological adaptations to suspension (Smayda and Boleyn 1966a, b), though some morphological adaptations (like the production of chitin fibres by *Thalassiosira weissflogii*, see Walsby and Xypolyta 1977) may contribute to an increase in the coefficient of form resistance which will slow the sinking speed of the cell. Cell buoyancy may depend on the light and nutrient status of the organism (Steele and Yentsch 1960, Bienfang et al. 1982, Bienfang et al. 1983,

Table 2.1: List of symbols and definitions for Chapter 2.

Symbol	Definition	Value	Units
V	Cell sinking rate	variable	m s^{-1}
g	Acceleration due to gravity	9.8	m s^{-2}
ρ	Intracellular density	variable	kg m^{-3}
ρ'	Seawater density	variable	kg m^{-3}
μ	Dynamic viscosity of seawater	variable	kg m^{-1} s^{-1}
r	Cell radius	variable	m
ϕ_r	Coefficient of form resistance	variable	dimensionless
PAR	Photosynthetically available radiation	variable	µmol quanta m^{-2} s^{-1}
t	time	variable	d
Chl_t	Chlorophyll concentration at time t	variable	mg m^{-3}
$Chl_{t-\Delta\tau}$	Chlorophyll concentration on previous day	variable	mg m^{-3}
K_{max}	Maximum specific growth rate	variable	d^{-1}
N	Nitrate concentration	variable	µM
K_S	Half saturation constant for nitrate uptake	variable	µM
W	Total loss rate	variable	d^{-1}
T_s	Timescale for increased sinking	variable	d
w_s	Maximum specific loss rate	variable	d^{-1}
t_d	Time since N depletion	variable	d
P	Significance level		dimensionless

Bienfang and Harrison 1984, Granata 1987, Waite et al. 1992a,b) and may require significant inputs of metabolic energy (Waite et al. 1992c).

Buoyancy changes give phytoplankton distinct ecological advantages. For example, it can be advantageous for cells to have low excess density so they will remain suspended in the illuminated waters of the euphotic zone. Often, however, nutrient levels in illuminated waters do not become significant until well below the euphotic zone (e.g. Hayward 1991). Thus, buoyancy changes that cause cells to sink to deeper layers to obtain nutrients are also of great potential benefit. Sinking of cells following diatom blooms is thought to be a survival strategy whereby cells become "resting stages" in dark, cold water and are then ready to seed a new population when conditions are right (Smetacek 1985).

Changes in buoyancy may also cause cell sinking rates to slow, and often result in accumulation of cells in subsurface maxima near nutrient gradients (Steele and Yentsch 1960, Heaney et al. 1989). Lande and Wood (1987) calculated residence times of cells in the surface mixed layer and nutricline of a two-layer model of the upper ocean. Cells whose sinking rates slowed to 1 m d^{-1} at the top of the nutricline (from 4 m d^{-1} in the mixed layer) were shown to spend a substantially longer time in the mixed layer than cells with sinking rates that did not change, because the more slowly sinking cells had greater probability of being mixed back up to the surface. Prolonged cycles of sinking and resuspension meant that cells were "shuttled" between nutrient-rich (deeper) waters, and higher irradiance surface layers (Lande and Wood 1987).

In this section, I focus on the buoyancy of a relatively small coastal marine diatom, and on the connection between cell buoyancy, nutrient status, and cellular chemical composition. Experiments performed in a 2.1 m tall laboratory water column showed that a population of nutrient-replete *Thalassiosira weissflogii* was almost neutrally buoyant, but once nutrients ran out the nearly-neutral buoyancy was lost. To determine the mechanism of sinking, I examined changes that occur in carbohydrate and protein during nutrient depletion and how changes in these constituents may affect cell sinking rates. Results are

discussed in terms of the ecological advantages of buoyancy changes, both with respect to increased sinking rates upon nutrient depletion and decreased sinking rates when nutrient-replete. Finally, I discuss the potential biogeochemical consequences of buoyancy changes through unbalanced growth.

2.2 Methods

2.2.1 Tank experiments

Unialgal cultures of the marine diatom *Thalassiosira weissflogii* (Provasoli-Guillard Center for Culture of Marine Phytoplankton strain #1336) were grown in 10 l polycarbonate carboys which contained 8 l of sterile-filtered artificial sea water (ASW)-based f/2 medium (Guillard 1972) with nitrate concentration adjusted to 440 μM. Sterile filtration was done using a 0.2 μm Culture Capsule filter (Gelman Sciences, Ann Arbor, Michigan). Cells were grown at 20°C, on a 16h:8h light:dark (L:D) cycle. Illumination was from 7 Vita-Lite fluorescent lamps providing a quantum scalar irradiance of 150 μmol m^{-2} s^{-1} (photosynthetically active radiation, PAR) as measured by a Biospherical Instruments QSL-100 4π sensor placed just outside the culture containers

Experiments were conducted in a 2.1 m tall, 0.29 m inner diameter (i.d.) opaque polyvinylchloride cylinder (Fig 2.1; see Heaney and Eppley 1981, Cullen and Horrigan 1981). The bottom of the tank was surrounded by a barrel through which 9°C water was circulated to produce temperature stratification. The top portion of the tank was wrapped with an insulating blanket to conserve heat and to maintain a stable temperature gradient. Illumination was provided from above on a 12h:12h L:D cycle (lights on from 08:00 to 20:00) using a 250-watt metal halide Grow Lamp (Applied Hydroponics, Inc., San Rafael, CA) shining through a running-water heat filter made of clear acrylic. Irradiance just below the surface water of the tank was approximately 150 μmol m^{-2} s^{-1} PAR as measured with a QSL-100 submersible sensor. Room temperature averaged 20°C, though variations (± 3°C)

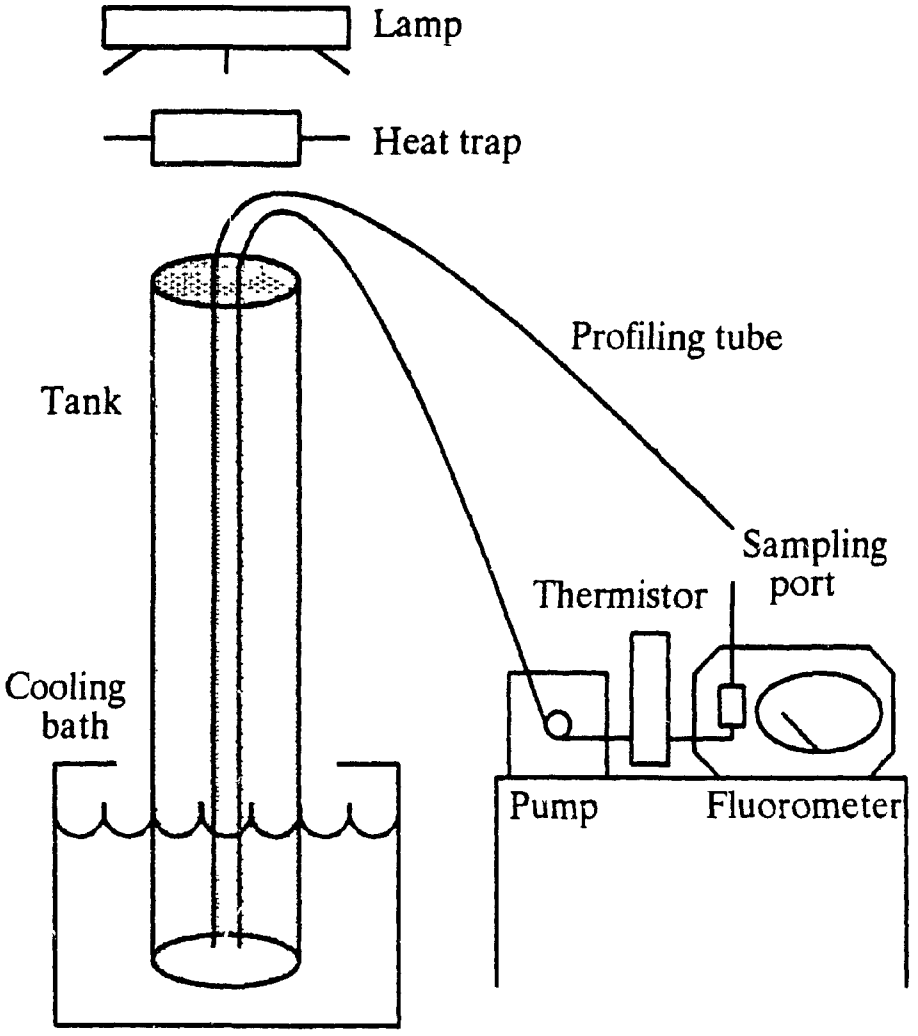

Figure 2.1: Schematic of tank experiment apparatus.

occurred due to heating by the lamp during the day and cooling of the ambient air at night; variations in water temperature were minimized by the insulating blanket.

The tank was filled with 100 l of sterile-filtered ASW-based f/2 medium without nitrate, and was inoculated with the 8 l culture of exponential phase *Thalassiosira weissflogii* described above. Nearly uniform vertical distribution of the culture was achieved by pumping the inoculum of *T. weissflogii* into the tank using a Masterflex peristaltic pump with 5 mm i.d. silicone tubing, while simultaneously mixing the tank by pulling the tube up and down. This resulted in an initial chlorophyll concentration of approximately 7 mg m^{-3}, an initial nitrate concentration of 30 μM, and an initial temperature of 20°C. Once these conditions were established, the 9°C water was circulated through the barrel surrounding the bottom of the tank, and a sharp thermocline at about 150 cm depth was established within 12 h of inoculation. This thermocline remained nearly constant for the duration of the experiment (Fig. 2.2a). Cells were allowed to adjust to tank conditions for approximately 4 days, after which routine sampling began.

Vertical profiles were conducted using a double-tube profiling system much like that described by Cullen and Horrigan (1981) (refer to Fig. 2.1). Weighted silicone tubing (i.d. 1.6 mm) was lowered into the tank. One end of the tube ran from the tank, through a Masterflex peristaltic pump (flow rate approx. 30 ml min^{-1}) to the micro-flow-through cell of a Turner Designs Model 10-005R fluorometer. A return-flow tube carried this water to the depth from which it came, with little disruption of temperature stratification in the water column. Daily monitoring of 3 (3,4-dichlorophenyl)-1, 1-dimethylurea (DCMU)-induced fluorescence ratios (Roy and Legendre 1979, Vincent 1980) indicated no deleterious effects of pumping to photosynthetic capacity of cells. A thermistor was attached near the intake tube which gave vertical profiles of temperature. Using this double-tube system, profiles of fluorescence and temperature were performed at depth intervals of 20 cm. Vertical profiles were taken for 20 days, 6 times daily (at 01:00, 07:30, 11:00, 14:00, 17:00, and 20:00).

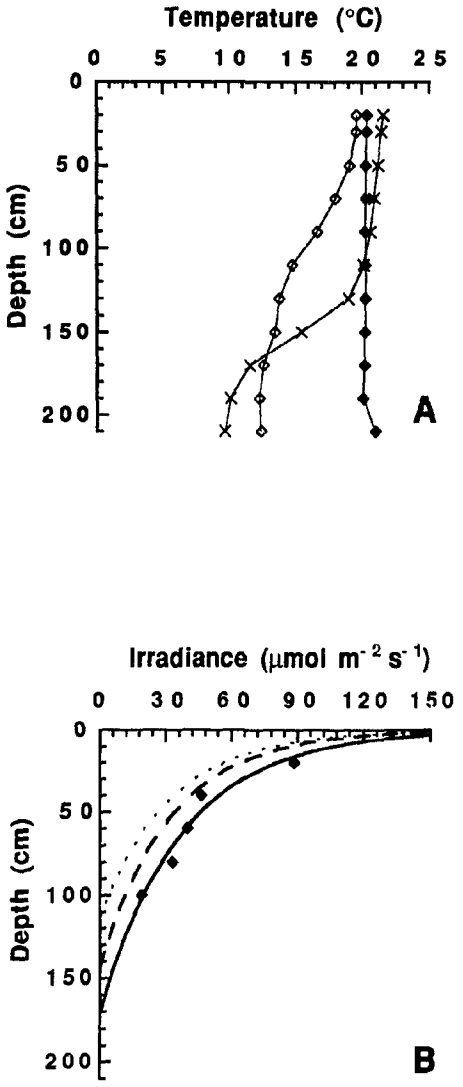

Figure 2.2: (A) Temperature profiles at three time points during the tank experiment, Day 1 (◆), Day 4 (◊), and Day 10 (x). (B) Irradiance profiles measured with distilled water in the tank (no cells) (◆, with exponential curve fit as solid line) and modeled curves for Day 5 (---) and Day 10 (···) of the experiment.

Sampling times included one point at the end of the dark period (the 07:30 profile) and one point at the end of the light period (20:00).

Samples for cell counts, chlorophyll, and nitrate concentration were removed from a T-connector in the return flow tube at 3 to 5 depths per profile. Depths chosen for sampling depended upon observed vertical distributions of fluorescence. Chlorophyll concentrations were determined by fluorescence after at least 24 h extraction in 90% acetone in the dark at -10°C (Strickland and Parsons 1972). Nitrate concentrations were determined by a Technicon Auto-Analyzer II, and cell counts were done with an inverted microscope on cells preserved with a 1% solution of paraformaldehyde and glutaraldehyde (1:1 by volume) to a final concentration of 0.01%. Fluorescence measurements were converted to chlorophyll concentration using a conversion factor calculated from determinations of chlorophyll at 3 to 5 depths in each profile, with intermediate values determined by linear interpolation of fluorescence:chlorophyll ratios. Specific rate of increase (k in d^{-1}) of cells from the surface of the tank were determined by non-linear least squares regression analysis of an exponential growth curve, fit to the chlorophyll time series before depletion of ambient nitrate.

A profile of irradiance is shown in Fig. 2.2b. Due to the bulkiness of the light profiling apparatus, and its detrimental effects on thermal stratification in the tank, a light profile was determined only prior to the beginning of the experiment when the tank was filled with distilled water and there were no diatoms present. A rough approximation of the incremental attenuation of PAR due to increased chlorophyll throughout the experiment was modeled assuming a direct light path with attenuation due solely to absorption, with a specific absorption coefficient for phytoplankton of 0.015 m^2 mg chl $^{-1}$ (Kirk 1994) (Fig. 2.2b).

2.2.2 Batch culture experiments

For batch culture experiments, triplicate cultures of *Thalassiosira weissflogii* were grown in 10 l polycarbonate carboys which contained 7 l of ASW-based f/2 medium with nitrate concentration adjusted to near 30 μM. Cells were grown at 20°C on a 12h:12h L:D cycle, and were illuminated with Vita-Lite fluorescent lamps providing an irradiance of 150 μmol m^{-2} s^{-1} measured just outside culture containers. A time-course experiment was conducted during which triplicate samples from each culture were taken morning and evening (just before lights on and off) for analysis of chlorophyll, nitrate, protein, and carbohydrate. Chlorophyll and nitrate were analyzed as described for tank experiments, protein was analyzed by the Biuret-Folin method of Dorsey et al. (1978) using bovine serum albumin (BSA) as standard, and carbohydrate was measured as glucose equivalents by the phenol-sulphuric acid method of Dubois et al. (1956). Samples were taken before and after depletion of nitrate from the culture medium. Cells were allowed to go without nitrate for 3 days, after which 100 μM of $NaNO_3$ was added to observe recovery of cells and accompanying changes in the accumulation of cellular constituents. Specific growth rates (k in d^{-1}) were determined by non-linear least squares regression analysis of an exponential growth curve, fit to the chlorophyll time series obtained before depletion of ambient nitrate.

2.3 Results

2.3.1 Nearly-neutral buoyancy in nitrate-replete *Thalassiosira weissflogii* grown in the experimental water column

A total of 103 profiles were performed during the 20-day tank experiment. Under nitrate-replete conditions, *Thalassiosira weissflogii* had a specific rate of increase of 0.3 d^{-1} at the surface of the tank, reaching chlorophyll concentrations of 100 mg m^{-3} after 10 days

(Fig. 2.3a). Cells exhibited nearly-neutral buoyancy during this period. This assertion is based upon the following observations: i) growth rates of cells at the surface of the tank were the same as cells in batch cultures under similar conditions (0.3 d^{-1}, discussed below), indicating that significant numbers of cells were not lost to sinking, ii) chlorophyll yield was as predicted for an initial nitrate concentration of 30 µM (using a nitrate:chlorophyll relationship of 0.3 µmol μg^{-1} established during batch culture work), and iii) there was no noticeable accumulation of cells at the bottom of the tank (210 cm) until after nitrate was depleted from upper layers (see Fig. 2.3a to 2.3c and Fig. 2.4).

Chlorophyll profiles done at 20:00 each day (Fig. 2.4) show increases near the surface with minimal accumulation at depth until after day 10, at which time the profile changed dramatically showing accumulation at mid-depth (Fig. 2.4), then deep in the tank (Fig. 2.4). Cell counts (Fig. 2.5) confirm that cells disappeared from surface waters. Cell count data and surface chlorophyll data (Fig. 2.3a) showed that cells did not sink immediately upon depletion of nitrate from the medium. Qualitative examination of chlorophyll data shows a time lag of approximately 48 h; a slightly longer lag (60 h) is indicated by cell count data. The difference is consistent with a change in chlorophyll per cell after depletion of nitrate from culture medium (Fig. 2.5).

A diel series of profiles taken between 01:00 and 20:00 on a typical day before nitrate depletion shows rapid accumulation of chlorophyll between 11:00 and 14:00 with profiles keeping their characteristic shape throughout the day (Fig. 2.6).

2.3.2 Growth of cells and changes in carbohydrate and protein during batch culture experiments

Batch culture experiments examined changes in chlorophyll, protein, and carbohydrate during nitrate-replete and nitrate-depleted growth of *Thalassiosira weissflogii*. Initially, cells grew exponentially at a rate of 0.3 ± 0.01 d^{-1} (mean ± SE of triplicate cultures) reaching chlorophyll levels of near 100 mg m^{-3} after 6.3 days (Fig. 2.7a). By that

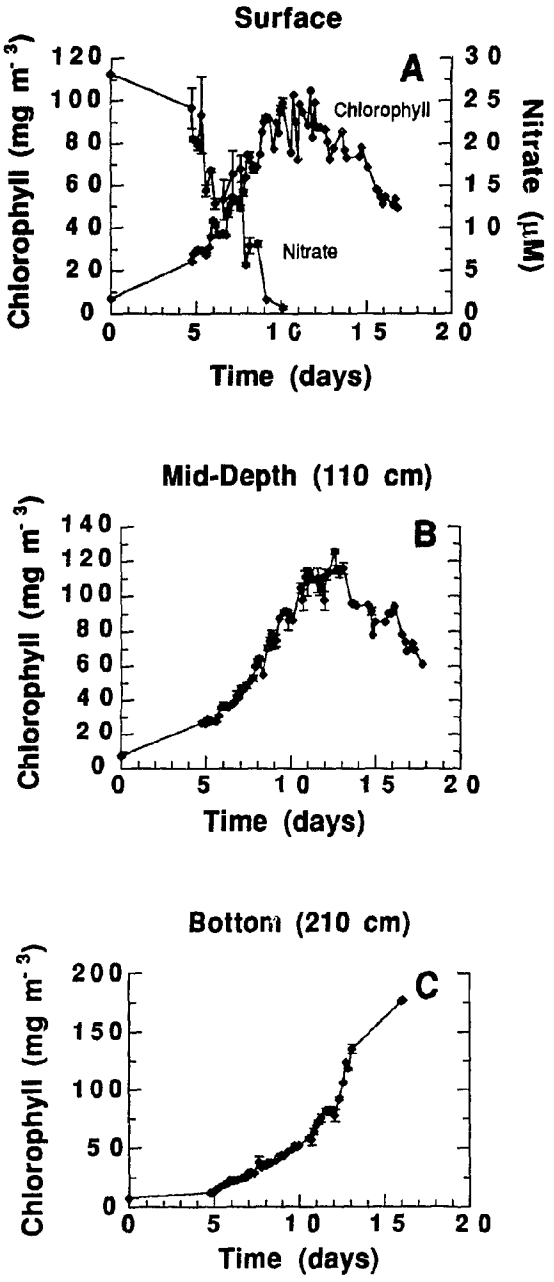

Figure 2.3: Time-course of (A) chlorophyll (◆) and nitrate (◊) in tank surface waters, (B) chlorophyll at mid-depth (110 cm) and (C) at the bottom (210 cm) during growth of *Thalassiosira weissflogii* in the tank. Error bars are ± SE of triplicate measurements. Symbols with error bars are true chlorophyll determinations, those without error bars are chlorophyll values converted from fluorescence profiles.

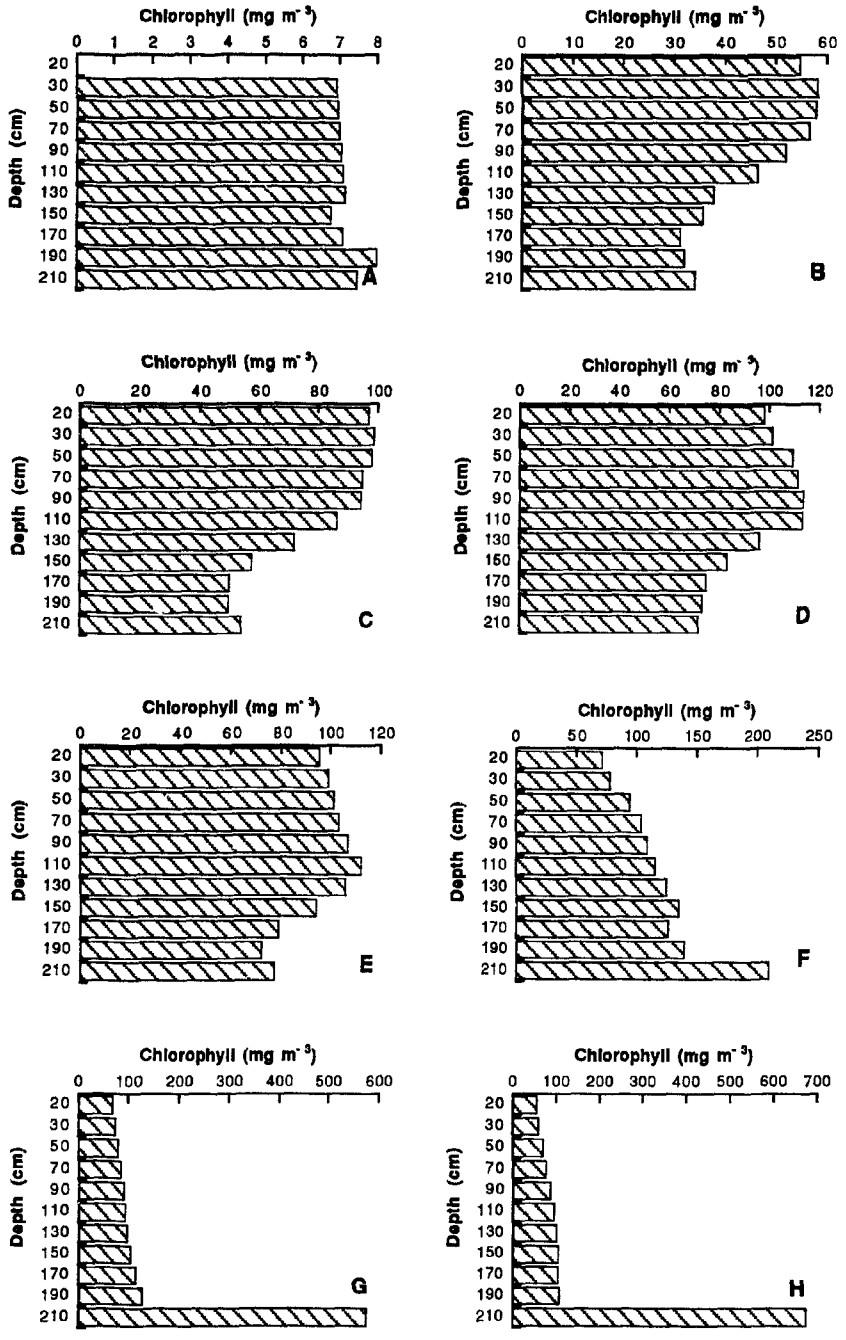

Figure 2.4: Representative chlorophyll profiles done at 20:00 daily during the tank experiment. (A) Profile on Day 1 (initial), (B) Day 7, (C) Day 10, (D) Day 11, (E) Day 12, (F) Day 13, (G) Day 15, and (F) Day 16. Ambient nitrate was depleted after Day 10 of the experiment.

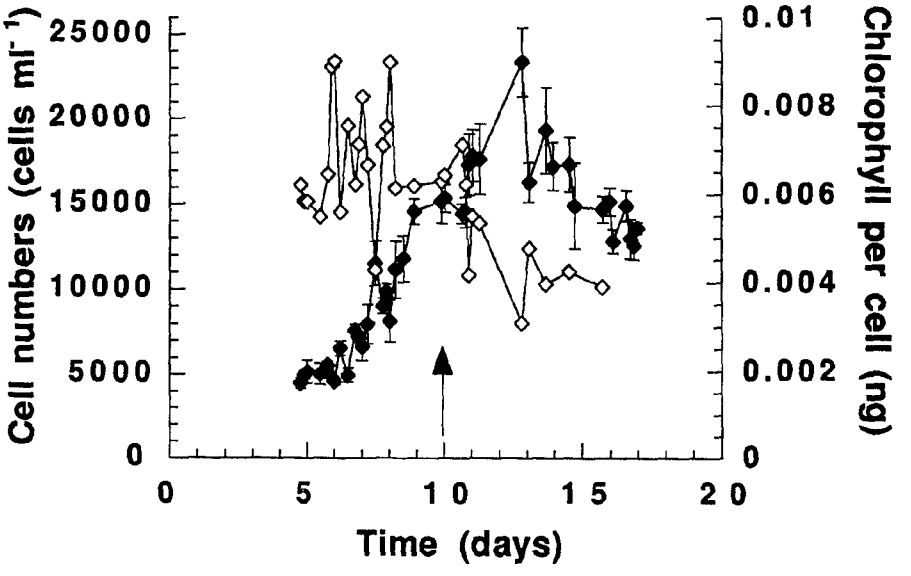

Figure 2.5: Time course of cell counts (◆) and chlorophyll per cell (◊) of *Thalassiosira weissflogii* taken from surface water of the experimental tank. Error bars are ± SE of triplicate measurements. Arrow indicates time at which nitrate was depleted from surface waters.

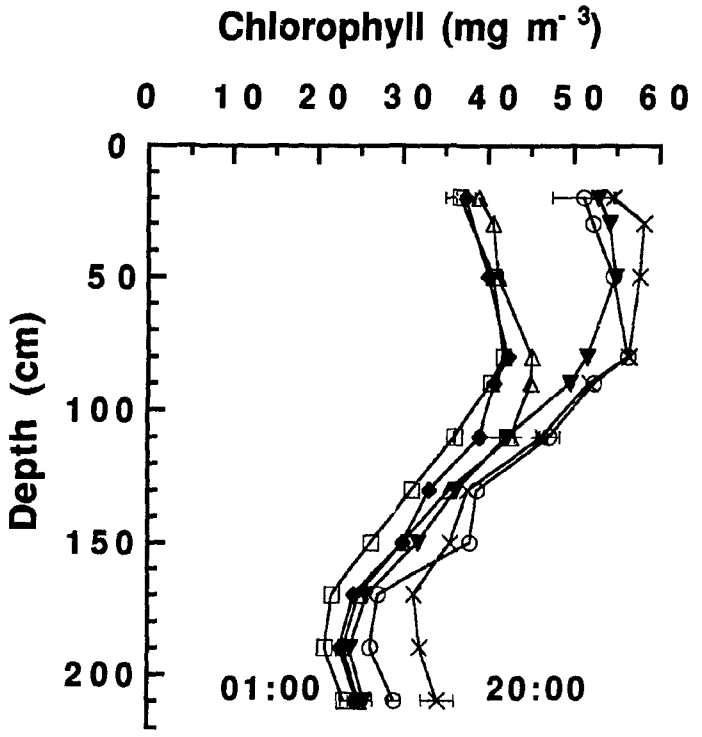

Figure 2.6: Diel series of chlorophyll profiles done on a representative day (Day 8) before depletion of nitrate from surface waters of the tank. Profiles were done at 01:00 ( ), 07:30 (◆),11:00 (Δ),14:00 (▼),17:00 (O), and 19:30 (x). The 07:30 profile is just before lights-on; 19:30 is just before lights-off. Error bars are ± SE of triplicate measurements.

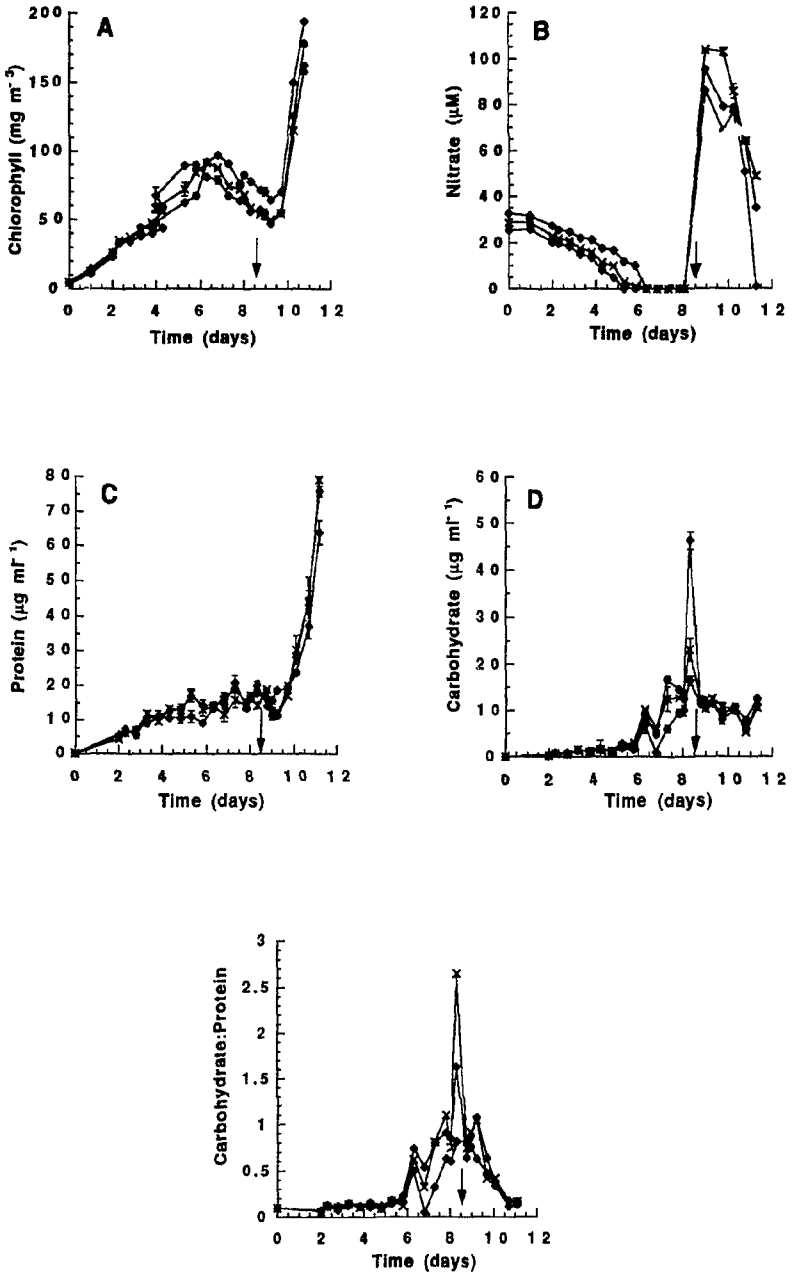

Figure 2.7: Time-course of (A) chlorophyll, (B) nitrate, (C) protein, (D) carbohydrate, (E) carbohydrate:protein ratio during batch culture experiments with *Thalassiosira weissflogii*. Symbols represent triplicate cultures treated identically. Arrow indicates time at which nitrate was added back to the medium. Error bars are ± SE of triplicate measurements.

time, ambient nitrate had disappeared (Fig. 2.7b), protein synthesis had slowed (Fig. 2.7c), but cells continued to synthesize carbohydrate in a period of unbalanced growth (Fig. 2.7d). As in tank experiments, there was a noticeable decrease of chlorophyll after nitrate was depleted from culture medium (Fig. 2.7a). Overall, carbohydrate per ml of culture increased between 2.3 and 5.2 times during the nitrate-depleted phase of the experiment. Accordingly, time-course measurements of carbohydrate:protein ratios showed increases from pre-depletion values of 0.1 to values of over 2.5. When nitrate was re-introduced after close to 3 d of nitrate depletion, however, cells recovered completely (Fig. 2.7c, d, and e). Protein synthesis increased, carbohydrate levels declined rapidly, and carbohydrate:protein ratios returned to their original values within 2 d.

2.4 Discussion

2.4.1 A model of nitrate-dependent sinking

Daily profiles conducted during the growth of *Thalassiosira weissflogii* in the experimental water column showed that this diatom was almost neutrally buoyant under well-stratified conditions. Maintenance of buoyancy seemed closely tied to the nutrient status of the cells and changed after depletion of ambient nitrate. To quantify and examine this process, changes in chlorophyll and nitrate at the surface of the tank were described by an exponential growth equation modified by a Michaelis-Menten term for nitrate uptake and a loss term due to sinking:

$$Chl_t = Chl_{t-\Delta t} \cdot e^{\left(K_{max}\left(\frac{N}{N+K_s}\right)-W\right)\cdot\Delta t} \qquad (2.2)$$

where Chl_t and $Chl_{t-\Delta t}$ are chlorophyll concentrations (mg m^{-3}) at day t and t-Δt respectively, K_{max} is the maximum specific growth rate (d^{-1}), N is nitrate concentration (μM) at day t, K_S is the half saturation constant for nitrate (μM), Δt is the time since last time step in days, and W is a loss term (d^{-1}), due to sinking. Some component of this loss term is also due to chlorophyll degradation, as will be discussed later. These parameters are included in the list of symbols and definitions for this chapter (Table 2.1). Changes in surface water concentrations of chlorophyll and nitrate were modeled as discrete changes from an initial chlorophyll concentration of 7 mg m^{-3}, an initial nitrate concentration of 30 μM (initial values during the tank experiment), and a nitrate:chlorophyll ratio of 0.3 μmol μg^{-1} (determined during batch culture experiments). Generally, W was modeled as:

$$W = \frac{w_s}{1 + 100 \cdot e^{-\left(t - t_d / T_s\right)}} \tag{2.3}$$

where w_S is the maximum specific loss rate (d^{-1}), t is time in days, t_d is the time of nitrate depletion (d), and T_S is a time scale for increased sinking (d). This formulation varies W 100-fold, from 1% to 100% of the maximum specific loss rate, w_S, with a sigmoid function consistent with changes in chemical composition during unbalanced growth (Cullen and Lewis 1988); cells reach 10% of w_S at approximately 2.5 T_S.

Parameters for equations (2.2) and (2.3) were estimated by a least squares non-linear curve fitting routine in SYSTAT, version 5.2.1. The optimal combination of parameters was determined using a grid search method on a spreadsheet, where the aim was to minimize the sum of the squared deviations of the modeled vs. measured chlorophyll.

Four possible time-courses were modeled by varying the form of W, the loss term. Chlorophyll and nitrate distributions were modeled for the case where there was no sinking of cells upon nitrate depletion, that is, if W was set to zero through the entire time series (Fig. 2.8a), and for the case where W remained constant with time and was set to w_S, the value of which was determined by the grid search method (Fig. 2.8b). Tank experiment data showed that sinking losses were not detectable before depletion of ambient nitrate. Therefore, modeled distributions shown in Fig. 2.8c and Fig. 2.8d have sinking initiated *after* nitrate depletion. Chlorophyll and nitrate distributions are shown if sinking of cells occurred *immediately* after ambient nitrate depletion (Fig. 2.8c). In this case, T_S was set to the arbitrary low value of 0.0001 days. Finally, distributions are shown for the case where sinking of cells starts slowly after nitrate depletion, then accelerates (following a sigmoid function) to the maximum specific sinking rate (Fig. 2.8d). This was the best-fit equation as determined by F-ratio test (Moore and McCabe 1993) (see Table 2.2). According to this chlorophyll-based model equation, the time scale for increased sinking after depletion of ambient nitrate was 25 h (1.04 d). Thus, cells reach 10% of w_S approximately 62 h after nitrate depletion. The model equation also gave a maximum specific growth rate (K_{max}) of 0.3 d^{-1}, a K_S value of 1.95 μM, and a maximum specific sinking (loss) rate of 0.22 d^{-1}. This loss rate corresponds to a sinking rate of 0.04 m d^{-1} over an arbitrary surface stratum of 20 cm.

An unknown component of the loss term (which I have considered due entirely to sinking) is due to the degradation of cellular chlorophyll upon nitrate depletion. Quantification of the degradation component is difficult. The use of chlorophyll data from batch culture experiments (which are not confounded by sinking losses) predicts a chlorophyll degradation rate of 0.14 d^{-1}. If this rate is applied directly to the model immediately after nitrate depletion, it results in a gross overestimate of the actual loss of chlorophyll. In fact, it predicts that *all* the loss of chlorophyll from the surface of the tank could be from chlorophyll degradation. I know from cell count data, however, that cells

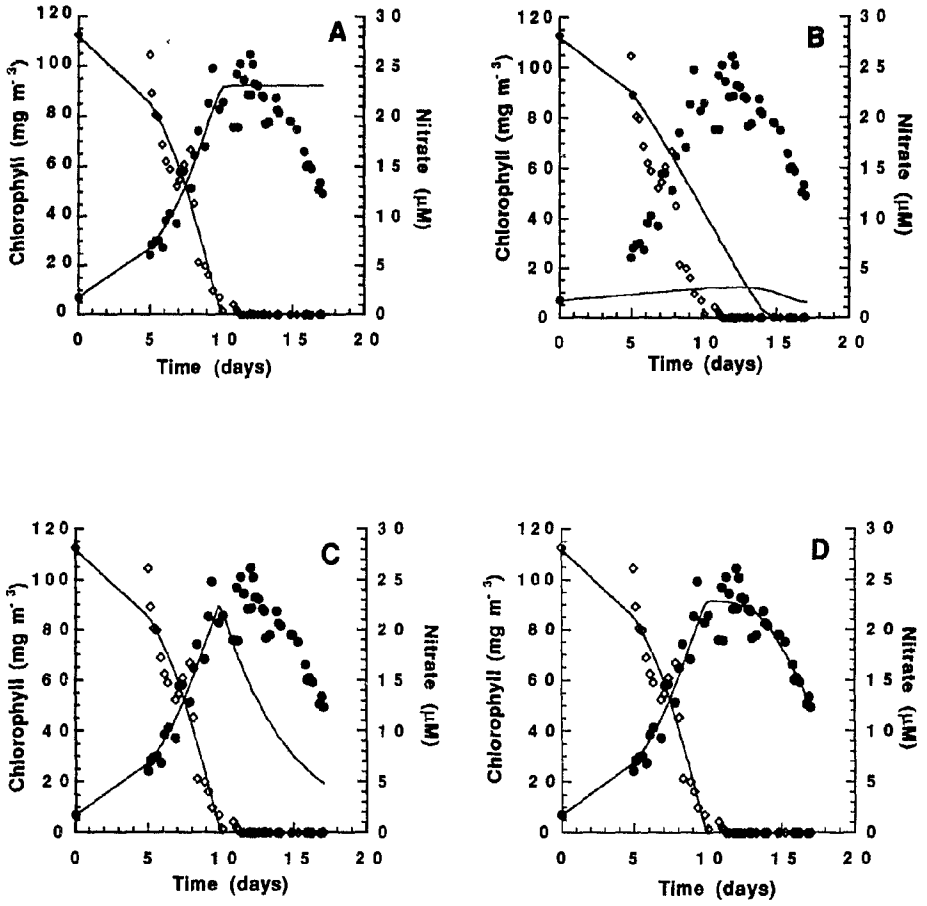

Figure 2.8: Fits of model equations (—) to observed chlorophyll (●) and nitrate (◊) data. (A) Fit of model equation with nitrate-dependent growth of cells but no sinking of biomass, (B) Fit of model equation with constant sinking rate, (C) Fit of model equation with no delay between depletion of ambient nitrate and initiation of sinking, (D) Fit of model equation with nitrate-dependent growth and nitrate-dependent sinking where cells reach 50% of their maximal sinking rate 115 h after depletion of ambient nitrate.

Table 2.2: F-ratio comparison of fits of four versions of Eq. (2.2) to observed surface chlorophyll distributions during growth of *Thalassiosira weissflogii* in the experimental tank. The 4 versions of Eq. (2.2) are: Model A = no sinking of biomass, Model B = constant sinking of biomass, Model C = immediate nitrate-dependent sinking, Model D = nitrate-dependent, sigmoid-shaped sinking function. I compare only the fit of Model D to the fits of the other three models. Values for sum of the squared deviations of modeled chlorophyll from observed values (=SS dev model - obs) were determined by spreadsheet calculations. Degrees of freedom (d.f.) are the number of parameters in each model. The F-statistic was determined according to the equation:

$$\text{F-statistic} = \frac{(\text{SS dev model 1} - \text{SS dev model 2})/(\text{d.f. model 2} - \text{d.f. model 1})}{(\text{SS dev model 2}/\text{No. of obs} - \text{d.f. model 2})}$$

where model 1 and model 2 were designated such that model 1 has the higher sum of squared deviations of the model from the observed data. F-ratio analysis shows that the fit of Model D was significantly better than the fits of the other three models at $p = 0.001$, as the calculated F-statistics were all greater than the critical value of 56.18 (according to Table F, Moore & McCabe 1993).

Comparison	SS dev Model - Obs	Degrees of Freedom	No. of Observations	Calculated F-statistic	Significant at p=0.001?
Model D to Model A	2121 13224	4 2	48 48	150.3	yes
Model D to Model B	2121 184247	4 3	48 48	3778.19	yes
Model D to Model C	2121 41170	4 3	48 48	810.15	yes

were lost from the surface. This decline in cell numbers actually represents a minimum estimate of sinking losses, because cell division continues after the depletion of ambient nitrate (Fig. 2.5). The absence of a clearly defined relationship between cell numbers and nitrate disappearance precluded modeling cell numbers vs. time, so the exact contribution of sinking to losses from the tank must lie somewhere between the minimum estimation from cell count data (0.1 d^{-1}, according to a least squares regression negative exponential curve fit) and the maximum specific loss rate of 0.22 d^{-1} determined by the model fit to chlorophyll data.

2.4.2 Neutral buoyancy and sinking upon nitrate depletion

Nutrient-replete *Thalassiosira weissflogii* exhibited nearly-neutral buoyancy. There are at least three previous reports of neutral buoyancy in marine diatoms. In a similar experiment with a much larger tank, Strickland et al. (1969) observed neutral buoyancy during nitrate-replete growth of the relatively large (cell length approx. 40 μm) diatom, *Ditylum brightwellii*, but they did not run the experiment to complete exhaustion of nutrients. Eppley et al. (1967) noticed neutral buoyancy in *Thalassiosira weissflogii* under specific culture conditions, and though they suspected that a fraction of these cells were neutrally buoyant in nature, they did no further investigation of this buoyancy or of the effects of nutrient depletion on buoyancy. Takahashi and Bienfang (1983) found that natural populations of ultraplankton (size range < 3 μm) were neutrally buoyant, i.e. they had no measurable sinking rates. Both neutral and positive buoyancy have been reported for the large (>100 μm) diatoms *Rhizosolenia* and *Ethmodiscus* (Villareal 1988, Villareal 1992).

My observation of nearly-neutral buoyancy in nitrate-replete *Thalassiosira weissflogii* was based upon the interpretation of chlorophyll profiles derived from *in vivo* fluorescence, which were then used as a proxy for biomass distribution. Though I recognize the inherent variability in fluorescence per chlorophyll and in chlorophyll per cell

(as discussed above), cell counts done on surface samples agree with the pattern of biomass distribution inferred from chlorophyll profiles and I believe that these profiles are representative of changes in overall biomass distribution. However, one clarification is necessary: the conversion from fluorescence profiles to chlorophyll profiles was done using 3 to 5 direct chlorophyll measurements as calibration points, while values between these points were determined by linear interpolation. There was not always a surface sample taken for each profile, so apparent decreases in chlorophyll near the surface (see Fig. 2.6, for example) may be artifacts of extrapolating outside the range of measurements.

Thalassiosira weissflogii sank under nutrient-depleted conditions. It could be argued that sinking might have occurred at some critical concentration of biomass even if cells were not depleted of nutrients (Jackson 1990), however, the timing of the sinking response was consistent with changes in chemical composition (discussed in the next section) and with results previously reported in the literature. Much attention has been paid to the effects of nutrient depletion on cell sinking rate, though results in the literature are often contradictory. Steele and Yentsch (1960) recognized early that nutrient status and cell buoyancy are closely related. Their experiments with *Skeletonema costatum* showed that sinking rates increased when nutrients were depleted from culture medium, but that sinking rates of nutrient depleted cells decreased considerably when cells were re-enriched and placed in the dark. Later work that measured sinking rates of cells in relatively small columns (Bienfang 1981a) found that nitrate depletion caused either a decrease (Bienfang et al. 1982) or no significant change (Bienfang 1981b, Bienfang and Harrison 1984, Bienfang et al. 1986) in cell sinking rates, though sinking rate increases were seen in response to depletion of other nutrients like phosphate and silicate (e.g. Bienfang and Harrison 1984). More recent work on the dynamics of the sinking of spring blooms showed that termination and sinking of blooms occurred consistently at limiting nitrate concentrations (Waite et al. 1992a) and that *Thalassiosira* species were the most nutrient-

sensitive, that is, their sinking rates increased most dramatically upon nitrate depletion (Waite et al. 1992b).

Some generalizations can be made between apparently contradictory evidence in the literature. Measurements which found no significant change in cell sinking rate with nitrate depletion were often done on natural populations which included a variety of phytoplankton types (e.g. Bienfang 1981b, Bienfang and Harrison 1984), and all phytoplankton do not necessarily respond to nitrate depletion in the same way. There seems to be at least genus-specific differences in sensitivity to nitrate exhaustion (Waite et al. 1992a, b) as well as variation in sinking rates due to the pre-conditioning nutrient history of the population (Bienfang 1981b) and growth phase (Bienfang 1981c), so it is not surprising that there could be no obvious overall changes in sinking rates due to nutrient depletion. Different cells may react differently to nitrate depletion, but no change in the sinking rate of the population would be observed if sinking rates of mixed populations are measured using bulk biomass (not taxon specific) estimates such as total chlorophyll.

The early work of Steele and Yentsch (1960) involved experiments with a monospecific culture (as was mine), while the later work of Waite et al. (1992a,b) dealt with blooms composed of only a few genera of diatoms (dominated by *Thalassiosira aestivalis*). Species-specific changes in cell sinking rates, therefore, should be more obvious for the case of monospecific populations than for more diverse assemblages of phytoplankton As well, the termination of spring blooms due to nitrate exhaustion is similar to my "bloom" and its termination in the tank.

The sinking of cells from surface waters of the tank occurred some time after the depletion of ambient nitrate. Chlorophyll data indicated that this sinking commenced approximately 24-48 h after ambient nitrate depletion. Cell count data, however, show that the time scale for increased sinking was closer to 60 h. The time scale is likely underestimated by the chlorophyll data, as results from batch culture experiments and measured chlorophyll per cell during the tank experiment both show evidence of

chlorophyll degradation. The model using chlorophyll as the biomass parameter thus overestimates actual sinking losses, as discussed earlier. Batch culture experiments showed little change in carbohydrate:protein ratios for the first 30 h after ambient nitrate depletion, then ratios increased rapidly to the end of the nitrate-depleted phase of the experiment. This indicates, perhaps, that cells were responding to depletion of internal nitrogen pools rather than to prevailing concentrations of nitrate, though no measurements of internal pools were made.

There is some support for delayed sinking in the literature. Bienfang (1981b) cites pre-conditioning nutrient history as a possible explanation for why he found no significant relationship between ambient nutrient concentrations and sinking rates of heterogeneous phytoplankton populations. In direct contrast to my work, however, Waite et al. (1992a) found that initiation of sinking of a spring bloom occurred before complete exhaustion of ambient nitrate, at threshold levels between 1-2 μM. It is not clear why these results differ, though increased aggregation of cells under low nutrient conditions (Kiørboe et al. 1990) may have played a role. I noticed no aggregation of *Thalassiosira weissflogii* during microscopic examination of surface samples taken from the tank.

2.4.3 Increased intracellular density through unbalanced growth

It is instructive to ask why nutrient depleted cells sank from surface waters of the tank. Changes in cellular carbohydrate and protein during batch culture experiments could be responsible for changes in cell buoyancy observed during the tank experiment, so I performed calculations using literature values to determine how changes in carbohydrate and protein affect intracellular density of a model cell. Initial values of carbohydrate and protein per cell were taken from Myklestad (1974) for nutrient-replete cultures of *Thalassiosira fluviatilis* and were converted to carbohydrate per μm^3 cell volume and protein per μm^3 cell volume using cell volume data of Conover (1974) for the same

organism. Resulting concentrations were 2.0 x 10^{-7} μg $μm^{-3}$ and 1.2 x 10^{-7} μg $μm^{-3}$ for carbohydrate and protein, respectively.

The model cell was composed only of carbohydrate, protein, and sea water. The total carbon pool of the cell, therefore, was determined by the total amount of carbon contained in carbohydrate and protein, assuming that carbohydrate (as laminarin) was 44.4% carbon and protein was 50% carbon by weight (West and Todd 1963). Starting from initial values stated above, the weight of a 1 $μm^3$ volume was computed and expressed as density in units of $kg·m^{-3}$. For this calculation, the densities of carbohydrate and protein were assumed to be 1600 kg m^{-3} and 1300 kg m^{-3}, respectively (Oliver and Walsby 1984). The remainder of the 1 $μm^3$ volume was assumed to be occupied by sea water. I then varied both the partitioning of total carbon (between carbohydrate and protein) and the total carbon pool to determine concurrent changes in intracellular density. To convert changes in intracellular density to changes in sinking rate of the model cell, I applied the equivalent changes in density to a cell of 7.5 μm radius, and computed sinking rate from Stokes' law for a sphere (Eq. 2.1), assuming a sea water density of 1029 $kg·m^{-3}$ and a dynamic viscosity of 1.072x10^{-3} kg m^{-1} s^{-1} at 20°C (Vogel 1981).

The relationship between sinking rate and carbohydrate:protein ratio was examined for three cases (Fig. 2.9). For case 1, I assumed that the total carbon content of the cell remained constant, but that the partitioning of carbon between carbohydrate and protein changed. Total volume of the cell was kept constant. Potential variations in cell volume due to changes in relative amounts of carbohydrate and protein were countered by changes in cell water content. For case 2, I assumed that cell protein remained constant, but that carbohydrate could increase or decrease. As with case 1, changes in volume occupied by carbohydrate were balanced by changes in water content so that total volume of the cell remained constant. For case 3, cell protein was held constant, carbohydrate was allowed to fluctuate, and the cell was allowed to get larger or smaller. Maximum change in cell radius within the range of the model was ± 8%.

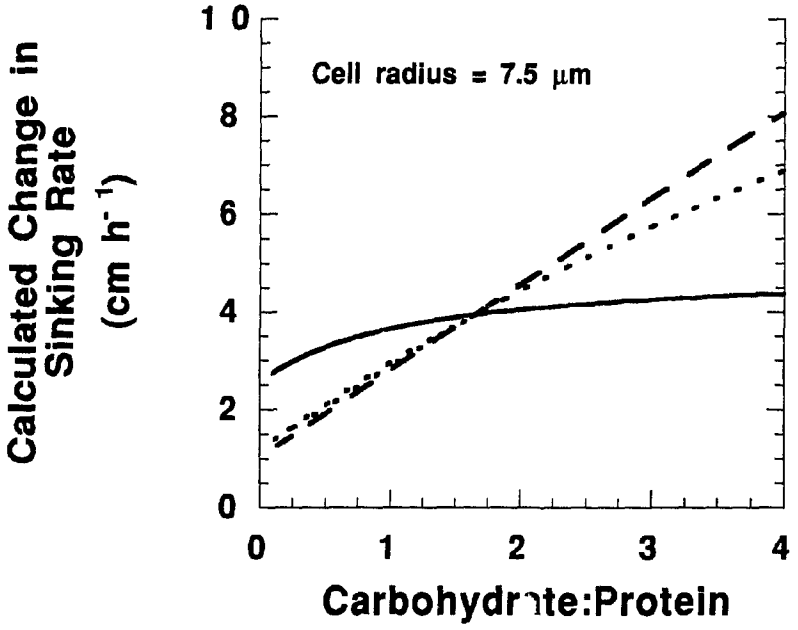

Figure 2.9: Model output of changes in sinking rate expected with concurrent changes in carbohydrate:protein ratio for a model cell of radius 7.5 µm (similar to the radius of *Thalassiosira weissflogii*). Solid line (—) shows expected sinking rate changes for a cell that keeps its total carbon content constant but shunts newly-acquired carbon into carbohydrate instead of protein (case 1). Dashed line (---) shows expected sinking rate changes if a cell increases its carbohydrate but keeps both its protein and cell volume constant (case 2). Dotted line (···) shows expected sinking rate changes if a cell increases its carbohydrate, keeps its protein constant, but gradually increases its overall cell volume (case 3).

Model calculations (Fig. 2.9) show that the smallest ballast-related changes in sinking speed would be experienced by a cell that keeps its total carbon content constant, and merely shunts carbon acquired under nitrogen depleted conditions into carbohydrate rather than protein. The greatest changes in cell sinking rate would be experienced by a cell that changes its cellular content of carbohydrate but keeps both its volume and its cellular content of protein constant. Intermediate between these values is the cell that changes its cellular carbohydrate and volume, but keeps its protein content constant. Over the course of nutrient depletion, that is, from carbohydrate:protein ratios of 0.1 to those of slightly less than 3.0, (the maximum range of carbohydrate:protein ratios determined during batch culture experiments, refer to Figure 2.7e), these cells could experience changes in cell sinking rates of up to 4.5 $cm \cdot h^{-1}$ or 1.1 $m \cdot d^{-1}$ (using Fig. 2.9). It would take approximately 60 h for these changes to occur, which agrees well with the range of time scales for increased sinking determined during the tank experiment. During batch culture experiments, reversal of carbohydrate:protein ratios was rapid. Within 24 h *after* nitrate was added back to the medium, carbohydrate:protein values decreased to 1.0 from a value close to 3.0 (using Fig. 2.7e), which could translate to a sinking rate decrease 2.8 cm h^{-1} or 0.7 m d^{-1} (using Fig. 2.9). Overall, these calculations indicate that increases in carbohydrate ballast alone could have caused the changes in cell buoyancy observed during growth of *Thalassiosira weissflogii* in the experimental water column.

Though batch culture experiments and modeling exercises showed that increases in intracellular carbohydrate due to nitrate depletion could have resulted in the changes in buoyancy observed during the tank experiment, our calculations assume that the cell is comprised only of carbohydrate, protein, and water. As this is untrue, calculated density changes and calculated sinking rates should be considered only as *relative* changes. They do not represent absolute values for cell sinking rates. True sinking rate of the cell will depend on many other factors, including silicification, ionic content, lipid content, and

morphological characteristics (see review by Smayda 1970). The model of density change which allowed cell volume to increase is the more ecologically-relevant, since cell volume tends to increase with growth of *Thalassiosira weissflogii* until cell division (Conover 1974).

Changes in intracellular density were calculated based only upon the measurement of carbohydrate as glucose equivalents which are detected by the phenol-sulphuric acid method. Any incorporation of carbon into storage products other than β-1,3-glucan was not measured and was not considered in our analysis. The incorporation of carbon into lipid, for example, would affect intracellular density as the density of lipid is much lower than that of carbohydrate and protein. This would affect cell sinking rate by counteracting increases in sinking rate due to accumulation of carbohydrate. The degree of accumulation of lipid under nitrogen stress varies with phytoplankton species between 10 and 40% of total ^{14}C incorporation (de Madariaga 1992).

2.4.4 Ecological consequences and biogeochemical implications of buoyancy changes and changes in chemical composition during unbalanced growth

I have shown that *Thalassiosira weissflogii* can be almost neutrally buoyant, and that its sinking rate can change significantly (perhaps by as much as 1 m d^{-1}) as the result of accumulation of carbohydrate through unbalanced growth. I have also shown that the chemical composition of *T. weissflogii* can revert rapidly upon exposure to nitrogen. These observations may have important ecological consequences. The model of Lande and Wood (1987) showed that cells whose sinking rates slowed under nutrient-replete conditions spend a substantially longer total time in the surface mixed layer because of greater probability of re-entrainment back into the mixed layer. I did *not* show that the rates of cells sinking from the surface of the tank slowed once they reached the nutrient gradient. Data from batch cultures, however, showed clearly that the physiology of these cells *is* plastic

enough to change intracellular density and thus permit fairly rapid buoyancy reversals. This would confer a distinct ecological advantage. According to the Lande and Wood (1987) model, nutrient-dependent buoyancy changes allow cells to be shuttled between the top of the nutricline (where there is low light but high nutrient concentrations) and shallower depths (where there is high light but low or no nutrients). Access to both high light and high concentrations of nutrients may result in greater overall levels of primary productivity and growth than if buoyancy changes were not possible.

The vertical movements of phytoplankton represent an input of nitrogen to the euphotic zone and are a form of new production as defined by Dugdale and Goering (1967). Because, in the dark, nitrate can be taken up without concurrent uptake of carbon (Terry 1982), cells will instead combine nutrients acquired at depth with carbon acquired in surface waters; that is, the processes of nutrient uptake and carbon uptake become uncoupled in space and time (Cullen 1985, Fraga et al. 1992). Thus, the input of nitrogen through vertical movements of cells is *not* coupled to the input of carbon in the Redfield ratio (Redfield 1958), as is the case for physically-transported dissolved nutrients (see Eppley and Peterson 1979). Since photosynthesis occurring in surface waters requires a carbon source, and since stoichiometric equivalents of carbon are not brought to the surface by cells in coupled transport with nitrogen, new production resulting from buoyancy-assisted uptake of nutrients could result in the net removal of carbon from oceanic surface waters which, in turn, could affect the air-sea exchange of carbon dioxide.

A clear example of the uncoupled movements of carbon and nitrogen due to vertical movements of phytoplankton was shown by Fraga et al. (1992) through their measurements of Broecker's parameters (Broecker 1974). These parameters, known as "NO", "CO", and "PO", are intended to be conservative properties that characterize water masses. If biochemical reactions in the water mass are occurring in Redfield proportions, each of Broecker's parameters will be constant with depth. During a red tide of the dinoflagellate *Gymnodinium catenatum*, however, Fraga et al. (1992) found distinct

vertical differences in their measurements of Broecker's parameters indicating that biochemical reactions in the water mass were not occurring in Redfield ratios. They attributed these deviations to vertical migrations by the dinoflagellates, whereby carbohydrate synthesis at the surface and nutrient uptake at depth resulted in a carbon deficit near the surface and a nitrogen deficit below.

The ecological consequences of uncoupled carbon and nitrogen uptake have been outlined previously by Goldman et al. (1992). Similar to my observations during batch culture experiments with *Thalassiosira weissflogii*, Goldman et al. found uncoupling between photosynthesis and nutrient uptake in cultures of the diatom *Stephanopyxis palmeriana*. Carbon accumulation continued well into stationary phase of the growth of this diatom, long after nutrients were depleted from the growth medium. Though C:N uptake ratios during exponential (nutrient-replete) growth were in Redfield proportions (approximately 6:1), large deviations from Redfield stoichiometry occurred during the nutrient-depleted period of carbon accumulation (to C:N ratios of 12:1). These observations are not restricted to laboratory experiments: removal of carbon from nutrient depleted waters of the North Atlantic has been noted by Sambrotto et al. (1993) and Michaels et al. (1994). Goldman et al. (1992) point out the ecological consequences of unbalanced growth: the conventional definition of new production assumes that the flux of particulate organic carbon (POC) as new production can be calculated by multiplying new production as particulate organic nitrogen (PON) by the Redfield ratio of 6.6 (by atoms). It assumes a balance between the input of nutrients to the euphotic zone and the flux of organic matter to the deep ocean, even over short time scales. If, however, C:N ratios are higher due to excess carbon accumulation during unbalanced growth, then the conventional definition of new production must be revised. By failing to consider the continuation of photosynthesis by some phytoplankton species after nutrient depletion, estimates of new production could be grossly underestimated (Goldman et al. 1992).

Goldman et al. (1992) also recognized the potential contributions of excess carbon accumulation to increased sinking speed of cells. In their study, nutrient depleted cells formed highly condensed gelatinous masses, probably as the result of cellular excretion of complex heteropolysaccharides. Aggregation of these cells into large masses, and their subsequently high sinking speeds, would lead to direct export of cells from the euphotic zone with minimal losses to grazing. The loss of "photosynthetically heavy" cells from the euphotic zone, however, is not necessarily an irreversible process. As I have shown by my batch culture experiments with *Thalassiosira weissflogii*, cells that have been accumulating carbon during unbalanced growth have the capacity to respond rapidly to increased nutrients, even after fairly long periods of nutrient deficiency (in this case up to 3 d). Rather than considering unbalanced growth and sinking as a one way process, then, perhaps the process should be viewed as a cycle. That is, carbon accumulation provides adequate ballast to increase sinking speed, but the recovery from nutrient deficiency (perhaps to return to a state of increased buoyancy) allows cells to more easily *return* to the well-lit waters of the euphotic zone. The observed recovery of cells from nutrient deficiency also lends support to the purported ability of cells to migrate vertically in nature (Villareal et al. 1993).

Thus, changes in cell buoyancy may be viewed as inherent consequences of cell physiology. The increase in cellular excess density provided by carbohydrate as the result of unbalanced growth followed by slowing of sinking rate due to uptake of nutrients and the use of stored carbohydrate is, in effect, a built-in buoyancy regulating mechanism. Rapid increases of cell sinking rate upon nutrient depletion, and rapid returns to increased buoyancy when nutrient replete may represent an ecological adaptation to environments where light and nutrients are spatially-separated.

Chapter 3

Physiological properties of *Rhizosolenia formosa* in the context of open ocean vertical migration

3.1 Introduction

Large diatoms of the genus *Rhizosolenia* (cell volumes up to 10^7 μm^3) are commonly found in open ocean ecosystems such as the Sargasso Sea (Carpenter et al. 1977, Villareal 1988, Villareal and Lipschultz 1995), the Caribbean (Carpenter et al. 1977, Villareal 1988), the Eastern Pacific Ocean (Alldredge and Silver 1982, Martinez et al. 1983) and the Central North Pacific Gyre (Villareal and Carpenter 1989, Villareal et al. 1993). *Rhizosolenia* cells can be solitary, or can exist in the form of chains, multi-species mats, or rafts (Venrick 1974, Villareal and Carpenter 1989) and can be both positively and negatively buoyant (Villareal 1988, Villareal and Carpenter 1989). Mats of *Rhizosolenia*, for example, can ascend at average rates of 3.6 m h^{-1} (Villareal and Carpenter 1989). Observations of pronounced changes in its buoyancy state first led to the hypothesis that *Rhizosolenia* may undergo vertical migrations in nature (Villareal and Carpenter 1989), similar to migrations of dinoflagellates (Heaney and Eppley 1981, Cullen 1985, Watanabe et al. 1991). Later evidence strongly supported this hypothesis: particulate nitrogen of *Rhizosolenia* collected in nitrate-depleted surface waters of the Central North Pacific Gyre contained $\delta^{15}N$ signatures (i.e., ratios of the natural abundance of stable isotopes of N)

characteristic of cells that had exploited deep water sources of nitrate (Villareal et al. 1993). As well, positively buoyant *Rhizosolenia* had significantly higher internal nitrate concentrations than sinking cells, consistent with vertical movements between surface and deep (>100 m) waters (Villareal et al. 1993, Villareal and Lipschultz 1995). Vertical migrations to deep sources of nutrients gives cells a distinct ecological advantage in areas such as the Central North Pacific Gyre, where nitrate does not become available until well below the euphotic zone (e.g. Hayward 1991). Access to both saturating irradiance at the surface and high concentrations of nutrients at depth may result in greater overall levels of primary productivity and growth than if migrations were not possible (Gran 1929), and may explain the relative success of large phytoplankton in areas otherwise dominated by picoplankton and highly regenerative food webs. The importance of large phytoplankton in open ocean regions is becoming better-recognized (Sancetta et al. 1991, Goldman et al. 1992, Goldman 1993) and has led to hypotheses about their potential roles in biogeochemical cycling (Goldman et al. 1992, Villareal et al. 1993) and in the air-sea exchange of carbon dioxide (Yoder et al. 1994).

Migrating phytoplankton may have significant effects on water column chemistry through their influence on the cycling of nutrients like carbon, nitrogen, phosphorus, and oxygen (Fraga et al. 1992). When nitrate is taken up at depth and transported to the euphotic zone by vertical movements of phytoplankton, the resulting growth represents a form of new production as defined by Dugdale and Goering 1967 (Moore 1994, Richardson and Cullen 1995). Further, in many oceanic regimes, the top of the nutricline is below the euphotic zone (see Hayward 1991) so uptake of nitrate will occur in the dark without accompanying uptake of carbon (see Terry 1982). Cells will instead combine nutrients acquired at depth with carbon acquired in surface waters; that is, the processes of nutrient uptake and carbon uptake become uncoupled in space and time (Cullen 1985, Fraga et al. 1992). Thus, the input of nitrogen through the vertical movements of cells is not coupled to the input of carbon in the Redfield ratio (Redfield 1958) as is the case for

physically-transported dissolved nutrients (see Eppley and Peterson 1979). Because photosynthesis occurring in surface waters requires a carbon source, and since stoichiometric equivalents of carbon are not brought to the surface in coupled transport with nitrogen, new production resulting from vertical movements of phytoplankton could result in the net removal of carbon from oceanic surface waters if migrating organisms are in sufficient concentrations. This, in turn, could affect the air-sea exchange of carbon dioxide (Richardson and Cullen 1995).

When this work was initiated, evidence supporting purported vertical migrations of *Rhizosolenia* had been collected mainly from field experiments; relatively little work had been done in the laboratory. Accordingly, laboratory experiments using cultures of *Rhizosolenia formosa* were performed to determine whether physiological characteristics of this large diatom were consistent with the ability to migrate vertically in the open ocean. Time-course experiments examined changes in chemical composition and buoyancy during nitrate (N)-replete growth, N-starvation and after re-introduction of N to culture medium in order to simulate conditions that would be experienced by cells migrating in nature. Nitrate uptake rates were determined for batch cultures under varied conditions of light and nutrients. Photosynthesis vs. irradiance (P-I) measurements under N-replete and N-depleted conditions were used to determine whether the photosynthetic capabilities of *R. formosa* show adaptations consistent with vertical migrations in nature. Determination of rates of carbon and nitrate uptake are also necessary first steps towards examining potential larger-scale effects of *Rhizosolenia* on biogeochemical cycling.

3.2 Methods

3.2.1 Culture conditions.

Unialgal cultures of the marine diatom *Rhizosolenia formosa* (Clone B8, isolated from the Sargasso Sea near Bermuda in August 1992 by T.A. Villareal) were grown in 4 l

glass Erlenmeyer flasks containing 3 l of MET-44 medium (Schöne and Schöne 1982), with trace metals and vitamins adjusted to K/20 and K medium concentrations, respectively (Keller et al. 1987). The medium was filter-sterilized using a 0.2 μm Culture Capsule filter (Gelman Sciences, Ann Arbor, Michigan). Cells were grown at 20°C, on a 14:10 h L:D cycle with illumination provided from the side by 5 Cool-White fluorescent lamps. Two layers of blue LEE gel filters (#061) separated the lamps and culture containers, giving a quantum scalar irradiance of approximately 50 μmol quanta m^{-2} s^{-1} (photosynthetically active radiation, PAR) as measured with a Biospherical Instruments QSL-100 4π sensor placed just outside the culture containers.

Large diatoms are notoriously difficult to culture (Goldman 1993). Members of the genus *Rhizosolenia,* in particular, are fragile and very sensitive to disturbance. Growth rates are reduced significantly and often cultures do not survive when routine (i.e. frequent) sampling procedures are used. All experiments in this study were constrained by the frequency with which cells could be sampled (every 3 d or so at best). Ambient nitrate could be measured more frequently, as cultures could be sampled gently and thorough mixing (to obtain an evenly dispersed sample of cells) was not required.

3.2.2 Chemical composition time-course experiment

A time-course experiment was conducted to examine changes in chemical composition of *Rhizosolenia formosa* during N-replete growth and N-starvation. Six 3 l cultures of *R. formosa* were grown as described above, but nitrate was adjusted to an initial concentration of 10 μM. Samples for chlorophyll, cell counts, particulate carbon and nitrogen, carbohydrate, protein, and ambient nitrate were taken initially, at one time point before N-depletion, and at one time point after N-depletion. Ambient nitrate was monitored more frequently to determine approximate time of N-depletion. Once ambient nitrate was exhausted, the six cultures were divided into three groups of two. Duplicate cultures were left for 24 h, 30 h, or 53 h without nitrate, after which nitrate was re-introduced to the

culture medium to a final concentration of approximately 15 µM. Cells were left for a further 24 h to allow for incorporation of nitrate before the final samples were taken. Chlorophyll *a*, corrected for phaeopigment, was determined fluorometrically using a Turner Designs model 005R fluorometer calibrated with pure chlorophyll *a* (Sigma Chemical Co., St. Louis, MO, USA). Samples were collected in triplicate on Whatman GF/C filters and were extracted in 10 ml of 90% acetone in the dark for at least 24 h at -10°C. Cell counts were done with an inverted microscope on cells preserved with acid Lugol's solution (Throndsen 1978). Ambient nitrate was determined with a Technicon Autoanalyzer II on GF/C-filtered samples. Particulate carbon and nitrogen were determined using a Perkin-Elmer 2400 CHN Analyzer on material collected on precombusted GF/C filters. Precombusted GF/C filters were used as blanks; acetanilide was used as a calibration standard. Carbohydrate was determined as glucose equivalents by the phenol-sulfuric acid method (Dubois et al. 1956), and protein was analyzed by the heated biuret-folin method (Dorsey et al. 1978) using bovine serum albumin (BSA) as a standard. Since protein measurements were inconsistent with measurements of particulate nitrogen and uptake of inorganic nitrogen, BSA standard curves were scaled by measurements of particulate nitrogen using the assumptions of Dorsey et al. (1978) assuming that protein is 16% nitrogen by weight (West and Todd 1963). Growth rate of *Rhizosolenia formosa* was determined by non-linear least squares regression analysis of a negative exponential curve fit to changes in ambient nitrate with time. Similarly, growth rates based on increases in particulate nitrogen, particulate carbon, and chlorophyll were estimated from data points before depletion of ambient nitrate from culture medium.

3.2.3 Buoyancy time-course experiment

A time-course experiment was conducted to determine whether changes in chemical composition might affect cell buoyancy. Triplicate 3 l cultures of *Rhizosolenia formosa* were grown as described above, with initial nitrate adjusted to 10 µM. Samples for

particulate carbon and nitrogen analyses and ambient nitrate were taken initially, at one time point before N-depletion and at two time points after N-depletion (which was at least 48 h after cells exhausted the ambient nitrate). Cell buoyancy measurements (described below) were done on cells before and after N-depletion; measurements done on cells before N-depletion were done at mid-day, those on N-depleted cells were done just before the end of the normal photoperiod (20:00). At the end of the photoperiod, nitrate (final concentration 40 μM) was added back to culture medium and cells were placed immediately in darkness overnight to allow for incorporation of nitrate. Cell buoyancy measurements and sampling for particulate carbon and nitrogen analyses were repeated after re-introduction of N to culture medium, once prior to the normal photoperiod (07:00) and once near the end of the photoperiod (19:00).

Cell buoyancy was determined by placing an evenly mixed sample from each culture into one of three sinking columns (each with a total volume of 420 ml) as described by Bienfang (1981a). Each column was surrounded by a water jacket through which 20°C water was circulated from a water bath. This ensured that the columns remained isothermal to minimize convection (see Bienfang 1981a). Cells were allowed to settle for 1 h, during which time they separated into three arbitrarily-defined fractions: the top 70 ml, the middle 265 ml, and the bottom 85 ml of each column. The volume of each fraction was determined by the location of sampling ports. Cell buoyancy measurements on N-replete and N-depleted cells were done with columns illuminated from the side by 2 Cool-White fluorescent lamps. One blue LEE gel filter (#061) separated the lamps from the columns, resulting in an irradiance of 50 μmol quanta m^{-2} s^{-1} PAR. Buoyancy measurements on cells after re-addition of nitrate were done either in the dark (for measurements prior to the photoperiod) or with columns illuminated as described above (for measurements at the end of the photoperiod). The percentage of cells in the top, middle, and bottom fractions of each sinking column was expressed as a percentage of the total population by dividing the number of cells in each fraction by the total number of cells in the column multiplied by

100. The number of cells in each fraction was determined from cell count data; the average number of cells from triplicate determinations was multiplied by the total volume of water in that fraction.

The sinking velocity of negatively buoyant cells was calculated from average changes in the percentage of cells in the top fraction of the columns over the 1 h incubation, as follows. The top fraction represents 17% of the total volume of the column. Assuming that cells are uniformly distributed after being mixed and placed into each column, 17% of the cells should be found in the top fraction. The change in the percentage of cells, i.e. the initial percentage minus the percentage in the top fraction after the 1 h incubation, was expressed as a fraction of the initial 17%, resulting in a specific loss rate (h^{-1}). This was then multiplied by the height of the top fraction of the column (0.1 m) giving the sinking velocity of the negatively buoyant portion of the population. This sinking velocity may be underestimated to the extent that cells from below rise into the upper fraction.

3.2.4 Nitrate uptake experiments

Nitrate uptake rates were determined for triplicate cultures of N-replete and N-depleted cells, both in the dark and in the light. Nitrate concentrations were determined as described above. For dark nitrate uptake experiments, disappearance of nitrate was calculated for an overnight incubation of triplicate cultures of both N-replete and N-depleted *Rhizosolenia formosa*. For N-replete cells (nitrate =30 μM) samples for ambient nitrate, cell counts, and particulate carbon and nitrogen were taken from exponential phase cultures at the beginning of the dark period of the normal L:D cycle. From the same cultures sampled initially, identical post-incubation samples were taken at the end of the dark cycle (before lights-on), approximately 10 h later. Exact incubation time was calculated as the time from lights-off in the culture room to the time of filtration of each culture. All culture containers were covered with black plastic bags to exclude light until samples were filtered. Cell counts and particulate carbon and nitrogen analyses were as described above.

For N-depleted cells (nitrate < 0.5 μM for 24 h before the experiment), samples for ambient nitrate, cell counts, and particulate carbon and nitrogen analyses were taken from exponential phase cultures at the beginning of the dark period of the normal L:D cycle. Nitrate (5 μM) was added to each culture, a sample for ambient nitrate was taken, and cells were incubated overnight (approximately 10 h). Post-incubation samples for ambient nitrate, cell counts, and particulate carbon and nitrogen analyses were taken just before the end of the dark period, and incubation time was calculated as described above for N-replete cells. Nitrate was never fully depleted by the end of the incubation period. Cell counts and particulate carbon and nitrogen analyses were done as described above.

For determination of nitrate uptake rates in the light, disappearance of nitrate was calculated for incubations N-replete and N-depleted cells incubated during the light phase of the normal L:D cycle. Initial samples for ambient nitrate, chlorophyll, cell counts, and particulate carbon and nitrogen analyses were taken just before lights-on, then identical post-incubation samples were taken just before lights-off (approximately 14 h later). Nitrate was added to N-depleted cells as described above. Statistical analysis of all nitrate uptake data was done by a two-way analysis of variance (ANOVA) using SYSTAT for Macintosh version 5.2.1.

3.2.5 Photosynthesis vs. Irradiance

A modified method of Lewis and Smith (1983) was used to measure photosynthesis as a function of irradiance (P-I) in cultures of *Rhizosolenia formosa* grown as described above. Samples of 400 ml were inoculated with ^{14}C-bicarbonate (final radioactivity was 0.01 μCi ml^{-1}) and 36 aliquots of 10 ml each were dispensed into 20 ml capacity glass scintillation vials. Total ^{14}C in each sample was determined by subsampling 50 μl into scintillation vials containing 10 ml of Ecolume fluor and 500 μl of phenylethylamine. Phenylethylamine reacts rapidly with CO_2 to form carbamates which are stable in liquid scintillation cocktails, thereby avoiding the problem of losing labeled

inorganic carbon from acidic (pH ~ 6.0) fluor (Iverson et al. 1976). A range of irradiances was provided from below with four 250 W ENH tungsten-halogen projection lamps directed through a heat filter of circulating water, and attenuated with a range of neutral density screens and a blue LEE # 061 gel filter. Irradiance in each position was measured with a Biospherical Instruments QSL-100 4π sensor inserted into an empty scintillation vial. Inoculation and sub-sampling were conducted in very low light, and three time-zero aliquots were taken for each experiment. Time-zero samples were 10 ml of labeled culture added to scintillation vials containing 500 µl of buffered formalin. Incubations began within 15 min of ^{14}C inoculation, and were terminated after 45 min by the addition of 500 µl of formalin to each vial. Temperature during the incubations was held at $20 \pm 0.5°C$ and was kept constant with a circulating water bath. Dissolved inorganic carbon was driven off by adding 1 ml of 6 M HCl and agitating the open vials for at least 4 h (usually overnight) in a fume hood. Ten ml of Ecolume fluor were added to each vial, each vial was mixed vigorously, and vials were allowed to sit overnight before counting with a Beckman LS 3801 Liquid Scintillation Counter. The H# method was used to correct counts for quenching. Total dissolved inorganic carbon was assumed to be 2.2 mM and no correction for isotope discrimination was made.

Triplicate P-I curves were determined for each of triplicate cultures of both N-replete and N-depleted cells, with the exception of one culture of N-replete cells for which only two P-I curves were determined. Nitrate-replete cultures had approximately 30 µM ambient nitrate, while N-depleted cultures had less than 0.5 µM nitrate for at least 48 h prior to the experiment (determined by frequent monitoring of ambient nitrate near to N-depletion). Chemical composition of cultures used for P-I experiments is summarized in Table 3.1. Ambient nitrate, particulate carbon and nitrogen, and cell counts were determined as described above. Chlorophyll was determined spectrophotometrically, as described by Richardson et al. (1996).

Results were modeled using the equation of Platt et al. (1980):

Table 3.1: Chemical composition of N-replete (NR) and N-depleted (ND) *Rhizosolenia formosa* used for P-I experiments. Values are averages ± standard errors. Initial concentration of nitrate in culture medium was 40 µM for NR cultures and 10 µM for ND cultures.

Culture	Nitrate (µM)	Chl (mg m^{-3})	Cell counts (cells l^{-1})	POC (mg m^{-3})	PON (mg m^{-3})	C:N (g:g)	C:Chl (g:g)	Cell volume (x 10^6 μm^3)
NR	27.4 ± 0.8	12.2 ± 0.3	24 200 ± 870	1 200 ± 74	200 ± 17	6.0	99	4.0 ± 0.6
NR	28.8 ± 1.1	12.6 ± 0.4	26 800 ± 3350	1 130 ± 50	200 ± 12	5.5	89	4.0 ± 1.1
NR	28.9 ± 1.1	12.1 ± 0.5	21 900 ± 2200	1 190 ± 41	200 ± 8	5.9	98	3.8 ± 0.6
Avg ± s.e.	**28.4 ± 0.5**	**12.3 ± 0.2**	**24 300 ± 1400**	**1 170 ± 23**	**200 ± 1**	**5.8 ± 0.1**	**95 ± 3.0**	**3.9 ± 0.1**
ND	0.14 ± 0	6.8 ± 1	22 900 ± 900	1 100 ± 110	110 ± 5	10.3	162	5.0 ± 0.8
ND	0.17 ± 0	7.4 ± 0.1	21 100 ± 1700	1 100 ± 23	100 ± 5	11.6	155	4.4 ± 0.7
ND	0.21 ± 0	9.9 ± 1	22 400 ± 750	1 400 ± 36	110 ± 9	12.2	136	4.2 ± 0.8
Avg ± s.e.	**0.17 ± 0**	**8.0 ± 1**	**22 105 ± 520**	**1 200 ± 77**	**110 ± 4**	**11 ± 1**	**150 ± 8**	**4.5 ± 0.2**

$$P^B = P_s^B\left(1 - e^{\left(-\alpha I/P_s^B\right)}\right)\left(e^{\left(-\beta I/P_s^B\right)}\right) \quad (3.1)$$

where P^B is the rate of photosynthesis normalized to chlorophyll (g C g Chl^{-1} h^{-1}), $P^B{}_s$ is the maximum rate of photosynthesis in the absence of photoinhibition (g C g Chl^{-1} h^{-1}), I is irradiance (µmol quanta m^{-2} s^{-1}), α is the initial slope of the P-I curve (g C g Chl^{-1} h^{-1} (µmol quanta m^{-2} $s^{-1})^{-1}$), and β is a parameter which characterizes photoinhibition (g C g Chl^{-1} h^{-1} (µmol quanta m^{-2} $s^{-1})^{-1}$). These parameters are included in the list of symbols for this chapter (Table 3.2). Curves were fitted to P-I data using a least-squares nonlinear curve-fitting routine in Kaleidagraph for Macintosh, version 3.0.1, which uses a Levenberg-Marquardt algorithm. For fitting the data, the intercept, P_0 (g C g Chl^{-1} h^{-1}), was included as a parameter. The inclusion of P_0 means that the curve is not forced through a zero intercept, resulting in an increase in the variability explained and an improvement in the distribution of residuals. Values for $P^B{}_{max}$, the realized maximum rate of photosynthesis, and I_k, the conventional index of light saturation (Talling 1957), were calculated using the method of Platt et al. (1980) from values of $P^B{}_s$, α, and β determined by curve fitting. Statistical analyses of differences between N-replete and N-depleted cultures were done by Student's t-test for difference of means (Sokal and Rohlf 1981).

3.3 Results

3.3.1 Chemical composition time-course experiment

During N-replete growth, the six cultures of *Rhizosolenia formosa* reached chlorophyll concentrations of 6.7 to 9.1 mg m^{-3} (Fig. 3.1a) and cell concentrations of

Table 3.2: List of symbols and definitions for Chapter 3.

Symbol	Definition	Value	Units
Chl	Chlorophyll	variable	g
C	Carbon	variable	g
N	Nitrogen	variable	g
P	Photosynthesis	variable	g C g Chl h^{-1}
I	Irradiance	variable	µmol quanta m^{-2} s^{-1}
PAR	Photosynthetically available radiation	variable	µmol quanta m^{-2} s^{-1}
P^B	Photosyntheic rate	variable	g C g Chl h^{-1}
P^B_{max}	Maximum realized rate of photosynthesis	variable	g C g Chl h^{-1}
P^B_s	Potential rate of photosynthesis	variable	g C g Chl h^{-1}
α	Initial slope of the P-I curve	variable	g C g Chl^{-1} h^{-1} (µmol quanta m^{-2} s^{-1})$^{-1}$
β	Photoinhibition parameter	variable	g C g Chl^{-1} h^{-1} (µmol quanta m^{-2} s^{-1})$^{-1}$
P_o	Intercept of P-I curve	variable	g C g Chl^{-1} h^{-1}
I_k	Irradiance where P is maximal	variable	µmol quanta m^{-2} s^{-1}
N_{top}	Cells in top fraction of sinking column	variable	cells
N_{mid}	Cells in middle fraction of column	variable	cells
N_{bott}	Cells in bottom fraction of column	variable	cells
C_o	Initial concentration of cells in column	4	cells ml^{-1}
V	Total volume of sinking column	420	ml
Fl	Fraction of rising cells	variable	dimensionless
Si	Fraction of sinking cells	variable	dimensionless
P	Significance level		dimensionless

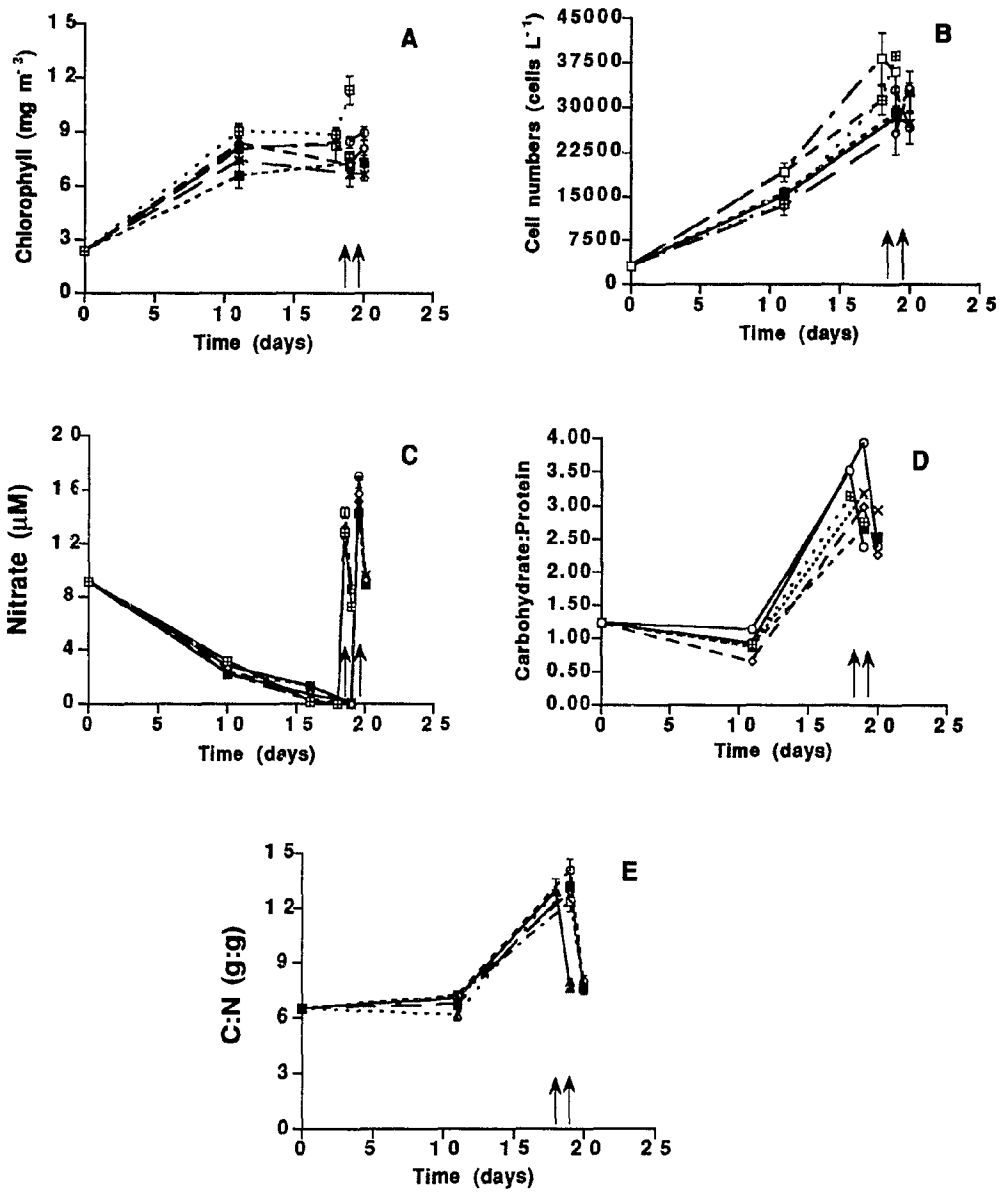

Figure 3.1: Time-course measurements of A) chlorophyll, B) cell numbers, C) nitrate, D) carbohydrate:protein, and E) C:N ratio for cultures of *Rhizosolenia formosa*. Different symbols represent replicate cultures. Error bars represent standard errors of triplicate measurements for each culture. Arrows indicates times at which nitrate was re-introduced into the medium (varied with culture).

15 000-20 000 cells l^{-1} after 11 days from initial conditions of approximately 9 μM nitrate and 2 mg m^{-3} chlorophyll (Fig. 3.1b). Cells divided at least once after the sampling on Day 11, reaching concentrations of 25 000-30 000 cells l^{-1} by Day 18 (Fig. 3.1b). Growth rate determined by disappearance of nitrate from culture medium was 0.14 d^{-1}. The estimated growth rate of *R. formosa* based on chlorophyll measurements during the N-replete phase of growth was 0.10 d^{-1}, while similar rates of increase of 0.14 d^{-1} and 0.10 d^{-1} were estimated from increases in particulate nitrogen and particulate carbon, respectively, over the N-replete portion of the experiment.

Depending on the culture, nitrate was depleted from the medium between Days 16 and 18 (Fig. 3.1c). After depletion of nitrate, cellular chemical composition changed noticeably. The ratio of C:Chl increased from an average value of 120 (g:g) for N-replete cells to 200 after depletion of ambient nitrate (Table 3.3). Carbohydrate ml^{-1} of culture increased and protein, on average, stayed constant during the N-depleted phase of the experiment (Table 3.3). Thus, carboyhydrate:protein ratios increased from pre-depletion values of 1.0 to values between 3 and 4 (Fig. 3.1d), while C:N (g:g) changed from values of just above 6 to values close to 13 (g:g) (Fig. 3.1e).

Cultures were allowed to go between 24 h and 53 h without nitrate. After each nitrate-depleted phase, cultures were re-enriched with nitrate to concentrations of approximately 15 μM. Within 24 h, ambient nitrate had once again decreased by between 5.2 μM and 7.7 μM (Fig. 3.1c). In most cultures, carbohydrate ml^{-1} of culture decreased and protein ml^{-1} of culture increased after re-introduction of nitrate to the medium. As a result, the observed increases in carbohydrate:protein, C:Chl, and C:N during N-depleted growth reverted, with average values tending towards pre-depletion values independent of the amount of time that cells were left without nitrate (Fig. 3.1d and 3.1e).

Table 3.3: Ambient nitrate concentrations and chemical composition of *Rhizosolenia formosa* before and after depletion of nitrate and after re-introduction of nitrate to culture medium. N-replete cells are those sampled at the pre-depletion point (Day 11) in the time-course experiment. N-depleted cells were sampled after 24 h (Cultures A and B), 53 h (Cultures B and C), or 30 h (Cultures E and F) without ambient nitrate. Carbos refers to carbohydrate concentration ($\mu g\ ml^{-1}$).

	Culture	A	B	C	D	E	F	Overall Avg± s.e.
N-repl	C:Chl (g:g)	161	146	115	109	77	109	120±17
	Carbos ($\mu g\ ml^{-1}$)	0.6±0.1	0.6±0.2	0.6±0.2	0.5±0.2	0.6±0.3	0.8±0.3	0.6±0.1
	Protein ($\mu g\ ml^{-1}$)	0.69± 0.04	0.73± 0.04	0.71± 0.03	0.8± 0.02	0.67± 0.02	0.72± 0.09	0.72± 0.03
N-depl	C:Chl (g:g)	179	201	221	226	171	199	200±13
	Carbos ($\mu g\ ml^{-1}$)	2.1±0.5	2.1±.3	2.4±.3	2.3±.5	2.4±.3	2.2±.7	2.3±0.1
	Protein ($\mu g\ ml^{-1}$)	0.55± 0.07	0.73± 0.06	0.76± 0.02	0.76± 0.07	0.69± 0.03	0.73± 0.08	0.7± 0.05
N re-add	C:Chl (g:g)	167	197	208	195	146	190	183±13
	Carbos ($\mu g\ ml^{-1}$)	1.8±0.2	1.7±0.2	1.7±0.3	1.9±0.3	2.3±0.3	2.0±0.4	2±0.1
	Protein ($\mu g\ ml^{-1}$)	0.76± 0.01	0.73± 0.05	0.57± 0.02	0.82± 0.04	0.84± 0.08	0.9± 0.02	0.77± 0.07

3.3.2 Changes in buoyancy with N status

For N-replete cells, an average of 11 ± 2% of cells were found in the top fraction (Fig. 3.2a), 44 ± 1% of cells were found in the middle fraction (Fig. 3.2b), and 44 ± 3% of cells were found in the bottom fraction of the settling column (Fig. 3.2c) after the 1 h incubation. After N-depletion, the percentage of cells found in the top fraction decreased to 4 ± 0.3% (Fig. 3.2a) and the percentage of cells found in the middle fraction decreased to 17 ± 4% (Fig. 3.2b), while the percentage of cells in the bottom fraction increased to 79 ± 4%. Twelve hours after re-addition of N to culture medium, the percentage of cells in the top fraction of the column increased (compared to values for N-depleted cells) to 9 ± 0.6% (Fig. 3.2a); there were correspondingly small (but detectable) decreases in the percentage of cells in the bottom fraction to values of 73 ± 4% (Fig. 3.2c). Twenty four hours after N-readdition, at the end of the photoperiod, the percentage of cells in the top fraction (8 ± 1%) was still greater than for N-depleted cells, while the percentage of cells in the bottom fraction had decreased further to average values of 70 ± 3%. Regardless of nitrate status, visual inspection showed that essentially all cells found in the top fraction of the settling column after the 1 h incubation were found in the top 2.5 ml of the 70 ml total volume. That is, the cells were concentrated against the top surface of the settling column rather than being dispersed throughout the entire top fraction.

The average sinking velocity of cells sinking from the top fraction of the column was 0.04 m h^{-1} when cells were N-replete, but this increased to 0.08 m h^{-1} when cells became N-depleted (Table 3.4). After N re-supply, sinking velocities slowed to 0.05 m h^{-1} for measurements done both in the dark and in the light. Increased and decreased sinking velocities were consistent with increased and decreased C:N ratios (Fig. 3.3). It should be noted that these sinking velocities are minimum estimates as they are a function of the height of the column over which the calculation is performed.

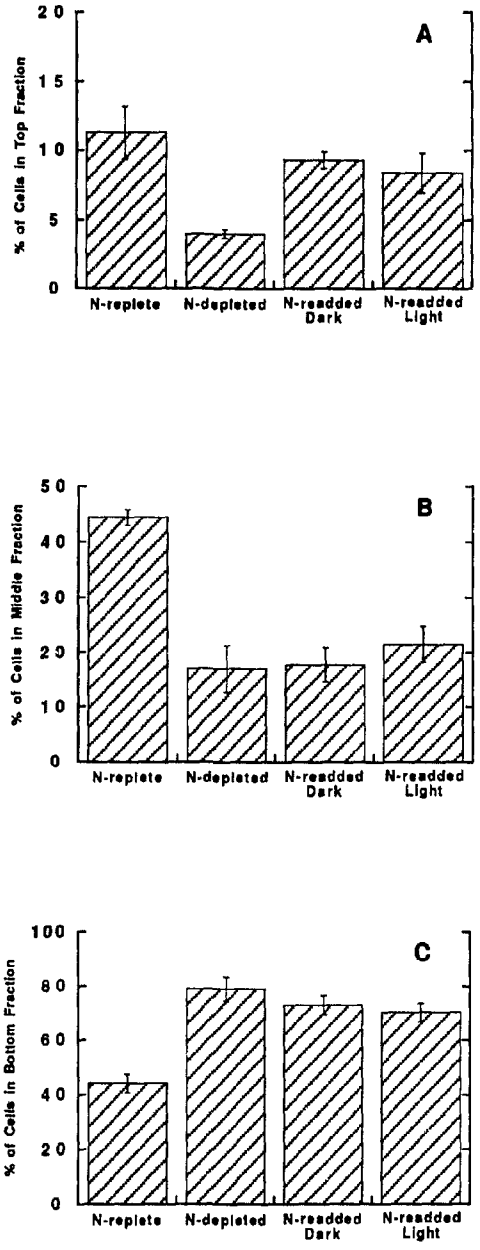

Figure 3.2: The percentage of nitrate-replete, nitrate-depleted, and nitrate-resupplied cells found in the A) top, B) middle, and C) bottom fractions of settling columns. Note that the axes are scaled differently to reflect differences between treatments.

Table 3.4: Calculation of minimum estimates of sinking velocities of negatively buoyant *Rhizosolenia formosa* with variations in N status.

Treatment	Initial % of total cells in top fraction (A)	% present after 1 h (B)	% Change (A-B=C)	Specific loss rate (h^{-1}) (C/A)	Depth of top fraction (m) (D)	Sinking velocity ($m\ h^{-1}$) (D x C/A)
N-replete	17	11	6	0.35	0.1	0.04
N-depleted	17	4	13	0.76	0.1	0.08
N re-supplied Dark	17	9	8	0.47	0.1	0.05
N re-supplied Light	17	8	9	0.52	0.1	0.05

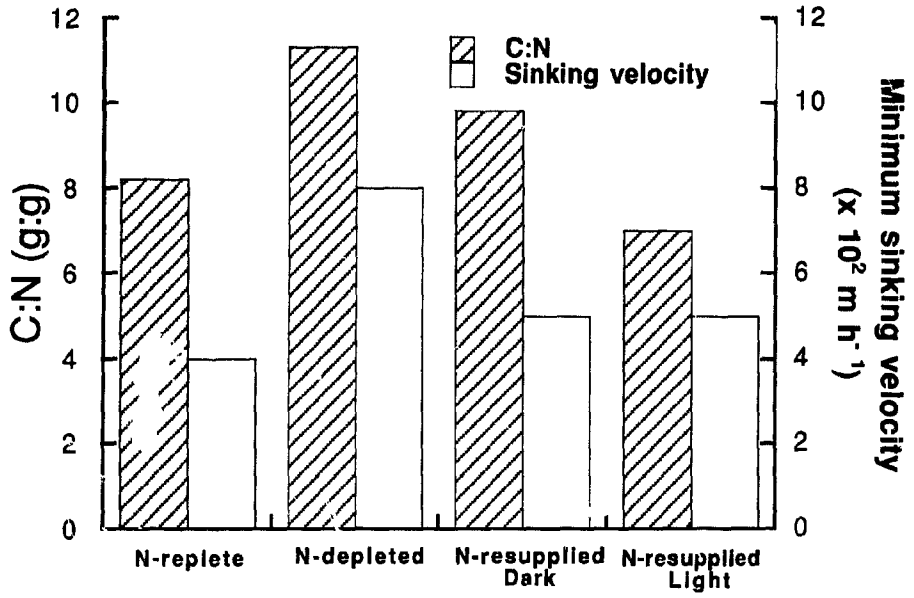

Figure 3.3: Calculated minimum sinking velocities and C:N ratios of negatively buoyant *Rhizosolenia formosa* with variations in N status.

3.3.3 Nitrate uptake experiments

Biomass concentrations, chemical composition, and absolute and specific nitrate uptake rates were determined for N-replete and N-depleted *Rhizosolenia formosa* in the light and in the dark (Table 3.5). Average rates of nitrate uptake were always higher for N-depleted cells, and rates were slightly higher in the light than in the dark. According to atwo-way ANOVA, however, there were no significant differences between any of the treatments (calculated P value for irradiance treatment = 0.367, for nutrients P = 0.308; P values > 0.05 were not considered significant). This reflects the fact that variation within a group (e.g. within triplicate N-replete cultures) was greater than variation between groups (e.g. N-replete vs. N-depleted cells). The two-way ANOVA also indicated no significant interaction between nutrient and irradiance treatments (P = 0.86).

3.3.4 Photosynthesis vs. Irradiance

Measurements of P-I were done for both N-replete (Fig. 3.4) and N-depleted (Fig. 3.5) cultures. Nitrate-replete cultures of *Rhizosolenia formosa* had average P^B_{max} values of 2.6 ± 0.1 g C g Chl^{-1} h^{-1} (Table 3.6), while values of P^B_{max} for N-depleted cells were significantly lower (Table 3.6) with an average P^B_{max} of 1.0 ± 0.1 g C g Chl^{-1} h^{-1}. Values of α, β, and I_k were both significantly lower for N-depleted cells than for N-replete cells (Table 3.6).

3.4 Discussion

3.4.1 Growth rate and chemical composition

The growth rate of *Rhizosolenia formosa* calculated from nitrate disappearance during the time-course experiment was 0.14 d^{-1}. A growth rate of 0.14 d^{-1} converts to a doubling time of almost 5 d. This is a slow growth rate if compared to smaller diatoms (see

Table 3.5: Biomass concentrations, chemical composition, and rates of nitrate uptake in the light and the dark by N-replete and N-depleted *Rhizosolenia formosa.* NRLT and NDLT refer to N-replete and N-depleted triplicates, respectively, where measurements were done in the light. NRDK and NDDK indicate N-replete and N-depleted triplicates, respectively, where measurements were done in the dark.

Culture	Average cell conc. (cells l^{-1})	Average POC ($\mu g\ l^{-1}$)	Average PON ($\mu g\ l^{-1}$)	C:N (g:g)	Uptake rate (nmol $cell^{-1}\ h^{-1}$)	Specific uptake rate (h^{-1})
NRLT	3730	260	39	6.7	0.015	0.020
NRLT	4770	290	51	5.7	0.010	0.013
NRLT	3680	260	40	6.5	0.016	0.020
Average ± s.e.	**4060 ± 360**	**270 ± 9**	**44 ± 4**	**6.3 ± 0.3**	**0.014 ± 0.002**	**0.017 ± 0.003**
NDLT	10650	630	71	8.8	0.004	0.008
NDLT	4850	620	69	9.0	0.044	0.044
NDLT	8650	670	76	8.8	0.017	0.027
Average ± s.e.	**8050 ± 1700**	**640 ± 14**	**72 ± 2**	**8.9 ± 0.1**	**0.022 ± 0.012**	**0.03 ± 0.01**
NRDK	19 900	890	149	6.0	0.005	0.01
NRDK	14 700	690	109	6.3	0.004	0.006
NRDK	16 000	600	98	6.1	0.009	0.02
Average ± s.e.	**16 900 ±1600**	**730 ± 85**	**119±16**	**6.1 ± 0.1**	**0.006 ± 0.002**	**0.012 ± 0.004**
NDDK	7190	630	79	8.0	0.014	0.018
NDDK	5230	570	76	7.4	0.007	0.006
NDDK	6900	550	71	7.7	0.022	0.031
Average ± s.e.	**6440 ± 600**	**580 ± 25**	**75 ± 2**	**7.7 ± 0.2**	**0.014 ± 0.005**	**0.018 ± 0.007**

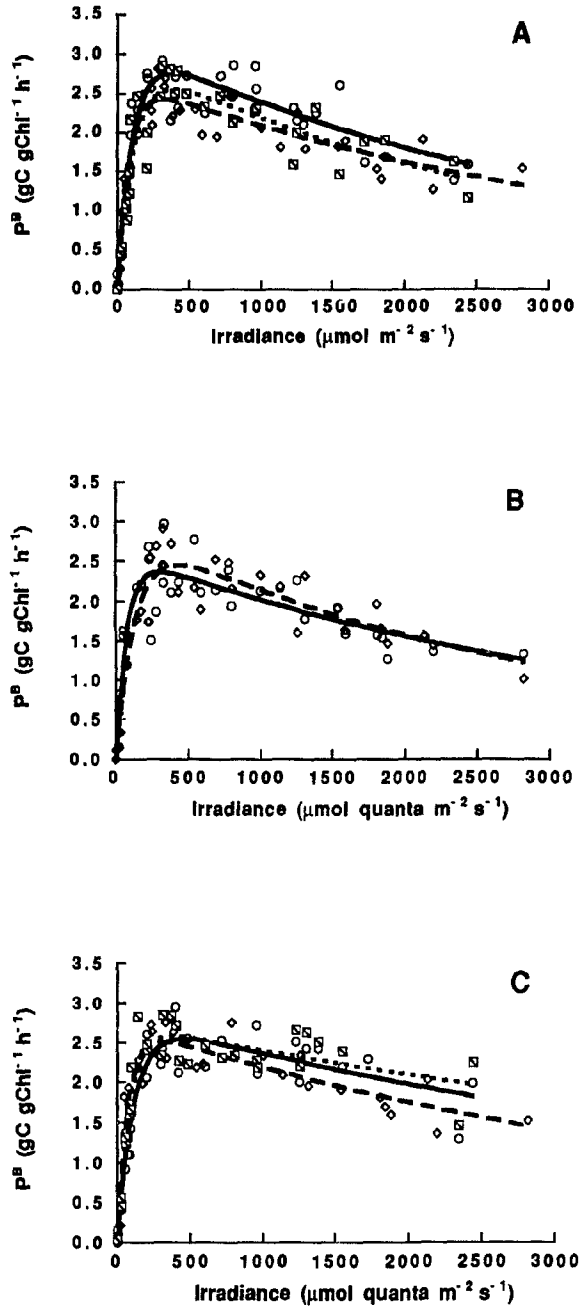

Figure 3.4: Photosynthesis vs. irradiance (P-I) curves for N-replete cultures of *Rhizosolenia formosa*. A), B), and C) are triplicate cultures of *R. formosa*, each of which had triplicate determinations of P-I as indicated by dotted, dashed, and solid lines (with the exception of B) which had only two P-I determinations).

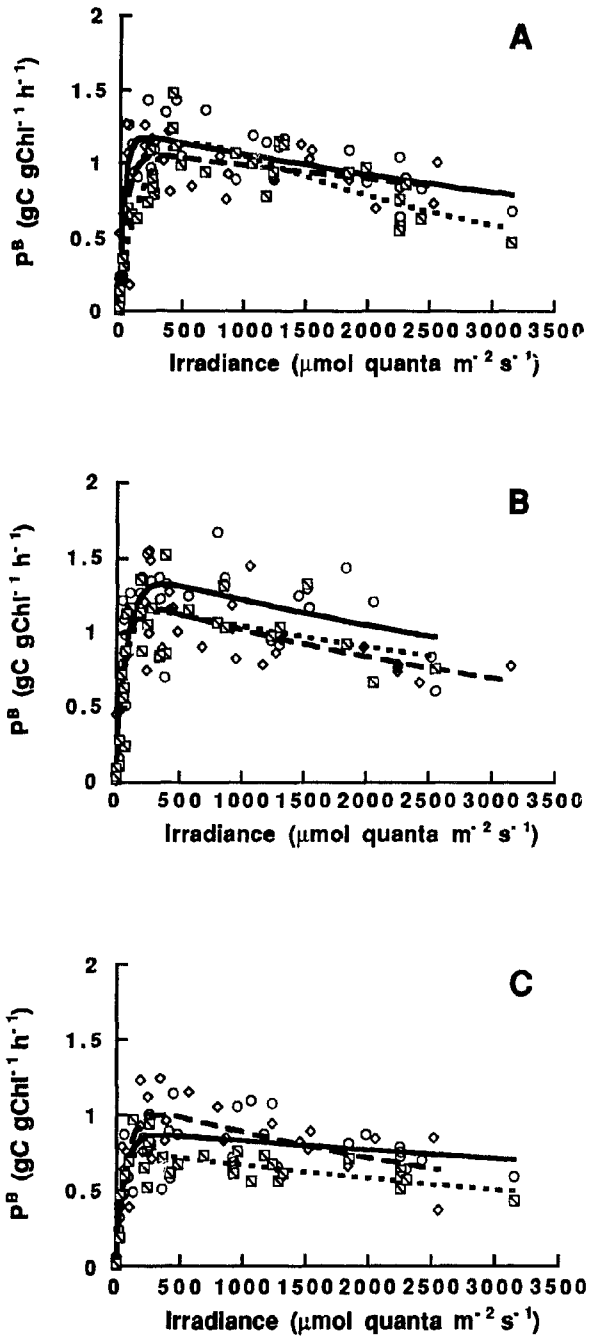

Figure 3.5: Photosynthesis vs. irradiance (P-I) curves for N-depleted cultures of *Rhizosolenia formosa.* A), B), and C) are triplicate cultures of *R. formosa*, each of which had triplicate determinations of P-I as indicated by dotted, dashed, and solid lines.

Table 3.6: Summary of parameters determined from photosynthesis vs. irradiance (P-I) experiments done with N-replete (NR) and N-depleted (ND) *Rhizosolenia formosa*. Values reported are averages of triplicate measurements from each culture ± standard error of the mean, except for the second NR culture for which only two P-I curves were determined. Values for the overall averages of N-replete and N-depleted parameters are compared using a Student's t-test for comparison of means. Calculated values of the t-statistic are compared with the critical value of t (2.1318) at the 0.05 significance level and 4 degrees of freedom.

Culture	P^B_{max} (gC gChl^{-1} h^{-1})	α (gC gChl^{-1} h^{-1} (µmol m^{-2} s^{-1})$^{-1}$)	β (gC gChl^{-1} h^{-1} (µmol m^{-2} s^{-1})$^{-1}$)	I_k (µmol m^{-2} s^{-1})
NR	2.6±0.1	0.029±0.001	0.0009±0.00007	361±21
NR	2.5±0.1	0.028±0.007	0.0008±0.0001	368±65
NR	2.6±0.0	0.032±0.004	0.0005±0.0001	378±44
Overall avg± s.e.	**2.6 ± 0.1**	**0.03 ± 0.002**	**0.0007 ± 0.0001**	**370 ± 20**
ND	1.0±0.09	0.017±0.006	0.0002±0.0001	259±57
ND	1.2±0.05	0.016±0.0002	0.0002±0.00004	334±19
ND	0.8±0.04	0.015±0.003	0.00014±0.0001	301±51
Overall avg± s.e.	**1.02 ± 0.1**	**0.016 ± 0.002**	**0.0002 ± 0.00004**	**298 ± 13**
t-statistic	15.2	10.1	4.6	3.2
Sig. Diff?	**Yes**	**Yes**	**Yes**	**Yes**

Geider 1984, Goldman et al. 1992), yet it is near rates predicted by allometric relationships (Geider et al. 1986) and those determined previously for this diatom (Moore 1994). These relatively low growth rates are also consistent with C:Chl ratios determined during this study (90 to 120 (g:g) for N-replete cells and close to 200 (g:g) for N-depleted cells) which are high compared with values for smaller diatoms at similar irradiances (see Geider 1984). Cells with high C:Chl ratios tend to grow slowly because cells have to photosynthesize more at a given irradiance (than cells with lower C:Chl) to double their relatively large amount of carbon. Growth rate predicted from P^B at growth irradiance (approximately 1 g C g Chl^{-1} h^{-1}) and a C:Chl ratio of 100 (g:g) was 0.14 d^{-1}, which agrees well with estimates by nitrate disappearance and by increases in POC and PON.

In the present study, C:N ratios for N-replete cells ranged from 5.5 (g:g) to 7.2, while values for N-depleted cells ranged from 9.1 to 14.0 (g:g). Both C:N and C:Chl ratios agree well with values for *Rhizosolenia* mats collected in the field. Carpenter et al. (1977) reported average C:N ratio of mats from the Sargasso Sea of 9.7, while Martinez et al. (1983) gave values of 7.2±1.3. Villareal and Carpenter (1989) found C:N ratios of 7.4±2.8 (mol:mol) and C:Chl ratios of 150±100 in mats from the Central North Pacific Gyre. Villareal et al. (1996) divided mats into ascending and sinking assemblages during two cruises in the Central North Pacific Gyre, and analyzed C:Chl, C:N, and carbohydrate:protein ratios. Values of C:N for ascending (and presumably N-replete) mats were 7.4 and 8.1 (during two different cruises), while values for sinking (and presumably N-depleted) mats were between 9.6 and 11.3. Ratios of C:Chl for ascending mats were 115±21 and 146±24, while sinking mats had higher ratios (187±43 and 174±47).

Carbohydrate:protein ratios determined for cultures in the lab differ somewhat from ratios determined for field samples. Villareal et al. (1996) found that ascending mats of *Rhizosolenia* had carbohydrate:protein ratios of 0.87 and 0.62 during two different cruises. Sinking mats had ratios of 1.5 and 1.6. These values from those of the present study (1.0 for N-replete cells and between 3 and 4 for N-depleted cells). This may be because

protocols used for analysis of carbohydrate and protein differed between our study and that of Villareal et al. (1996), but the extent to which this may have influenced the overall carbohydrate:protein ratios is not known. It should be noted, however, that even though the absolute values for carbohydrate:protein ratios differ, the trend of higher ratios in sinking mats is the same as the higher values observed for N-depleted cells.

3.4.2 Nitrate uptake, changes in chemical composition, and cell buoyancy

The chemical composition time-course experiment showed that C:N, C:Chl, and carbohydrate:protein increased noticeably upon depletion of ambient nitrate. Similarly, cell buoyancy (as indicated by percent of cells in the top fraction of the settling column) decreased, and the sinking velocity of cells leaving the top fraction of the column increased. Changes in chemical composition indicate clearly that cells were in a state of unbalanced growth (Eppley 1981), that is, the uptake of carbon continued well after the depletion of ambient nitrate. The uncoupling of photosynthesis from nutrient acquisition has been noted previously in the diatoms *Stephanopyxis palmeriana* (Goldman et al. 1992) and *Thalassiosira weissflogii* (Richardson and Cullen 1995), and it seems likely that this is a general phenomenon. Goldman et al. (1992) found large deviations from Redfield stoichiometry, and Richardson and Cullen (1995) observed large increases in carbohydrate:protein ratio, during nutrient-depleted periods of carbon accumulation. These observations are not restricted to the laboratory: removal of carbon from nutrient-depleted waters of the North Atlantic (consistent with carbon uptake out of Redfield ratio) has been reported by both Sambrotto et al (1993) and Michaels et al. (1994).

After re-introduction of nitrate to the culture medium, the chemical composition of *Rhizosolenia formosa* reverted, tending towards pre-depletion values. All cultures took up nitrate after the period of N-depletion and most cultures showed concomitant reductions in carbohydrate and increases in protein. This is consistent with the mobilization of carbohydrate combined with the use of newly-acquired nitrogen for the production of

protein (Cuhel et al. 1984, Cullen 1985). Two cultures, however, showed no increase in protein to account for the disappearance of nitrate from the culture medium, though there were decreases in cellular carbohydrate. It is possible that nitrate was still being stored in the vacuole as intracellular nitrate, and that protein synthesis had not yet been initiated at the time of sampling. The role of carbon storage compounds such as lipid was not investigated during this study. I assume that lipids make only small contributions to the total pool of carbon in these cells. Calculations of the relative contribution of lipid to the total carbon pool (by weight) show that lipids may account for 25% of the total carbon pool in N-replete *R. formosa* and only 12% of the carbon pool in N-depleted cells, assuming that the majority of total cellular carbon is in the form of carbohydrate, protein, and lipid. Carbon in carbohydrate accounted for 64% of the total cellular carbon in N-depleted cells, thus I will assume that changes in carbohydrate make the highest relative contributions to changes in cell buoyancy, discussed below.

Overall, reversion of chemical composition occurred whether cells were without nitrate for 24 h, 30 h, or 53 h. No significant mortality of cells was observed even though two cultures were without detectable nitrate for over 2 d. These reversions have important ecological implications, as will be discussed below. The recovery of cells from almost 3 d of nitrate depletion was also observed by Richardson and Cullen (1995) using the smaller coastal diatom *Thalassiosira weissflogii* while Strickland et al. (1968) noted similar reversions in chemical composition when cultures of the dinoflagellate *Cachonina niei* grown in a deep tank were depleted of nitrogen for 5 d, and then re-inoculated with nitrate.

Changes in cell buoyancy were noted when nitrate was re-introduced to culture medium. The percentage of cells in the top fraction of the settling column increased and the percentage of cells in the bottom fraction decreased in response to nitrate re-addition, though shifts were small percentages in either direction. The sinking velocity of cells leaving the top fraction also decreased after re-introduction of nitrate to culture medium.

Although they represented only a small percentage of the total population (4-10%), cells were always present in the top fraction of the sinking column after the 1 h incubation. Their presence could be explained in at least three ways. First, assuming that the entire population of cells was negatively buoyant, these cells could represent the most slowly sinking portion of the population, i.e. cells that were still present because they did not sink out of the top fraction during the 1 h incubation time. It could be argued that if the experiment was left longer than 1 h then the number of cells in the top fraction would decrease with time. Second, these could have been neutrally buoyant cells which had no detectable sinking rate and thus were there when the experiment started. Third, cells in the top fraction could have been positively buoyant cells which rose to the top during the 1 h incubation. Using the settling column method alone it is not possible to prove that any one or combination of the above reasons is correct. However, visual observations of cells in the upper layer support the contention that cells found in the top fraction of the columns after the incubation period were positively buoyant, because cells were not found dispersed through the entire fraction but were instead concentrated within the top 2.5 ml of the 70 ml upper fraction. *Rhizosolenia formosa* in culture also shows similar behavior: the majority of cells are found on the bottom of the culture vessel, but a layer of cells is always found floating at the surface (T. L. Richardson, T. A. Villareal, J. K. Moore, pers. obs.).

The contention that cells in the upper fraction were concentrated near the surface, and, thus, were positively buoyant can be supported by an algebraic calculation of the positively, neutrally, and negatively buoyant fractions. The calculation uses the volumes of each fraction of the column, the total volume of the column (V), the initial concentration of cells in the column (C_0), and the number of cells observed in each fraction of the column after the 1 h incubation (N_{top}, N_{mid}, and N_{bott}), as follows:

$$N_{top}= [C_0 \times 0.17\ V]+[Fl\ (C_0 \times 0.83\ V)]-[Si\ (C_0 \times 0.17\ V) \qquad (3.2)$$

$$N_{mid}=[C_0 \times 0.63\ V]-[Si\ (C_0 \times 0.63\ V)]-[Fl\ (C_0 \times 0.63\ V)] \quad (3.3)$$

$$N_{bott}=[C_0 \times 0.20\ V]-[Fl\ (C_0 \times 0.20V)]+[Si\ (C_0 \times 0.80\ V)] \quad (3.4)$$

The initial concentration of cells, C_0 (cells ml^{-1}) is the concentration of cells at time zero (4 cells ml^{-1} for the N-replete experiment), V is the total volume of the column (420 ml), and Si and Fl are the fractions of sinking and floating cells, respectively (dimensionless numbers with values less than 1). The top fraction occupies 17% of the total volume (0.17 V), the middle fraction occupies 63% (0.63 V) and the bottom fraction occupies 20% (0.20 V). The calculation assumes that all positively buoyant cells have left the middle and bottom fractions of the column (together occupying 0.83 V) and that all negatively buoyant cells have left the top and middle fractions of the column (together occupying 0.80 V) by the end of the 1 h incubation. The limitations of this assumption are discussed below.

To solve for Fl and Si, only two of the above equations are needed. Equations 3.2 and 3.3 were solved simultaneously using data from the N-replete experiment (where N_{top} = 238 cells and N_{mid} = 772 cells) which gave values of Fl=0.017 (1.7%) and Si=0.25 (25%). By subtraction, the proportion of neutrally buoyant cells would then be 0.733, or 73.3%. These values are substantially different from those obtained by calculations using the settling column. However, the calculation assumes that the cells are distributed evenly throughout the entire volume of the top and bottom fractions and the calculation is sensitive to the concentration of cells as opposed to the number of cells.

Knowing that the cells found in the top and bottom fractions were concentrated against the top and bottom of the column in volumes of approximately 2.5 ml, this calculation was repeated with the volumes of each fraction adjusted accordingly. The equations then become:

$$N_{top}= [C_0 \times 0.006\ V]+[Fl\ (C_0 \times 0.994\ V)]-[Si\ (C_0 \times 0.006\ V) \quad (3.5)$$

$$N_{mid}=[C_O \times 0.988\ V]-[Si\ (C_O \times 0.988\ V)]-[Fl\ (C_O \times 0.988\ V)] \quad (3.6)$$

$$N_{bott}=[C_O \times 0.006\ V]-[Fl\ (C_O \times 0.006V)]+[Si\ (C_O \times 0.994\ V)] \quad (3.7)$$

Values for N_{top}, N_{mid}, V, and C_O remained the same. Using equations 3.5 and 3.6, values for Fl and Si were calculated to be 0.14 (14%) and 0.40 (40%), respectively, making the neutrally buoyant fraction 0.46 (46%). These calculated values are much closer to those determined during buoyancy experiments on N-replete cells (11%, 44%, and 44% for cells in the top, middle, and bottom layers) and, overall, these calculations show that the cells in the top and the bottom fractions were concentrated in volumes much smaller than the volume of the entire arbitrarily-defined fraction. The concentration of cells in the top of the column was due to the positively buoyant nature of the cells and thus, from now on, the cells in the top, middle, and bottom fractions of the column will be referred to as positively, neutrally, and negatively buoyant, respectively.

In general, the percentage of positively buoyant cells (for either N-replete or N-depleted cells) determined during this study are lower than values determined previously for *Rhizosolenia* (Moore 1994). This may be due to decreases in cell size. The extent to which a diatom can control its buoyancy is partly determined by the ratio of total cell volume to internal cell volume. Assuming equal thickness of cells walls, smaller cells will have smaller capacities for changing internal cell density. In Moore's (1994) study, 40% of cells 129 µm in diameter were positively buoyant at an irradiance of 50 µmol quanta m^{-2} s^{-1} (used for experiments in the present study), but this number decreased to 0% for cells 117 µm in diameter. The cultures used for the present study are the same strain as that of Moore (1994), however the cultures are now older and have decreased in size as the culture has aged (attempts at inducing auxospore formation have not been successful). Measurements done on cells during P-I experiments showed that these cells now have a

maximum diameter of 90 µm, consistent with the expected decrease in percentage of positively buoyant cells compared to 129 µm diameter cells, though 11% of the N-replete cells were still positively buoyant even at this relatively small cell size. The percentage of positively buoyant cells in natural populations may be much higher values (as high as 30%) as *Rhizosolenia* will be reproducing naturally and should not experience reductions in size with successive divisions. High concentrations of positively buoyant cells in nature have been observed by Barber et al. (1994) and Yoder et al. (1994) who describe concentrations of *Rhizosolenia* at a convergence region in the Equatorial Pacific; concentration of cells in convergence regions requires them to be positively buoyant. As well, cultures of the same *Rhizosolenia formosa* used for buoyancy experiments were grown in an experimental mesocosm and, after inoculation and a short period of adjustment, all cells floated to the top of the tank and remained there for several days (T. L. Richardson, unpublished data). This infers that there may also be "container effects" which prevent cells from expressing their full range of buoyancy control. That is, cells exposed to a gradient of light in the large volume experimental mesocosm behaved differently than cells in the smaller volume settling columns where the light environment was relatively constant.

The low values of positively buoyant cells observed during my study may also be a result of the settling column method used to estimate the percentages of positively buoyant, neutrally buoyant, and negatively buoyant cells. The study of Moore (1994) did not use a settling column but instead used a standard laboratory petri dish in which an evenly mixed sample of cells was left for 5 min. then the number of cells at the top and bottom of the dish were counted and compared to the total number of cells in the dish. The timescale of Moore's (1994) measurements (5 min vs. 1 h for the present study), and the spatial scale over which measurements were made (1.5 cm vs. 50 cm) were vastly different from the ones employed here. Cells that are only slightly positively buoyant (i.e. with very low ascent rates) would be identified as positively buoyant using Moore's (1994) method, but may not reach the top of the settling column to be counted as such by my method.

Similarly, cells that are only slightly negatively buoyant may not reach the bottom fraction and thus may be included in the neutrally buoyant fraction (as would the slowly ascending positively buoyant cells) even though not truly neutrally buoyant. However, the settling column method does not take into account the fraction of neutrally buoyant cells already present in the top and bottom sections of the column, which may be mistakenly counted as positively or negatively buoyant, respectively. As calculated above and as experimentally determined, this fraction may be as high as 46%.

As has already been discussed, the absolute values of the percentages of positively, neutrally, and negatively buoyant cells are likely not representative of natural populations and measurements from this study differ even from measurements performed on the same organism using another protocol. However, consideration of the trends in the data show that both the direction of buoyancy changes in response to nutrient deprivation and re-supply, and the timescales of these buoyancy changes are both consistent with vertical migrations: the percentage of negatively buoyant cells increased when cells ran out of nitrate, and more cells became positively buoyant when re-enriched with nitrate even within 12 h of nitrate re-addition. It is these relative changes in buoyancy that may be important within the context of vertical migration.

The results of time-course experiments showed clearly that the physiology of *Rhizosolenia formosa* is extremely flexible, an attribute consistent with vertical migrations in nature. *Rhizosolenia formosa* could maintain unbalanced growth for at least 53 h without nitrate. Since cells are expected to spend some portion of their migration cycle in N-depleted waters and since internal nitrogen stores will eventually run out, *Rhizosolenia* must be capable of accumulating large amounts (perhaps one full cell quota or more) of carbon during this N-depleted, but illuminated, phase of migration. Cellular capacity for changes in chemical composition will be determined by the extent to which photosynthate can be stored for later use after nutrient acquisition. As shown by buoyancy experiments, the nutritional status of the cell also affects cell buoyancy. The percent of positively

buoyant cells decreased upon N-depletion, possibly due, in part, to increases in cellular carbohydrate. Carbohydrate has been shown to play a significant role in the regulation of buoyancy of blue-green algae such as *Trichodesmium* (Romans et al. 1994, see also review by Oliver 1994) because of its fairly high density (1600 kg m^{-3}).

Reversion to negative buoyancy would remove cells from illuminated, N-depleted waters and would allow them to sink to deeper waters which contain high concentrations of nutrients. I have shown that *Rhizosolenia formosa* is capable of resuming uptake of nitrate upon returning to N-replete waters. In the open ocean, nitrate often does not become detectable until well-below the euphotic zone (see Hayward 1991) so it is necessary for *R. formosa* to have the ability to take up nitrate in the dark if migrations are to be ecologically useful. Buoyancy experiments also showed that N-depleted cells can revert to positive buoyancy when re-enriched with nitrate in the dark. The resumption of nitrate uptake after prolonged unbalanced growth, the ability to take up nitrate in the dark, and the reversal of buoyancy upon N-repletion are all consistent with, and critical to, the ability of *Rhizosolenia* to migrate vertically in nature.

Nitrate uptake measurements verified that both N-replete and N-depleted cells can take up nitrate in the dark, and that rates in light and darkness were comparable. Calculation of an overall average from nitrate uptake data yielded an N-specific uptake rate of 0.02 h^{-1}. Previous work has shown that prior N-starvation often increases the specific rate of (or induces) nitrate uptake in phytoplankton (e.g. Harrison 1976, see also Syrett 1981); however, the variability within treatments made it impossible to detect the effects of treatments such as N-depletion on uptake rate.

Moore (1994) provided the first evidence that *Rhizosolenia formosa* could take up nitrate in the dark. During the dark period of a 24 h time-course experiment, intracellular nitrate of *R. formosa* increased by at least 6 mM over a 6 h time period. The uptake of nitrate in the dark has also been observed in other diatoms and in other vertically-migrating phytoplankton (Harrison 1976, Bhovichitra and Swift 1977, Syrett 1981, Cullen 1985).

Bhovichitra and Swift (1977) found that the large dinoflagellate *Pyrocystis fusiformis* took up nitrate at comparable rates during both day and night. Nocturnal uptake of nitrate is a well-known phenomenon in coastal dinoflagellates, and may contribute to the formation of dinoflagellate blooms (Eppley and Harrison 1975, Harrison 1976, Cullen 1985).

Nitrogen-specific uptake rates (0.02 h^{-1} which converts to 0.48 d^{-1}) were higher than estimated N-specific growth rates (0.15 d^{-1}). This indicates that over a short time scale cells have the ability to take up nitrate in excess of that necessary for immediate metabolic requirements. Nitrate can be stored in the relatively large vacuole of *Rhizosolenia* (see Moore 1994, Villareal and Lipschultz 1995); from which it can be mobilized, reduced, and combined with carbon acquired during photosynthesis in surface waters to make proteins. The enhanced ability of a cell to take up nitrogen in excess of its immediate requirements has been demonstrated for other marine phytoplankton (McCarthy and Goldman 1979, Glibert and Goldman 1981, Horrigan and McCarthy 1981, 1982). The last authors showed that *Thalassiosira pseudonana* and *Skeletonema costatum* had enhanced uptake of ammonium and urea even for nutrient-saturated cultures. Enhanced uptake allows phytoplankton to exploit the episodic pulses of nutrients often encountered in the marine environment, thereby satisfying their daily quota of nitrogen (see also Glover et al. 1988). For the case of migrating *Rhizosolenia*, the "patchiness" of its nutrient environment is in the form of intermittent exposures to sources of nutrients deep within the water column.

3.4.3 Photosynthetic physiology of *Rhizosolenia formosa*

The photosynthetic physiology of *Rhizosolenia formosa* and possible adaptations to vertical migration were examined through measurements of P-I and *in vivo* and *in vitro* absorption. Overall, values for P^B_{max} determined here for N-replete *R. formosa* (average= 2.6 g C g Chl^{-1} h^{-1}) are in good agreement with production rates calculated previously for cultures of *R. formosa* in the laboratory, and with ^{14}C determinations of primary productivity of mats collected in the field. Moore (1994) calculated an apparent production

rate for nutrient-replete *R. formosa* of 2.9 g C g Chl^{-1} h^{-1} from experimentally-determined growth rates and C:Chl ratios. In the Equatorial Pacific at temperatures > 25°C, Yoder et al. (1994) determined a daily production rate of 68 g C g Chl^{-1} d^{-1} which converts to approximately 5.7 g C g Chl^{-1} h^{-1} assuming a 12 h photoperiod. Alldredge and Silver (1982) measured the primary productivity of mats of *Rhizosolenia castracanei* and *R. imbricata* var. *shrubsolei* in the boundary waters of the Central North Pacific Gyre and found average maximal photosynthetic rates of 5.8 g C g Chl^{-1} h^{-1}. In mats of similar species composition, Carpenter et al. (1977) found that primary productivity was variable, but ranged between 2.8 and 10.4 g C g Chl^{-1} h^{-1}. More recent estimates of the primary productivity of *Rhizosolenia* mats based on O_2 evolution rates gave C fixation rates of 4.7 g C g Chl^{-1} h^{-1} for sinking mats and 7.3 g C g Chl^{-1} h^{-1} for floating mats (Villareal et al. 1996).

Photosynthetic rates determined for N-replete cells agree with those determined in the field, but rates for N-depleted cells from this study are generally lower than observed field values. It is possible that the growth temperature of *Rhizosolenia formosa* in culture has affected its maximal photosynthetic rate when compared to natural populations. Li and Morris (1982) examined the effects of growth temperature on P^B_{max} of *Phaeodactylum tricornutum* and found that P^B_{max} increased as growth temperature increased with a Q_{10} of about 2.6. Thus, I would not expect *R. formosa* grown in the laboratory at 20°C to have exactly the same P^B_{max} as mats of *Rhizosolenia* collected from 28-30°C surface waters in the open ocean. Also, *Rhizosolenia* mats collected in the field are assemblages of various species, and therefore should not necessarily reflect the P_{max} of any particular species.

Values of P^B_{max} and α measured during this study for N-depleted *Rhizosolenia formosa* were significantly lower than those determined for N-replete cells. Similarly, Villareal and Lipschultz (1995) found decreases in both P^B_{max} and α during progressive depletion of internal nutrient stores of the vertically-migrating diatom *Ethmodiscus*. Decreases in P^B_{max} and α in N-depleted cells were likely due to the dependence of cellular

physiology on available nitrogen as reduction in available nitrogen will decrease the production of chlorophyll and accessory pigments (Zevenboom 1986, Sosik and Mitchell 1991, Latasa and Berdalet 1994). The effects of nutrient depletion on phytoplankton photosynthesis have been examined previously (e.g. Yentsch and Lee 1966, Welschmeyer and Lorenzen 1981, Prézelin and Matlick 1983, Cleveland and Perry 1987). Welschmeyer and Lorenzen (1981), for example, found that both α and the quantum yield of photosynthesis decreased as cultures of *Thalassiosira pseudonana* entered stationary phase.

Average values for the saturation parameter, I_k, determined during P-I experiments were 370 µmol quanta m^{-2} s^{-1} for N-replete cells and 298 µmol quanta m^{-2} s^{-1} for N-depleted cells. Since there is a direct dependence of I_k on P^B_{max} (Henley 1993) and the rate of the dark reactions of photosynthesis decrease during N-depletion, it was not surprising that I_k shifted to lower light intensities (see Yentsch and Lee 1966). It is likely that I_k has been influenced by growth irradiance (50-100 µmol quanta m^{-2} s^{-1}) (see Kana and Glibert 1987a), however, values of I_k determined by Villareal et al. (1996) for field samples of *Rhizosolenia* generally agree well with these data: sinking mats had I_k = 140±22 µmol quanta m^{-2} s^{-1} while I_k for floating mats was 241±36 µmol quanta m^{-2} s^{-1}. Examples of I_k values considered indicative of a truly high-light adapted population were found by Jitts et al. (1976), who determined saturation irradiances of approximately 600 µmol quanta m^{-2} s^{-1} for surface phytoplankton collected at 3°S in the Pacific Ocean, and Takahashi et al. (1989), who found I_k values of over 700 µmol quanta m^{-2} s^{-1} for phytoplankton collected at 10 m in the Pacific Ocean off Japan. Finally, values of I_k determined for another vertically-migrating diatom, *Ethmodiscus* , averaged 575±191 µmol quanta m^{-2} s^{-1} (Villareal and Carpenter 1994). Comparisons of I_k data from different sources should be done with caution, however. Henley (1993) outlines clearly the potential problems with comparing I_k data determined by different methods, including the fact that the I_k for net photosynthesis (as would be determined by O_2 evolution) is not the same as that for gross

photosynthesis (determined by ^{14}C uptake). The value for I_k for net photosynthesis is that for gross photosynthesis minus the compensation irradiance (Henley 1993).

The parameter of photoinhibition, β, determined during this study ranged from an average of 0.0007 g C g Chl^{-1} h^{-1} (μmol quanta m^{-2} $s^{-1})^{-1}$ for N-replete cells to 0.0002 g C g Chl^{-1} h^{-1} (μmol quanta m^{-2} $s^{-1})^{-1}$ for N-depleted cultures. Photoinhibition is defined as the depression of photosynthesis at supra-optimal light (Neale 1987) and is a complicated phenomenon. Thus, values for β generated in the laboratory cannot be used to make any concrete conclusions as to the potential for photoinhibition of cells in nature.

The parameter of photoinhibition for N-depleted cells was significantly lower than that for N-replete cells. A possible reason for this is because N-depleted cells may lack the photoprotective mechanism that deactivates Photosystem II reaction centers thereby reducing short term photosynthesis at high irradiance, but promoting survival (see Neale 1987; Henley 1993). This would be manifested as a lower β, but the lack of photoprotection means that cells would not survive indefinitely.

In general, measurements of I_k suggest that *Rhizosolenia formosa* is moderately high-light adapted. Some degree of high-light adaptation would be useful for cells migrating to high-irradiance surface waters, but because cells move vertically throughout the euphotic zone and are not confined to a particular depth stratum, maximal photosynthetic performance at high irradiance is not necessary for their survival. The shape of the P-I curve and the high ratio of I_k to growth irradiance both suggest that the photosynthetic physiology of *Rhizosolenia formosa* is flexible and that cells may be able to adapt to changes in irradiance as they move vertically through the water column (Sakshaug et al. 1987). Cells also show evidence of "excess photosynthetic capacity" (Kana and Glibert 1987b). Using measurements of particulate carbon taken during P-I experiments, values of P^B_{max} normalized to carbon were calculated to be 0.026 h^{-1} or 0.3 d^{-1}. This value is three times the estimated C-specific growth rate of the diatom, indicating that its photosynthetic capabilities are flexible enough to respond to changing irradiance, and it has

the capability to "shift up" its photosynthetic rate in response to episodic exposures to high irradiance. The assimilation of carbon in excess of immediate metabolic requirements in high irradiance surface waters was observed also by Rivkin et al. (1984) in a study of migrations of the open ocean dinoflagellates *Pyrocystis noctiluca* and *Pyrocystis fusiformis*.

3.4.4 Potential role of *Rhizosolenia* in new production and biogeochemical cycling

This work has shown that the physiological characteristics of *Rhizosolenia formosa* are consistent with, and sometimes advantageous to, vertical migration. The capacity for unbalanced growth and for return to balanced growth as shown by changes in chemical composition is compatible with cells spending prolonged periods of time in N-depleted waters, and with the return to N-rich deep water. Their nitrate uptake machinery allows them to exploit deep sources of nutrients, and to take up nitrate in excess of their daily requirements. Finally, their photosynthetic physiology indicates that they are well-adapted to the continually changing irradiances encountered during vertical migrations, and their pigment composition affords some degree of protection against photoinhibition in high irradiance surface waters. Let us now consider the possible contribution of these migrations to new and primary production.

It is becoming better-recognized that large diatoms like *Rhizosolenia* are ubiquitous in oligotrophic regions of the world's oceans (Goldman et al. 1992, Goldman 1993). Not only are they present, but they may make substantial contributions to global primary production and new production, and hence to the export of carbon from the euphotic zone (Michaels and Silver 1988, Sancetta et al. 1991, Goldman et al. 1992, Goldman 1993). These contributions have been largely overlooked, because the numerical abundance of large phytoplankton has likely been underestimated by traditional sampling with small volume bottles (Alldredge and Silver 1982; Michaels and Silver 1988; Goldman 1988;

Sancetta et al. 1991; Carpenter and Romans 1991; Goldman 1993), and by traditional sampling strategies which miss episodic blooms of large diatoms (Goldman 1993).

Biological transport of nitrogen to the euphotic zone by migrations of *Rhizosolenia* represents a novel form of new production (Moore 1994; Richardson and Cullen 1995). If these organisms are sufficiently abundant, their migrations may contribute significantly to global levels of new and primary production. I have shown that *Rhizosolenia formosa* can take up nitrate in the dark, and, because this dark uptake will occur without concurrent uptake of carbon, cells will instead combine nitrate acquired at depth with carbon acquired in surface waters. That is, the processes of nutrient uptake and carbon uptake become uncoupled in space and time (Cullen 1985, Fraga et al. 1992). Fraga et al. (1992) showed uncoupled movements of carbon and nitrogen by their measurements of Broecker's parameters (Broecker 1974) during a red tide of the dinoflagellate *Gymnodinium catenatum*. Broecker's parameters ('NO', 'CO', and 'PO') are intended to be conservative properties that characterize water masses. If biochemical reactions in the water mass are occurring in Redfield proportions, each of Broecker's parameters will be constant with depth. Fraga et al. (1992) found distinct vertical differences in Broecker's parameters during the red tide, indicating that biochemical reactions were not occurring in Redfield proportions. They attributed these departures from Redfield stoichiometry to vertical migrations by the dinoflagellates, whereby carbohydrate synthesis at the surface and nutrient uptake at depth resulted in a carbon deficit near the surface and a nitrogen deficit below. Nitrogen deficits below the euphotic zone may also be exhibited as negative preformed nitrate signals. Emerson and Hayward (1995) cite nitrate uptake by migrating diatom mats as a possible explanation for the layer of negative preformed nitrate observed in the subtropical North Pacific Ocean.

Input of nitrogen to the euphotic zone during migrations of *Rhizosolenia* is not coupled to the input of carbon, as is the case for physically-transported dissolved nutrients (Eppley and Peterson 1979). Since photosynthesis occurring in surface waters requires a

carbon source, and since stoichiometric equivalents of carbon are not brought to the surface by cells in coupled transport with nitrogen, new production resulting from vertical migrations might result in the net removal of carbon from oceanic surface waters if migrating organisms are abundant. This, in turn, could affect the air-sea exchange of carbon dioxide (see also Richardson and Cullen 1995).

Calculation of the potential contribution of *Rhizosolenia* to new and primary production relies on having robust estimates of nitrate and carbon uptake, thus, differences in photosynthetic rates between N-replete and N-depleted cells should be considered in estimates of total carbon consumption during migrations. Since *Rhizosolenia* may be N-depleted during part of the migration cycle, carbon uptake would be overestimated if only N-replete rates are used. Determination of rates of carbon and nitrate uptake also help determine the timescale of the migration cycle, which will in part determine the timescale of the flux of nitrogen to the surface. The exact contribution of *Rhizosolenia* to new and primary production relies on robust estimates of cell abundance, but the geographical coverage of abundance estimates is not yet sufficient to determine the overall biogeochemical importance of *Rhizosolenia*.

Chapter 4

Potential contributions of vertically-migrating *Rhizosolenia* to nutrient cycling and new production in the open ocean

4.1 Introduction

Although open ocean regions are often dominated by small plankton and highly regenerative food webs (Eppley and Peterson 1979), the occurrence and significance of large phytoplankton (>100 μm, after Goldman 1988) in open ocean areas is now well documented (Beers et al. 1975, Alldredge and Silver 1982, Goldman 1988, Villareal 1988, Carpenter and Romans 1991, Karl et al. 1992, Villareal et al. 1993, Yoder et al. 1994). Large phytoplankton typically found in these regions include the cyanobacterium *Trichodesmium* (e.g. Bowman and Lancaster 1965, Villareal and Carpenter 1990, Carpenter and Romans 1991, Karl et al. 1992) and diatoms of the genera *Ethmodiscus* and *Rhizosolenia* (e.g. Villareal 1992, Villareal et al. 1993). In general, open ocean regions like the Central North Pacific Gyre are characterized by chronically low levels of nutrients in surface waters (Hayward 1991, Karl et al. 1992) which places large cells with small ratios of surface area to volume at a disadvantage in terms of nutrient uptake (Munk and Riley 1952, Pasciak and Gavis 1974, see also review by Chisholm 1992). However, large

phytoplankters found in these regions have developed mechanisms to cope with the scarcity of nutrients. *Trichodesmium*, for example, can fix atmospheric nitrogen, easing the burden of nitrogen limitation, and uses buoyancy reversals to migrate below the nutricline to acquire phosphorus (Carpenter and Romans 1991, Karl et al. 1992). Recent evidence supports the hypothesis (Villareal and Carpenter 1989) that the mat-forming diatom *Rhizosolenia* and the single-celled diatom *Ethmodiscus* also use their ability to change buoyancy to undergo vertical migrations, allowing them to exploit sources of nutrients in deeper water (Villareal et al. 1993, Villareal and Carpenter 1994, Villareal and Lipschultz 1995). For *Rhizosolenia*, this evidence includes $\delta^{15}N$ signatures (i.e. ratios of the natural abundance of stable isotopes of N) of surface-collected samples which are characteristic of cells that had exploited deep sources of nutrients (Villareal et al. 1993), and significantly higher internal nitrate concentrations in ascending cells than in sinking cells, consistent with the concept of nutrient replenishment by vertical movements between surface and deep waters (Villareal et al. 1993, Villareal and Lipschultz 1995). The large central vacuole of both *Rhizosolenia* and *Ethmodiscus* effectively increases the ratio of surface area to metabolic cell volume, permitting the accumulation of nutrients and facilitating buoyancy regulation (Villareal 1992)

Movement of phytoplankton between nitrate-rich deep waters and nitrate-poor surface waters to support growth results in an upward transport of nitrogen to the euphotic zone, a form of new production as defined by Dugdale and Goering (1967). Since sources of nutrients are often located well-below the euphotic zone (Hayward 1991), the uptake of nitrate may occur in the absence of photosynthesis, that is, without the accompanying uptake of carbon (Moore 1994, Richardson et al. 1996). Therefore, the input of nitrogen to the euphotic zone by migrating phytoplankton is without accompanying inputs of carbon, as is the case for physically-transported dissolved nutrients (Eppley and Peterson 1979). Since photosynthesis requires a carbon source, and since no carbon is brought to the surface in coupled transport with nitrogen, cells will instead combine nutrients acquired at

depth with carbon acquired in surface waters. New production resulting from vertical movements of phytoplankton, therefore, could result in the net removal of carbon from oceanic surface waters as cells sink from the surface layer if cells are sufficiently abundant.

The potential contribution of diatom migrations to the vertical flux of nutrients and to new production in the open ocean are not considered in current models of biogeochemical cycling (e.g. Fasham et al. 1990). The contributions may be important, as oceanic habitats are responsible for most of the global ocean primary productivity (Martin et al. 1987). Areas such as the central ocean gyres are significant contributors to the export of carbon from the euphotic zone (Karl et al. 1992), mostly due to their large geographical area. It is difficult to estimate the potential contributions of diatom migrations to biogeochemical cycling as data on the abundance of migrating diatoms in these regions, the amount of nutrient assimilation associated with each migration cycle, and the frequency of vertical cycling are scarce. Accordingly, a numerical model of migrations of *Rhizosolenia* in a hypothetical open ocean region was developed to estimate fluxes of carbon and nitrogen (and hence new production) due to migrations of *Rhizosolenia*. The model also predicts the specific rate of increase of *Rhizosolenia*, the total migration cycle time, and the vertical distribution of a population of *Rhizosolenia* under steady state conditions, with a view towards using abundance data collected in the field to predict associated fluxes of carbon and nitrogen.

4.2 Description of the Base Model

4.2.1 Physical Structure

The model represents a community of *Rhizosolenia* mats in the upper water column of an oligotrophic open ocean region (Fig. 4.1). The general structure is based loosely on a model by Kromkamp and Walsby (1990). Physiological rates used to specify parameters in the model were taken from a laboratory study by Richardson et al. 1996. Phytoplankton

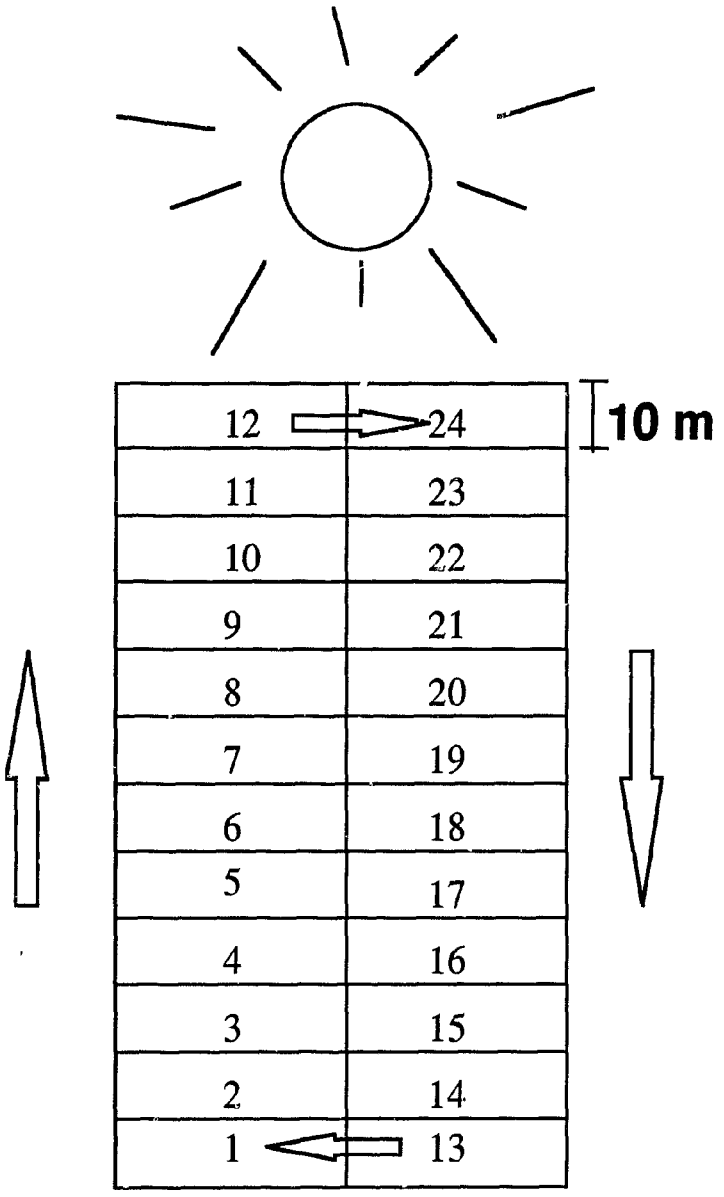

Figure 4.1: Schematic of a box model of a *Rhizosolenia* migration cycle. Numbered boxes 1, 12, 13, and 24 correspond to boxes referred to in equations 4.15 to 4.22 (see text). Biomass ascends through boxes on the left hand side of the figure and sinks through boxes on the right hand side. Transfer of biomass from ascending to sinking paths (and vice-versa) occurs only at the top and bottom boundaries (boxes 12, 24, 1 and 13). Irradiance is highest in the top boxes (12 and 24) and decreases exponentially with depth. Nitrate is available only in boxes 1 and 13.

biomass is represented as pools of particulate organic carbon (POC) and particulate organic nitrogen (PON) in 10 m intervals over a 120 m water column. The vertical structure simulates that found in oligotrophic regions of the world's oceans, where light and nutrients are spatially separated (see Hayward 1991). Nitrate is assumed to be undetectable in the upper 110 m, and becomes available in an unlimited supply (i.e. never goes to zero) only below the euphotic zone (110-120 m). Dissolved inorganic carbon is assumed to be in an unlimited supply. Photosynthetically available radiation (PAR) (after Morel 1978) varies with depth and with time of day. Variation of surface irradiance with time of day is according to

$$I_o = I_m \cdot \sin\left(\pi t / D_L\right) \qquad \text{for } 0 < t < D_L \qquad (4.1)$$

$$I_o = 0 \qquad \text{for } D_L < t < 24$$

(see Kirk 1994), while the variation of irradiance with depth is described by

$$I_z = I_o \cdot \exp(-kz) \qquad (4.2)$$

where I_0 is irradiance just below the sea surface (μmol quanta m^{-2} s^{-1}), I_m is maximal irradiance at the sea surface at noon (assumed to be 2000 μmol quanta m^{-2} s^{-1}), D_L is daylength (h, assumed to be 12 h), t is time (h), k is the vertical attenuation coefficient for PAR (0.06 m^{-1}, assumed constant with depth and with time), z is depth (m) and I_z is PAR at depth z (μmol quanta m^{-2} s^{-1}), taken to be the irradiance at the depth of the middle of each box. A complete list of symbols and parameters used in the model is found in Table 4.1.

Changes in POC or PON in each layer are the net result of uptake from pools of dissolved inorganic carbon or dissolved inorganic nitrogen and/or increases or decreases in

Table 4.1: Model variables and parameters. Multiple numbers in the Value column refer to rates for nitrate-replete biomass and rates for nitrate-depleted biomass, respectively, and are used to define the range between which the actual value in the model varies (see equations 4.9, 4.10, and 4.11 in text).

Symbol	Definition	Value	Units
I	Irradiance		µmol quanta m^{-2} s^{-1}
I_o	Surface irradiance	variable	µmol quanta m^{-2} s^{-1}
I_m	Max surface irradiance (noon)	2000	µmol quanta m^{-2} s^{-1}
D_L	Daylength	12	h
t	Time		h
z	Depth		m
Δz	Depth interval between boxes	10	m
k	Vertical attenuation coefficient	0.06	m^{-1}
POC_n	Particulate carbon in box n		mg m^{-3}
PON_n	Particulate nitrogen in box n		mg m^{-3}
Γ_n	Absolute C uptake		mg C m^{-3} h^{-1}
Ψ	Descent velocity	variable	m h^{-1}
A	Ascent velocity	variable	m h^{-1}
l_n	Specific loss rate in box n	variable	h^{-1}
R_n	Specific respiration rate in box n	variable	h^{-1}
P^N	N-specific carbon uptake rate		mg C mg N^{-1} h^{-1}
P^N_s	Maximum potential rate of photosynthesis	0.173, 0.085	mg C mg N^{-1} h^{-1}
α^N	Initial slope of the P-I curve	0.0016, 0.0013	(mgC mgN^{-1} h^{-1}) (µmol quanta m^{-2} s^{-1})$^{-1}$
β^N	Parameter of photoinhibition	4.4×10^{-5}, 1.31×10^{-5}	(mgC mgN^{-1} h^{-1}) (µmol quanta m^{-2} s^{-1})$^{-1}$
Σ	Absolute N uptake rate		mg N m^{-3} h^{-1}
V	N-specific nitrate uptake rate	0.02	h^{-1}

POC or PON due to migration into or out of the layer, and losses from the layer. Losses due to respiration also occur from the POC pool, and are modeled separately from other losses (assumed to be due to grazing, sinking, etc.). Ascending biomass has been modeled separately from sinking biomass (refer to Fig. 4.1), therefore, the total biomass in each layer is the sum of the ascending and sinking biomass. For ascending biomass (boxes on the left hand side of Fig. 4.1, excluding boxes 1 and 12 which will be discussed in section 4.2.2 below),the general equations describing changes in POC or PON are:

$$\frac{dPOC_n}{dt} = \left[\left(\Gamma_n\right) + \left(\left({}^{A_{n-1}}/_{\Delta z}\right) \cdot POC_{n-1}\right)\right] - \left[\left(\left({}^{A_n}/_{\Delta z}\right) \cdot POC_n\right) + \left(l_n \cdot POC_n\right) + \left(R_n \cdot POC_n\right)\right] \quad (4.3)$$

and

$$\frac{dPON_n}{dt} = \left[\left(\Sigma_n\right) + \left(\left({}^{A_{n-1}}/_{\Delta z}\right) \cdot PON_{n-1}\right)\right] - \left[\left(\left({}^{A_n}/_{\Delta z}\right) \cdot PON_n\right) + \left(l_n \cdot PON_n\right)\right] \quad (4.4)$$

where POC_n and PON_n are the concentrations of POC and PON (mg m^{-3}) in box n, POC_{n-1} and PON_{n-1} are the concentrations of POC and PON (mg m^{-3}) in box n-1 (which is below box n), Γ_n is the absolute carbon uptake (defined below) (mg C m^{-3} h^{-1}), A_{n-1} is the ascent velocity of material moving up from box n-1 (m h^{-1}), A_n is the ascent velocity of material leaving box n (m h^{-1}), Σ_n is the absolute nitrate uptake rate (defined below) (mg N m^{-3} h^{-1}), Δz is the depth interval between boxes (10 m), R_n is the specific respiration rate (h^{-1}) (see below), and l_n is the specific loss rate of material from box n (h^{-1}) due to processes other than respiration. In the base model, the specific loss rate was assumed to be constant with depth. To obtain a steady state solution, the value of l_n was adjusted iteratively so that losses balanced increases in surface POC and PON for at least 5 successive migration cycles and was later confirmed when calculated fluxes of POC and PON did not differ over at least 3 migration cycles. Thus, the model calculates specific rate of increase; losses due to respiration are also accounted for by first running the model with specific respiration rate set to zero, then re-running the model with specific respiration rate

set to 10% of the specific rate of increase determined by the previous model run. For all variations of the model, the loss term, l_n, represents the sum of all possible "losses" of biomass from the system, including grazing and irreversible sinking of biomass out of the system.

For sinking biomass (boxes on the right hand side of Fig. 4.1, excluding boxes 13 and 24 which will be discussed in section 4.2.2 below), changes in POC and PON were described by

$$\frac{dPOC_n}{dt} = \left[\left(\Gamma_n\right) + \left(\left({}^{\Psi_{n+1}}/_{\Delta z}\right) \cdot POC_{n+1}\right)\right] - \left[\left(\left({}^{\Psi_n}/_{\Delta z}\right) \cdot POC_n\right) + \left(l_n \cdot POC_n\right) + \left(R_n \cdot POC_n\right)\right] \quad (4.5)$$

and

$$\frac{dPON_n}{dt} = \left[\left(\Sigma_n\right) + \left(\left({}^{\Psi_{n+1}}/_{\Delta z}\right) \cdot PON_{n+1}\right)\right] - \left[\left(\left({}^{\Psi_n}/_{\Delta z}\right) \cdot PON_n\right) + \left(l_n \cdot PON_n\right)\right] \quad (4.6)$$

where POC_{n+1} and PON_{n+1} are the concentrations of POC and PON (mg m^{-3}) in box $n+1$ which is just above box n, Ψ_n is the descent velocity of material from box n (m h^{-1}) and Ψ_{n+1} is the descent velocity of material from box $n+1$ into box n.

In all equations, absolute carbon uptake, Γ_n, is defined as:

$$\Gamma_n = P^N \cdot PON_n \quad (4.7)$$

where P^N is the nitrogen specific carbon uptake rate (mg C mg N^{-1} h^{-1}) formulated according to the equation of Platt et al. (1980):

$$P^N = P_s^N \left(1 - e^{\left(-\alpha^N I / P_s^N\right)}\right)\left(e^{\left(-\beta^N I / P_s^N\right)}\right) \quad (4.8)$$

except that P^N is the rate of photosynthesis normalized to PON (mg C mg N^{-1} h^{-1}) rather than to chlorophyll, P^N_S is the maximum rate of photosynthesis in the absence of photoinhibition (mg C mg N^{-1} h^{-1}), I is irradiance (µmol quanta m^{-2} s^{-1}), α^N is the initial slope of the photosynthesis-irradiance (P-I) curve (mg C mg N^{-1} h^{-1} (µmol quanta m^{-2} s^{-1}) $^{-1}$), and β^N is a parameter which characterizes photoinhibition (mg C mg N^{-1} h^{-1} (µmol quanta m^{-2} s^{-1})$^{-1}$).

Values used for the parameters P^N_S, α^N, and β^N were determined experimentally by Richardson et al. (1996) (see Table 4.1). These values were determined at 20°C, thus the value for P^N_S in the surface (0-10 m) layer was multiplied by a Q_{10} of 2.6 (Li and Morris 1982) to account for the increase in P^N_S expected at a surface temperature of near 30°C. Values used for the photosynthetic parameters in the model also varied depending on whether the biomass was nitrate-replete or nitrate-depleted (see Richardson et al. 1996), thus P^N_S was allowed to vary as a function of C:N ratio according to

$$P_s^N = 0.25 + \left(-0.013 \cdot \left({}^{POC_n}/_{PON_n}\right)\right) \tag{4.9}$$

while α^N varied according to

$$\alpha^N = 0.0018 + \left(-4 \cdot 10^{-5} \cdot \left({}^{POC_n}/_{PON_n}\right)\right) \tag{4.10}$$

and β^N varied according to

$$\beta^N = \left(7 \cdot 10^{-5}\right) + \left(-4.4 \cdot 10^{-6} \cdot \left({}^{POC_n}/_{PON_n}\right)\right) \tag{4.11}$$

Equations 4.9, 4.10, and 4.11 are the equations that describe a linear increase or decrease in the parameter of interest between the range of values shown in Table 4.1. They are constrained by experimental measurements of the P-I parameters of *Rhizosolenia formosa* taken from Richardson et al. (1996).

The absolute nitrate uptake rate (Σ_n) was defined as:

$$\Sigma_n = V \cdot PON_n \tag{4.12}$$

where V is the N-specific uptake rate (h^{-1}). Nitrate uptake rates used for the model were determined experimentally for *Rhizosolenia formosa* (Richardson et al. 1996); V was set to a constant value of 0.02 h^{-1} as Richardson et al. (1996) showed that specific uptake rates of this diatom did not vary significantly with nutritional state or with incubation of cells in the light or in the dark. This value represents the average N-specific uptake rate determined during a 12 h incubation. This is not a maximal or a steady state uptake rate. A specific uptake rate of 0.02 h^{-1} allows luxury consumption of nitrate, that is, cells can take up nitrate in excess of their immediate metabolic requirements (Richardson et al. 1996).

In the base model, movements of biomass were modeled using ascent and descent velocities that varied with the C:N ratio of the biomass at a particular layer. Ascent velocity (A, m h^{-1}) was determined according to

$$A = 13 - \left({}^{POC_n}/_{PON_n}\right) \tag{4.13}$$

Thus, ascent velocity goes to zero when the C:N ratio of the biomass is 13 (mol:mol). During model runs, ascent velocities were never negative because ascending biomass did not exceed C:N ratios of 13. Descent velocity (Ψ) is similarly defined as a function of C:N ratio, as follows:

$$\Psi = \left({}^{POC_n}/_{PON_n}\right) - 8.3 \qquad (4.14)$$

Descent velocities were never negative as the C:N ratio of descending biomass did not fall below 8.3 during the descent. Because ascent and descent velocities are functions of C:N ratio, these values continually change as the C:N ratio of the biomass changes both on a diel basis and due to migration to more highly-illuminated layers, or to the nitrate-rich deep layer of the model. The movements of POC and PON were always in tandem; changes in the ratio of POC to PON in any layer, therefore, was due to differential uptake of DIC or DIN and was not due to differential migrations of POC and PON.

The C:N ratio of each layer was also used to determine when biomass would sink from the surface (0-10 m) layer and when biomass would float up from the deepest (110-120 m) layer. The base model was formulated such that biomass sank from the surface only when *POC/PON* >11.9; biomass ascended from the deepest layer only when *POC/PON* <8.3. Biomass accumulated in the surface or deepest layers until *POC/PON* reached these critical values. Parameterization of the critical values was based on C:N ratios of *Rhizosolenia* collected in the field by Villareal et al. (1996).

4.2.2 Boundary conditions

The model assumed no exchange of material across the air/sea interface and it had a closed bottom boundary. There was no horizontal advection, and there was no exchange between ascending and sinking biomass except at the top (0-10 m) and bottom (110-120 m) boundaries. Exchange of material occurred only when the C:N ratio of the top and bottom boxes reached 11.9 and 8.3 (mol:mol), respectively. Changes in POC and PON in the top boundary boxes (Boxes 12 and 24, refer to Fig. 4.1) can be described by the following equations. For Box 12:

$$\frac{dPOC_{12}}{dt} = \left[(\Gamma_{12}) + \left((A_{11}/\Delta z) \cdot POC_{11}\right)\right] - \left[(½ \cdot POC_{12}) + (l_{12} \cdot POC_{12}) + (R_{12} \cdot POC_{12})\right] \quad (4.15)$$

and

$$\frac{dPON_{12}}{dt} = \left[(\Sigma_{12}) + \left((A_{11}/\Delta z) \cdot PON_{11}\right)\right] - \left[(½ \cdot PON_{12}) + (l_{12} \cdot PON_{12})\right] \quad (4.16)$$

For Box 24:

$$\frac{dPOC_{24}}{dt} = \left[(\Gamma_{24}) + (½ \cdot POC_{12})\right] - \left[\left((A_{24}/\Delta z) \cdot POC_{24}\right) + (l_{24} \cdot POC_{24}) + (R_{24} \cdot POC_{24})\right] \quad (4.17)$$

and

$$\frac{dPON_{24}}{dt} = \left[(\Sigma_{24}) + (½ \cdot PON_{12})\right] - \left[\left((\Psi_{24}/\Delta z) \cdot PON_{24}\right) + (l_{24} \cdot PON_{24})\right] \quad (4.18)$$

The expression $½ \cdot POC_n$ or $½ \cdot PON_n$ represents the amount of biomass transferred between boxes in the same layer, i.e. one half of the biomass was transferred every hour. The specific transfer rate of ½ was chosen so that C:N ratios did not exceed the range of possible values established experimentally. Specific transfer rates greater than ½ did not noticeably affect model results. Changes in POC and PON in the bottom boundary boxes (1 and 13, refer to Fig. 4.1) are described by the following equations. For Box 1:

$$\frac{dPOC_1}{dt} = \left[(\Gamma_1) + (½ \cdot POC_{13})\right] - \left[\left((A_1/\Delta z) \cdot POC_1\right) + (l_1 \cdot POC_1) + (R_1 \cdot POC_1)\right] \quad (4.19)$$

and

$$\frac{dPON_1}{dt} = \left[(\Sigma_1) + (½ \cdot PON_{13})\right] - \left[\left((A_1/\Delta z) \cdot PON_1\right) + (l_1 \cdot PON_1)\right] \quad (4.20)$$

For Box 13:

$$\frac{dPOC_{13}}{dt} = \left[\left(\Gamma_{13}\right) + \left(\left(\Psi_{14}/\Delta z\right) \cdot POC_{14}\right)\right] - \left[\left(\tfrac{1}{2} \cdot POC_{13}\right) + \left(l_{13} \cdot POC_{13}\right) + \left(R_{13} \cdot POC_{13}\right)\right] \quad (4.21)$$

and

$$\frac{dPON_{13}}{dt} = \left[\left(\Sigma_{13}\right) + \left(\left(\Psi_{14}/\Delta z\right) \cdot PON_{14}\right)\right] - \left[\left(\tfrac{1}{2} \cdot PON_{13}\right) + \left(l_{13} \cdot PON_{13}\right)\right] \quad (4.22)$$

4.2.3 Initial conditions and other assumptions:

This model considers only the contributions of *Rhizosolenia* to carbon and nitrogen fluxes and assumes that diffusive processes and advective processes other than migration of the diatoms are negligible. The growth of *Rhizosolenia* is assumed to be dependent entirely on nitrate; there is no consideration of possible ammonia-based growth. It is also assumed that these *Rhizosolenia* contain no nitrogen fixing endosymbionts as had been observed by Alldredge and Silver (1982) and Martinez et al. (1983), but later challenged by Villareal (1987) and Villareal and Carpenter (1989).

The model starts with biomass evenly distributed from top to bottom in a C:N ratio of 8.3 (mol:mol). Variations in the initial distribution of biomass or in the initial C:N ratio did not alter the final results of the model. Initial abundances of POC and PON (180 μmol C m^{-2} and 22 μmol N m^{-2}) were determined from literature data on *Rhizosolenia* mats in the Central North Pacific Gyre. These abundances were calculated from average values of 0.3 mats m^{-3} and 2.5 μmol N mat^{-1} (Villareal and Carpenter 1989) integrated to 30 m depth. Initial POC was calculated by multiplying initial PON by 8.3 (mol:mol).

4.3 Variations in the Base Model

To test the sensitivity of the model to changes in various parameters, the base model was altered by changing either the function which determines ascent or descent velocities, the critical values of C:N at which biomass sinks from the top or floats up from the bottom, or the amplitude of the loss term with depth.

4.3.1 Variations in ascent and descent velocities

The effect of variations in ascent and descent velocities was determined by setting ascent and descent velocities to constant values of 3 m h^{-1}, 6 m h^{-1}, and 8 m h^{-1} instead of making them a function of C:N ratio as in the base model. Critical C:N ratios for sinking and floating were still applied, as in the base model. The range of ascent and descent velocities was chosen based on data for mats of *Rhizosolenia* in the Central North Pacific Gyre (Villareal and Carpenter 1989, Villareal et al. 1996). The velocity of 8 m h^{-1} is among the highest of ascent rates determined in the field, but was chosen to determine the sensitivity of the model to high ascent and descent velocities.

4.3.2 Variations in critical values of C:N for sinking and floating

To test the sensitivity of the model to choice of C:N criterion for sinking or floating, the critical C:N was varied as shown in Table 4.2. Choice of variations of the critical values was based partly on the range of C:N ratios of sinking and floating mats of *Rhizosolenia* in the Central North Pacific Gyre (Villareal et al. 1996), and partly on the minimum (7 mol:mol) and maximum (15 mol:mol) values of C:N obtained for N-replete and N-depleted cells during batch culture experiments (Richardson et al. 1996). Richardson et al. (1996) made measurements of cell buoyancy, though these measurements were on cultures of a single species of *Rhizosolenia* and not on multi-species mats found commonly in the Central North Pacific Gyre (Villareal et al. 1993, 1996), thus the data of Villareal et al. was

Table 4.2: Variations of critical C:N ratios (mol:mol) for sinking and floating.

C:N to sink	C:N to float
POC/PON > 11.9	POC/PON < 9.5
POC/PON > 10.7	POC/PON < 7.1
POC/PON > 15.4	POC/PON < 8.3

thought to be more relevant to this model of open-ocean vertical migration. As well, Villareal et al. (1996) had C:N ratios of mats that had been separated according to positive or negative buoyancy, thus better reflecting the composition of floating and sinking mats than C:N ratios done on a mixture of positively buoyant and negatively buoyant cells, as was done by Richardson et al. (1996).

4.3.3 Variations in the amplitude of loss term with depth

The base model had losses occurring equally from all layers. To test the sensitivity of the model to variations in specific loss rate with depth, the amplitude of the loss term was adjusted so that losses occurred 1) only from the top layer of the model (i.e., the specific loss rate of all other boxes was set to zero), 2) only from the bottom layer of the model, or 3) from the top and bottom layers only, but not from the middle boxes. As with the base model, the specific loss rate was adjusted to balance gains in surface POC and PON. The model was deemed to be in steady state when the net rate of increase of surface POC and PON was zero for at least 5 successive migration cycles; the model reached steady state no later than the third migration cycle of the model run. Rationale for the choice of the loss variations is in section 4.5.1.

4.3.4 Calculations

Equations 4.3 to 4.6 and 4.15 to 4.22 were solved by Euler integration with a time step of 0.25 h using Stella for Macintosh, version 2.2.1. Each model was run for 900 h (approximately 9 full migration cycles). Output from the model made possible the calculation of: 1) fluxes of POC and PON, 2) migration cycle times, 3) specific rates of increase, and 4) vertical distributions of POC and PON.

Fluxes of POC and PON into the euphotic zone were defined as the upward flux of biomass across the 110 m interface, i.e., from the 110-120 m layer to the 100-110 m layer (or, from box 1 to box 2 in Fig. 4.1). Fluxes of POC and PON out of the euphotic zone

were defined as the downward flux of biomass across the 110 m interface, i.e., from the 100-110 m layer to the 110-120 m layer (or, from box 14 to box 13 in Fig. 4.1). Fluxes were calculated as the product of the ascent or descent velocity and the concentration of biomass in each box at intervals of 0.5 h. Average flux was calculated for an entire migration cycle and was expressed as μmol C or μmol N m^{-2} d^{-1}, then, since there were small variations in the fluxes, an overall average was calculated for the last 3 migration cycles of the model run. Two types of fluxes were calculated, gross and net, net flux being calculated as the difference between gross upward and downward fluxes.

Initially, POC and PON were distributed uniformly with depth. However, the residence time required to reach critical C:N ratios for sinking or floating caused accumulations of biomass in the top and bottom layers. Thus, once the model was in steady state, the biomass moved as "waves" of POC and PON. As the biomass moved through a migration cycle, peaks were observed in surface POC and PON. The total migration cycle time, therefore, was determined by calculating the time difference between peaks of surface POC and PON, and was confirmed by calculating the time difference between peaks of upward and downward fluxes.

Vertical distribution of biomass in steady state was calculated by dividing the total amount of biomass in each layer (ascending plus sinking biomass) over a complete migration cycle by the total water column biomass over the same cycle. Vertical distribution was then expressed as a percentage of total POC or PON.

4.4 Results

4.4.1 Base Model Predictions

Using the initial biomass of 180 μmol C m^{-2} and 22 μmol N m^{-2}, the base model predicted a net downward flux of POC of 12 μmoles C m^{-2} d^{-1} and a net upward flux of

PON of 3 μmoles N m^{-2} d^{-1}. The specific rate of increase predicted by the model was 0.12 d^{-1}, while the total migration cycle time was predicted to be 4 d. The predicted vertical distribution of POC was approximately 22% in the surface 10 m, 26% in the bottom 10 m, with the remainder of the biomass distributed through the water column (Fig. 4.2a). Particulate organic nitrogen had a similar predicted distribution, with 21% of the PON being found in the surface box, 28% in the bottom box and the remainder of the biomass distributed approximately evenly through the remainder of the water column (Fig. 4.2a). An uncoupling of the distribution of PON from POC was observed, i.e., the percentage of PON found in the deepest layer was higher than the percentage of POC; the opposite was true for the surface layer. The base model had ascent and descent velocities that were a function of the C:N ratio of biomass in each layer. The range of C:N ratios throughout the model (i.e. considering biomass moving at all depths) was between 7.1 and 15 (mol:mol), which corresponds to ascent and descent velocities between 0 and 6 m h^{-1}. Ascent and descent velocities used for flux calculations (i.e. velocities of biomass moving up from and down to the deepest layer, respectively) varied between 3 and 6 m h^{-1}.

4.4.2 Variations in ascent and descent velocities

Variations in ascent and descent velocities affected the fluxes of POC and PON (Fig. 4.3), the specific rate of increase, and the total migration cycle time (Table 4.3) and the predicted vertical distribution of POC and PON (Fig. 4.2). Net flux of POC was in the downward direction and increased in a non-linear fashion with increasing ascent and descent velocity (Fig. 4.3). Net flux of PON was in the upward direction; net flux increased with increasing ascent and descent velocities until rates of 6 m h^{-1}, after which there was no increase in the net upward flux of nitrogen. Total migration cycle time decreased with increasing ascent and descent velocities until 6 m h^{-1}, beyond which changes were small. Increasing ascent and descent velocities to 10 m h^{-1} (output not shown) also resulted in no detectable increases in net upward flux of PON and migration

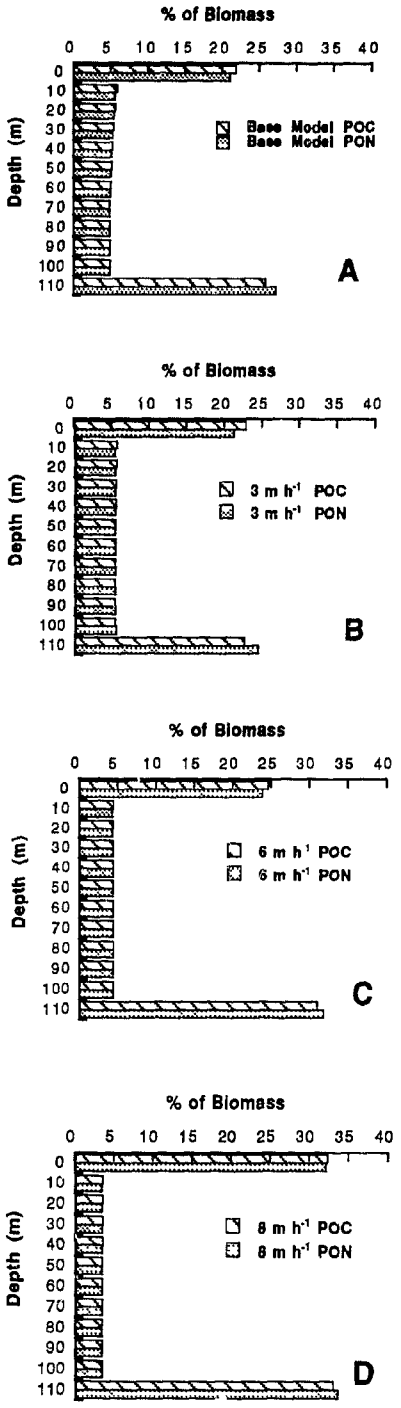

Fig. 4.2: Predicted vertical distributions of POC and PON for A) the base model, and for models with ascent and descent velocities set to constant values of B) 3 m h^{-1}, C) 6 m h^{-1}, and D) 8 m h^{-1}.

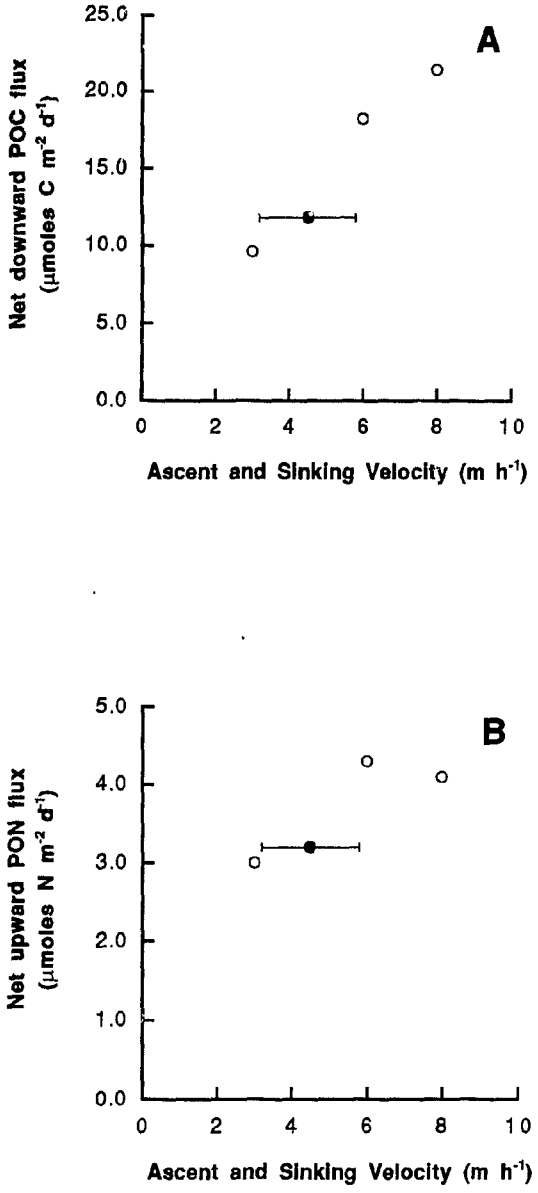

Fig. 4.3: A) Net downward flux of POC and B) net upward flux of PON for the base model (solid symbols) and for models where ascent and descent velocity are set at a constant values of 3 m h^{-1}, 6 m h^{-1}, or 8 m h^{-1}. As indictated by range bars on the solid symbols, the ascent and sinking velocity used for flux calculations from the base model varied between 3.3 and 5.8 m h^{-1}.

Table 4.3: Predicted upward, downward, and net fluxes of POC and PON, specific rates of increase, and total migration cycle times with variations in ascent and descent velocities.

Flux (μmol m^{-2} d^{-1})	Base Model	3 m h^{-1}	6 m h^{-1}	8 m h^{-1}
Upward POC	79.9	67.4	124.4	121.0
Downward POC	91.7	77.1	142.6	142.5
Net flux POC (down)	**11.8**	**9.6**	**18.2**	**21.4**
Upward PON	10.4	8.8	16.1	15.6
Downward PON	7.2	5.8	11.7	11.5
Net flux PON (up)	**3.2**	**3.0**	**4.3**	**4.1**
Specific rate of increase (d^{-1})	**0.12**	**0.11**	**0.14**	**0.15**
Total migration cycle time (d)	**4.0**	**5.0**	**3.0**	**3.0**

cycle time did not decrease. Specific rates of increase predicted by the model increased slightly with increased ascent and descent velocities. With respect to predicted vertical distribution of biomass, as ascent and descent velocity increased, the highest percentages of biomass were found at the surface and in the deepest layer (Fig. 4.2). All ascent and descent velocity variations showed an uncoupling between the percentages of POC and PON found at the surface and in the deep boxes as described for the base model, above.

4.4.3 Variations in critical C:N for sinking and floating

Variations in the C:N ratio at which biomass sank or floated affected the predicted vertical distribution of biomass (Fig. 4.4). In general, the lower or higher the critical C:N, the longer the amount of time required in the surface or deep box, respectively, to reach the critical C:N, the greater the percentage of total migration cycle time spent in the box, and, therefore, the greater the predicted percentage of biomass found in the box. A greater range between critical C:N ratios resulted in more time being spent in the top and bottom boxes, (and less time at mid-depths) and therefore a greater percentage of total POC and PON in the top and bottom boxes (see Fig. 4.4c).

Variations in the C:N ratio at which biomass sank or floated affected, to some extent, the magnitude of the predicted flux of POC, though there was no detectable difference in the flux of PON (Table 4.4). The total time of the migration cycle increased slightly compared to the base model when the critical C:N ratios were changed to 10.7 (for sinking) and 7.1 (for floating) and to 15.4 (for sinking) and 8.3 (for floating). Increases in specific rate of increase were detected only when the critical C:N ratio for sinking was increased to 15.4.

4.4.4 Variation of the amplitude of the loss term with depth

Variation of the amplitude of the loss terms affected the magnitude of the net fluxes of POC and PON (Table 4.5), but did not greatly affect the predicted vertical distribution of

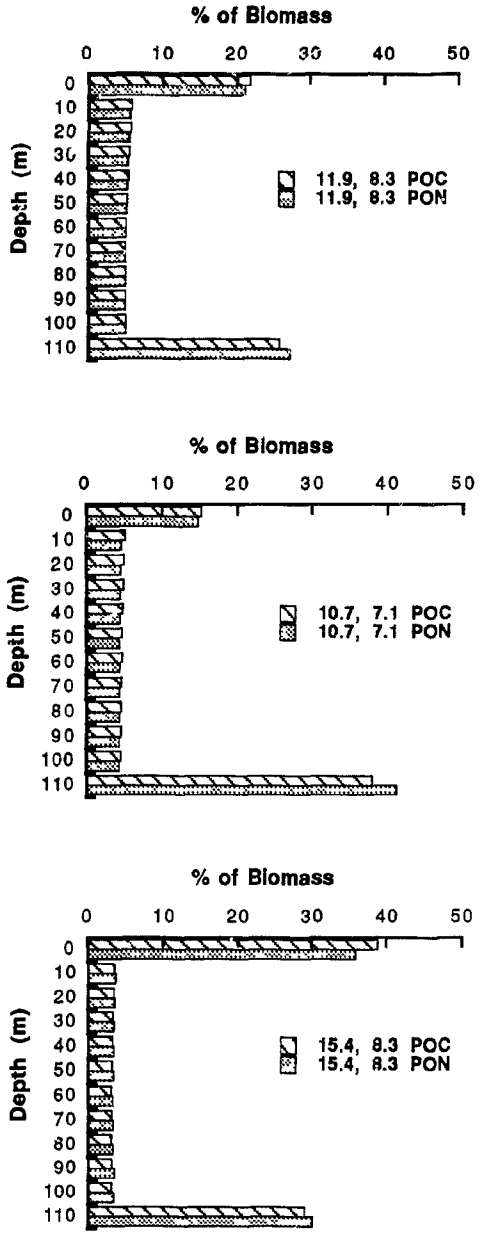

Fig. 4.4: Predicted vertical distributions of POC and PON for variations in critical C:N ratios (all mol:mol) for sinking and floating. A) base model, where sinking occurred when the C:N ratio reached 11.9 and floating occurred when biomass reached C:N = 8.3, B) sinking occurred when C:N reached 10.7 and floating when C:N reached 7.1, C) sinking occurred when C:N reached 15.4 and floating when C:N reached 8.3.

Table 4.4: Predicted upward, downward, and net fluxes, specific rates of increase, and migration cycle times for variations in critical C:N ratios (mol:mol) for sinking and floating.

Flux (μmol m^{-2} d^{-1})	Base Model C:N Sink = 11.9 C:N Float = 8.3	C:N Sink = 10.7 C:N Float = 7.1	C:N Sink = 15.4 C:N Float = 8.3
Upward POC	79.9	65.4	64.2
Downward POC	91.7	79.6	79.4
Net flux POC (down)	**11.8**	**14.2**	**15.2**
Upward PON	10.4	9.5	8.4
Downward PON	7.2	6.6	5.16
Net flux PON (up)	**3.2**	**2.9**	**3.2**
Specific rate of increase (d^{-1})	**0.12**	**0.12**	**0.14**
Migration Cycle Time (d)	**4.0**	**4.3**	**5.0**

Table 4.5: Predicted upward, downward, and net fluxes of POC and PON, specific rates of increase, and migration cycle times with variations in the amplitude of the loss term with depth. For models where losses were not uniform with depth, the specific rate of increase has been calculated from the actual loss rate used in the model and the percentage of total cycle time that the loss was applied. See Table 4.6 for unadjusted loss rates and conversion factors and see text for details.

Flux (μmol m^{-2} d^{-1})	**Base Model (Loss even with depth)**	**Top losses only**	**Bottom losses only**	**Top and bottom loss**
Upward POC	79.9	88.4	93.5	94.4
Downward POC	91.7	89.2	151.7	123.3
Net flux POC (down)	**11.8**	**0.8**	**58.2**	**28.9**
Upward PON	10.4	11.5	12.1	12.3
Downward PON	7.2	7.1	12.1	9.9
Net flux PON (up)	**3.2**	**4.4**	**0**	**2.4**
Specific rate of increase (d^{-1})	**0.12**	**0.12**	**0.12**	**0.12**
Migration Cycle Time (d)	**4.0**	**4.0**	**4.0**	**4.0**

biomass (Fig. 4.5). Total migration cycle time was not affected by variation in the amplitude of the loss term with depth (Table 4.5). As with all other models, the percentage of POC was predicted for the surface layer was higher than the percentage of PON, but higher PON than POC was predicted for the deepest box. Loss rates required to balance increases in POC and PON are shown in Table 4.6. Where losses were not applied uniformly with depth, loss rates were converted to specific rates of increase by multiplying the loss rate used in the model by the fraction of the total migration cycle time during which the loss rate was applied which is taken from the expected vertical distribution of biomass for the base model (see Table 4.6). The conversion of loss rate used for each variation of the base model to specific rate of increase resulted in rates identical to those of the base model (Table 4.6).

4.5 Discussion

4.5.1 Potential sources of error

The many assumptions made in this model should be outlined clearly. First, the model assumes that the net growth of *Rhizosolenia* is entirely dependent upon nitrate and that uptake and use of ammonia is negligible. The nitrogen preferences of *Rhizosolenia* have not been investigated, however, the $\delta^{15}N$ signature of material collected in the field suggests that the predominant source of nitrogen for *Rhizosolenia* is one relatively enriched in ^{15}N (Villareal et al. 1993). Enrichment in ^{15}N is indicative of a deep water source of N; near-surface sources are relatively enriched in ^{14}N (Altabet 1988). The deep water source of N may be nitrate, as high intracellular concentrations are found in this organism (Villareal and Lipschultz 1995, Villareal et al. 1996). The large size of *Rhizosolenia* may also preclude the use of nanomolar levels of ammonia found in areas such as the Central

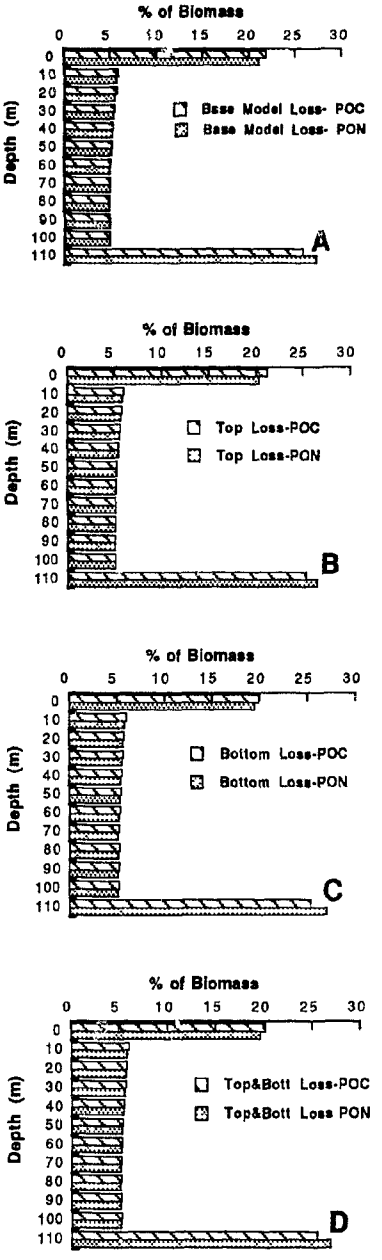

Fig. 4.5: Predicted vertical distributions of POC and PON for variations in the amplitude of the loss term with depth. A) base model, where losses occurred uniformly with depth at a specific loss rate of 0.12 d^{-1}, B) where losses occurred from the top layer of the model only, at a specific rate of 0.58 d^{-1}, C) where losses occurred only from the bottom layer of the model, at a rate of 0.46 d^{-1}, and D) where losses occurred from the top and bottom layers only, but not at mid-depths, at a rate of 0.26 d^{-1}.

Table 4.6: Calculation of adjusted loss rates for models where the amplitude of the loss term with depth was varied.

Loss model variation	Loss rate in model (d^{-1})	Fraction of migration cycle time applied	= Adjusted loss rate (d^{-1})
Top loss only	0.58	0.21	0.12
Bottom loss only	0.46	0.26	0.12
Top and bottom loss	0.26	0.22+0.26=0.48	0.12

North Pacific Gyre if the half-saturation constant of this organism is high enough to prevent uptake of enough ammonia to support growth (see Eppley et al. 1969).

The model assumes that buoyancy reversals and timescales of buoyancy changes are directly related to the C:N ratio of the biomass. The use of C:N criteria to determine buoyancy reversals was based primarily on data collected in the field, where mats of *Rhizosolenia* were sorted into positively buoyant, neutrally buoyant, and negatively buoyant fractions with C:N analysis being performed on the separate fractions (Villareal et al. 1996). Laboratory experiments have also shown that decreases in C:N ratio are correlated with increases in buoyancy, and that these increases occurred within 12 h of re-introduction of nitrate to culture medium (Richardson et al. 1996). Other mechanisms of buoyancy change (such as ionic regulation) may also be responsible (see Smayda 1970), The separate formulations of ascent and descent velocity takes these unknowns partly into account. For example, according to equations 4.13 and 4.14, a cell with a C:N ratio of 9.5 (mol:mol) could have either an ascent velocity of 3.5 m h^{-1} or a descent velocity of 1.2 m h^{-1}. While at first this may seem counterintuitive, it reflects the fact that C:N may not be the only determinant of buoyancy, and that cells of similar C:N ratio could have different buoyancy. The use of different formulations for ascent and descent velocity (and thus the potential for conflicting velocities) causes no problems in the model runs because ascending and sinking biomass were modeled separately and thus were only subject to one velocity formulation at a time.

By having a bottom boundary, the model assumes that biomass cannot sink deeper than 120 m. In nature, cells may sink more than 10 m (the depth of the bottom box in the model) before buoyancy reversals occur, thus they would exceed the 120 m vertical extent of the migration cycle imposed by the model. Thus, migration cycle times predicted by this model would be underestimated and the resulting fluxes of POC and PON would be overestimated. According to the model, biomass entering the bottom layer with a C:N ratio of 13 would be sinking at a rate of 4.7 m h^{-1}, which means that it would take only 2 h to

sink through the 10 m bottom layer. Decreases in descent rate will occur, however, as the C:N ratio of the biomass decreases because of uptake of nitrate from the bottom box.

Though ascent and descent velocities and the relationships between chemical composition and buoyancy used to parameterize the critical C:N ratios in the model were based on field data (Villareal and Carpenter 1989, Villareal et al. 1993), rates of nitrate uptake and photosynthesis were determined in the laboratory on monospecific cultures of *Rhizosolenia formosa* (Richardson et al. 1996). *Rhizosolenia* mats found in the open ocean are composed of several species, many of which are much larger than *R. formosa* and may differ physiologically (T.A. Villareal, pers. comm.). While acknowledging the differences between relatively small, monospecific cultures and multi-species mats of *Rhizosolenia*, and the application of rates determined from these cultures to a model of open ocean processes, I argue that the use of these rates was justified. First, no previous measurements of nitrate uptake rates had been made for this organism, thus, these were the only data available. Second, applying a Q_{10} of 2.6 to maximum photosynthetic rates of cells at the surface brought these values within the range of rates determined for *Rhizosolenia* in the field, at least for cells in the top layer of the model. Yoder et al. (1994) determined a P^B_{max} of 5.7 g C g Chl^{-1} d^{-1} for *Rhizosolenia* collected in the Equatorial Pacific and Alldredge and Silver (1982) measured a P^B_{max} of 5.8 g C g Chl^{-1} d^{-1} for cells from the North Pacific. These values are near the P^B_{max} used in the model. In comparable units for nitrate-replete cells, I used 2.6 g C g Chl^{-1} d^{-1} multiplied by a Q_{10} of 2.6 which converts to 6.8 g C g Chl^{-1} d^{-1}.

4.5.2 Migration cycle times and specific rates of increase

The time for one complete migration cycle was estimated by the model to be between 3 and 5 d. These values agree well with the range of 3.6 to 5.4 d estimated by Villareal et al. (1996) who used measurements of photosynthetic rates, ascent and descent velocities, estimates of nitrate uptake, and an implicit assumption of one migration cycle per

generation time. In general, migration cycle times decreased with increasing ascent and descent velocity. The fastest migration cycle times of 3 d were predicted by models that used a constant value of 6 and 8 m h^{-1} for ascent and descent velocity. However, because of the time required by cells to reach critical C:N ratios in the top and bottom layers of the model, the total cycle time was not significantly decreased by increasing ascent and descent velocity past 6 m h^{-1}. Total migration cycle time was increased to 5 d from 4 d when the critical C:N of the base model was altered to a critical C:N of 15 for sinking, due to the increased time required in the top layer to reach a C:N of 15. Variations in the amplitude of the loss term with depth did not significantly affect the total migration cycle time because migration cycle time is dependent upon ascent and descent velocities and on how fast carbon and nitrogen are accumulated so that the biomass reaches the critical C:N ratios, none of which are affected by changes in the amplitude of the loss term with depth.

Specific rates of increase in POC and PON predicted by the model varied between 0.11 and 0.15 d^{-1}; the lowest and highest rates being predicted by models with the slowest and fastest ascent and descent velocities. Increasing ascent and descent velocities increased the proportion of time that biomass could accumulate carbon and nitrogen, resulting in increased specific rates of increase.

4.5.3 Vertical distribution of *Rhizosolenia* in steady state

The vertical distribution of *Rhizosolenia* in steady state was affected by variations in ascent and descent velocities and by variations in the critical C:N ratios for sinking and floating, but was not affected by variations in the amplitude of the loss term with depth. As ascent and descent velocities increased, smaller percentages of biomass were found at mid-depths consistent with faster transit times between top and bottom layers. Variations in the critical C:N ratios for sinking and floating changed the expected vertical distribution as compared to the base model. A higher percentage of cells in the surface layer (>35%)

compared to the base model (20%) was predicted by the model that had a critical C:N ratio of 15 rather than 11.9, due to the increased amount of time necessary at the surface for biomass to reach a C:N ratio of 15. Similarly, the model with critical C:N for sinking of 10.7 had only 15% of the biomass found in the surface layer, as less time was required at the surface to reach a C:N ratio of 10.7 compared with 11.9 or 15.

Vertical distributions of biomass predicted by the model are only partly supported by observations of the vertical distribution of *Rhizosolenia* in nature. Accumulations of biomass at the surface gradually decreasing with depth have been reported (Alldredge and Silver 1982, Martinez et al. 1983, Villareal and Carpenter 1989, Villareal et al. 1993, Villareal et al. 1996), especially during periods of low winds over several days (Villareal et al. 1996). This is consistent with the predicted accumulation of *Rhizosolenia* in the top 10 m of the model. To date, however, no accumulations of biomass have been found near the top of the nutricline. This is not surprising because, in nature, there is no bottom boundary at which biomass can accumulate while there is a top boundary, i.e. the sea surface.

It is also important to note that, when running the model, I have made the assumption that the water column is completely static and that physical processes such as vertical and horizontal advection, upwelling, and wind-induced mixing are negligible. The effect of physical processes on the vertical distribution of biomass would be to distribute the biomass more evenly through the water column, the degree being dependent on the degree to which the water column is being mixed.

4.5.4 Fluxes of POC and PON

Fluxes of POC and PON due to migrations of *Rhizosolenia* were more greatly affected by variations in the amplitude of the loss term with depth than by variations in critical C:N ratios or ascent and descent velocities. Overall, variation in the amplitude of the loss term with depth affected the magnitude of gross and net fluxes due to differential effects on gains and losses of biomass. Variations of the model applied losses at different

stages of the migration cycle and, thus, for varying periods of time. A higher loss rate was required to balance increases in biomass when losses occurred only in the top layer, for example, because losses occurred only during the time the biomass was in the top layer and not during the entire migration cycle. The model was very sensitive to where (and therefore when) losses were applied as compared to where (and when) accumulations of biomass occurred.

When losses were applied only to the top layer of the model, the net downward flux of POC was reduced compared to the base model where losses were uniformly distributed with depth. This reduction in net downward flux of POC occurred primarily because the gross downward flux of POC was reduced (compared to the base model) because POC was removed from the top layer and therefore less was available to return to deeper layers. Also, the gross upward flux of POC was increased (compared to the base model) because POC was not lost (except to respiration) during residence in deeper layers. The application of losses only to the top of the model increased the net upward flux of PON slightly because no losses were applied at the depth where PON accumulated (the deepest box) resulting in an increase in the gross upward flux of PON.

Application of losses only to the bottom layer of the model also greatly affected both gross and net fluxes of POC and PON. First, the magnitude of both gross upward and downward fluxes was increased compared to the base model because losses were *not* applied to layers where most of the POC accumulated, i.e. losses were applied only in the poorly-illuminated bottom layer where POC increase was minimal. The absence of losses from surface layers (where most POC accumulation occurred) also resulted in a larger downward flux of POC. Both of these factors combined resulted in a greater overall net downward flux of POC as compared to the case where losses were applied uniformly with depth.

The application of losses to the top and bottom layers, but not to mid-depths, resulted in net and gross fluxes similar to those of the base model, though the net

downward flux of POC was slightly higher. This may be due to increases in POC that occurred during the transit time from the top to the bottom layer. Since nitrate was available only in the bottom layer, the flux of PON was not greatly influenced by the reduction of losses in the mid-depth range.

The choice of variations in the amplitude of the loss term with depth was somewhat arbitrary. Very little information exists about the fate of *Rhizosolenia* in the open ocean, especially about the vertical distribution of losses due to sinking and grazing. It was important, however, to examine whether concentration of losses at a particular depth made a difference to fluxes of POC and PON. Concentration of losses at the surface simulated possible grazing by copepods, euphausiids, and protozoans associated with dense surface aggregations of *Rhizosolenia* (Carpenter et al. 1977, Villareal and Carpenter 1989) as has been observed for the bloom-forming cyanobacterium *Trichodesmium* (O'Neil and Roman 1992). Generally, concentration of losses in the top layer assumes that *Rhizosolenia* will be aggregated near the surface (which has been observed in several studies, including Alldredge and Silver 1982, Villareal et al. 1993, and Villareal et al. 1996) and that the distribution of grazers will be directly correlated with food supply, i.e. mats of *Rhizosolenia* (see Longhurst and Harrison 1989). Concentration of losses in the bottom layer of the model simulated irreversible sinking of biomass from the euphotic zone, which might occur if cells were unable to recover from periods of nitrate depletion in surface waters, and any grazing that might occur due to concentration of zooplankton in deeper layers (see Venrick, McGowan, and Mantyla 1973). Losses occurring only from the top and bottom layers represented a combination of these possibilities, as did the uniform distribution of losses with depth. Considering the importance of the variation of loss rate with depth to the predicted fluxes of POC and PON due to migrations of *Rhizosolenia*, further research on associated loss processes is warranted.

In general, increases in ascent and descent velocities of biomass increased both the gross and net fluxes of POC and PON. Fluxes calculated using the base model were

intermediate between those of the model where ascent and descent velocities were held constant at 3 m h^{-1} and those of the model where velocities were held constant at 6 m h^{-1} because the ascent and descent velocities of the base model (used to calculate fluxes) varied as a function of C:N and ranged between 3.2 and 5.8 m h^{-1}. The most unexpected result of variations in ascent and descent velocities was that the net upward flux of PON did not increase past 6 m h^{-1} while the net downward flux of POC continued to increase, though only slightly. This saturation in the net upward flux of PON is the result of the time necessary in the bottom box for biomass to reach the critical C:N ratio for floating. Increasing the ascent velocity did not result in increased flux because the biomass was still "waiting" to reach the critical C:N for floating. Similarly, the total migration cycle time (discussed below) also did not decrease when the ascent and descent velocities were increased to 8 m h^{-1}. Time spent by biomass in the top and bottom layers constrained the total migration cycle time, such that increases beyond 6 m h^{-1} did not affect the total cycle time.

Variations in the critical C:N ratios at which biomass sank or floated only slightly affected the magnitude of the fluxes of POC and PON due to migrations of *Rhizosolenia*. The effects of changing the critical C:N ratios could be manifested in at least three different ways. First, because of the way that the ascent and descent velocities are formulated in the base model, changes in the critical C:N will determine the velocity with which biomass sinks from the top layer or floats up from the bottom layer, which will affect the calculation of flux. Second, the critical C:N will also determine how long the biomass spends in the top and bottom layers, which will in turn affect the total cycle time, and thus will affect the calculation of average flux on a daily basis. Third, the critical C:N determines the concentration of POC or PON that is allowed to accumulate in the top or bottom box, thus affecting the calculation of downward or upward (and therefore net) flux. Overall, however, the model was not particularly sensitive to the choice of critical C:N ratios, especially when compared to the effects of variations in the amplitude of the loss term with

depth on fluxes of POC and PON. In nature, therefore, differences in C:N ratios of cells will not be the key determinant of fluxes of POC and PON due to migrations of *Rhizosolenia*, rather, the vertical distribution of loss processes associated with their growth and their abundance in the water column (see below) will determine their relative contribution to fluxes of carbon and nitrogen.

4.5.5 Relative contributions of *Rhizosolenia* migrations to nutrient cycling and new production in the open ocean

This model so far has considered only one possible initial concentration of *Rhizosolenia* biomass when determining fluxes of POC and PON due to their migrations. The relationship between fluxes of POC and PON and the initial abundance of *Rhizosolenia* can be described by:

$$\phi = \frac{F}{C} \tag{4.23}$$

where F is the net flux of POC or PON (μmol m^{-2} d^{-1}), C is the integrated water column abundance of *Rhizosolenia* in the form of POC or PON (μmol m^{-2}), and ϕ is the flux of POC or PON due to migrations of *Rhizosolenia* normalized to the initial biomass (d^{-1}). Using values of net flux determined from the base model (see Table 4.3, 4.4, or 4.5), the initial abundance of POC and PON, and equation 4.23, the value of ϕ for net downward flux of POC was calculated to be 0.07 d^{-1}, while a value of 0.14 d^{-1} was determined for the net upward flux of PON. Values of ϕ for variations of the base model can be found in Table 4.7. Thus, no matter what the initial abundance of biomass, multiplication of integrated water column abundance by ϕ will yield an estimate of the net downward flux of POC or the net upward flux of PON, provided that the conditions in the water column are similar to those defined in the base model or to the chosen variation of the base model. The

Table 4.7: Calculated values of ϕ (d^{-1}) for variations of the *Rhizosolenia* migration model. The product of ϕ and the integrated water column abundance (μmol m^{-2}) of *Rhizosolenia* gives an estimate of net downward flux of POC or net upward flux of PON due to *Rhizosolenia* migrations.

Model Variation	ϕ for POC (d^{-1})	ϕ for PON (d^{-1})
Base	0.07	0.14
Top loss only	0.004	0.2
Bottom loss only	0.32	0
Top and bottom loss	0.16	0.11
Critical C:N 10.7, 7.1	0.08	0.14
Critical C:N 15.4, 8.3	0.08	0.14
A, Ψ= 3 m h^{-1}	0.05	0.14
A, Ψ= 6 m h^{-1}	0.10	0.19
A, Ψ= 8 m h^{-1}	0.12	0.18

values of ϕ tell us that, using the base model, the net downward flux of POC is approximately 7% of the standing crop of *Rhizosolenia* (measured as POC) per day and the net upward flux of PON is approximately 14 % of the standing crop of *Rhizosolenia* (measured as PON) per day.

It is now possible to determine the potential relative contribution of migrations of *Rhizosolenia* to fluxes of POC and PON, and thus to oceanic new production, by calculating fluxes based on a range of abundances obtained in the open ocean. Data on the abundance and distribution of *Rhizosolenia*, horizontally, vertically and on basin-wide spatial scales, are limited. Kilometre-scale estimates of *Rhizosolenia* abundance in the North Pacific Gyre range from values of 0.75 μmol N m^{-3} over the upper 4 m of the water column (Villareal and Carpenter 1989) to 1.75 μmol N m^{-3} over the top 16 m of the water column (Alldredge and Silver 1982). These concentrations were converted from units of mats m^{-3} using an average of 2.5 μmol N mat^{-1} given by Villareal et al. (1996), although the size of mats varies considerably (Villareal et al. 1993) and therefore the value of 2.5 μmol N mat^{-1} should be considered approximate.

In order to estimate net fluxes of POC and PON it is necessary to know integrated water column abundance. In general, it is difficult to determine the vertical extent of the *Rhizosolenia* mats, as measurements must be done by SCUBA divers who are limited to approximately 20 m of vertical descent. I will assume that the concentration of *Rhizosolenia* observed by Alldredge and Silver (1982) (1.75 μmol N m^{-3}) is found over the top 20 m of the water column instead of only the top 16 m. This may account for mats below 16 m which were not counted in their estimates, but is more conservative than integrating over a 120 m water column. This results in an integrated water column abundance of 35 μmol N m^{-2}. Using equation 4.23, and a value of $\phi = 0.14\ d^{-1}$ (from the base model), the estimated net upward flux of nitrogen to the euphotic zone would be at most on the order of 5 μmol N $m^{-2}\ d^{-1}$. This value is within the range of previous estimates of nitrogen flux due to migrations of *Rhizosolenia* in the open ocean. Villareal et al. (1996) calculated the upward

flux of nitrate-N carried by migrating *Rhizosolenia* to be between 3.9 and 40 μmoles N m^{-2} d^{-1}. It should be noted that Villareal's estimate takes into account only the upward flux of N, and doesn't consider the nitroger which returns to deep water during the downward phase of the migration cycle, however it was calculated using a slightly lower abundance of PON, thus the values are similar to those calculated using my model. From here on, I will use a net upward flux of 5 μmol N m^{-2} d^{-1} as the maximum potential contribution of migrations of *Rhizosolenia* to new production in the open ocean.

The importance of the predicted upward flux of N to total new production in open ocean regions can be estimated by comparing the predicted net upward flux of PON from the model to estimates of new production resulting from the turbulent diffusion of nitrate into the euphotic zone, new production from nitrogen fixation, and to estimates of export production from sediment traps.

Estimates of the flux of nitrate into the euphotic zone of the oligotrophic ocean due to the turbulent diffusion of nitrate vary by more than two orders of magnitude ranging from 3 μmoles N m^{-2} d^{-1} (Carr et al. 1995) to 1644 μmoles N m^{-2} d^{-1} (Jenkins 1988) (see Table 4.8). Not including the lowest (Carr et al. 1995) and highest (Jenkins 1988) fluxes, an average of these values is on order of 140 μmoles N m^{-2} d^{-1}. Thus, the upper limit of new production resulting from migrations of *Rhizosolenia* into the euphotic zone (5 μmoles N m^{-2} d^{-1}) may represent at most 4% of new production resulting from diffusive fluxes of N. Estimates of new production from nitrogen fixation are less variable than those from turbulent fluxes of nitrate, but variation still exists (Table 4.9). If 25 μmoles N m^{-2} d^{-1} is used as a rough estimate, then the net upward flux of N to the euphotic zone represents 20% of new production due to nitrogen fixation. In general, comparisons of new production due to *Rhizosolenia* migrations to that due to turbulent fluxes of nitrate should be done with caution. First, the variation in turbulent fluxes of nitrate (and in the estimates of new production due to migrations) is extremely high. This makes valid comparisons difficult. Second, none of the estimates of turbulent fluxes used for these comparisons

Table 4.8: Estimates of new production from turbulent fluxes of nitrate into the euphotic zone for comparison with vertical fluxes of N due to migrations of *Rhizosolenia* in the open ocean.

Location	Nitrate flux (μmoles N m^{-2} d^{-1})	Reference
Sargasso Sea	22-134	McCarthy and Carpenter 1983
Western Pacific Warm Pool	250-310	Pena et al. 1995
E. Atlantic 26°N, 28°W	27	Ledwell et al. 1993
Sargasso Sea, off Bermuda	1644	Jenkins 1988
E. Atlantic 28.5°N, 23°W	139	Lewis et al. 1986
Equatorial Pacific 10°N, 150°W	3	Carr et al. 1995

Table 4.9: Estimates of nitrogen fixation used for comparison with estimates of new production resulting from vertical migrations of *Rhizosolenia* in the open ocean.

Location	N_2 fixation (μmoles N m^{-2} d^{-1})	Reference
N. Atlantic (SW)	38	Goering et al. 1966
Caribbean	77	Carpenter and Price 1977
Sargasso Sea	1.4	Carpenter and McCarthy 1975

were done in regions where mats of *Rhizosolenia* are especially abundant (such as the Central North Pacific Gyre), so, again, comparisons must be made with caution.

Estimates of new (export) production from sediment trap measurements, however, have been made in the North Pacific Gyre and the variability in nitrogen fluxes measured by sediment traps in both the Atlantic and Pacific Oceans is somewhat less (see Table 4.10), though fewer measurements exist. At best, the net upward flux of nitrogen due to migrations of *Rhizosolenia* represents approximately 1% of new production as measured by sediment traps, using the new production estimate of 460 μmoles N m^{-2} d^{-1} of Martin et al. (1987).

In general, the relatively low estimated contribution of migrations of *Rhizosolenia* to open ocean new production is a result of their relatively low standing crop. At a VERTEX station in the Central North Pacific Gyre, Karl and Knauer (1984) found the standing crop of POC to be approximately 1700 μmoles m^{-3}, while the standing crop of PON was 160 μmoles m^{-3}. Abundance estimates of *Rhizosolenia* used for this model (based on field collected data) were 1.5 μmoles m^{-3} for POC and 0.2 μmoles m^{-3} for PON, a difference of three orders of magnitude. The abundance estimated by Alldredge and Silver (1982) (1.75 μmoles N m^{-3}) is slightly higher, but it is still well below the total standing crop of PON which includes organisms other than *Rhizosolenia*.

The contribution of *Rhizosolenia* to overall new production in the open ocean is small. These contributions can nonetheless be ecologically important because of the uncoupled nature of the cycling of carbon and nitrogen during migrations. Migrations of *Rhizosolenia* occur in regions where sources of light and nutrients are spatially separated. Often, nitrate does not become detectable until well-below the euphotic zone (see Hayward 1991), thus, uptake of nitrate by migrating *Rhizosolenia* will occur in the dark and, since photosynthesis requires light, the uptake of nitrate will not be accompanied by the uptake of carbon (see Richardson et al. 1996). Nitrate transported to the surface by migrating diatoms, then, will not be accompanied by stoichiometric equivalents of carbon, as is the

Table 4.10: Estimates of new production as export production measured by sediment traps for comparison with vertical fluxes of N due to migrations of *Rhizosolenia* in the open ocean.

Location	Export production (μmoles N m^{-2} d^{-1})	Reference
N. Pacific Subtropical Gyre	460	Martin et al. 1987
Sargasso Sea	770	Michaels et al. 1994
N. Pacific Subtropical Gyre	714	Karl and Knauer 1984

case for new production that results from the input of physically-transported dissolved nitrate to the euphotic zone (Eppley and Peterson 1979). Since photosynthesis at the surface requires a carbon source, and since carbon is not brought to the surface in coupled transport with nitrogen, photosynthesis at the surface may result in the net decrease of carbon from surface waters. The uncoupled uptake of carbon and nitrogen during vertical migrations of *Rhizosolenia* is potentially the greatest contribution that these migrations can make to biogeochemical cycling and new production.

In general, uncoupled uptake of carbon and nitrogen also has implications for the estimation of primary productivity. Usually, upward flux of nitrate to the euphotic zone (new production) is converted to primary production by multiplying by the Redfield ratio. Uncoupled transport of N by migrating diatoms, and periods of unbalanced growth that can occur in N-depleted surface waters (see Richardson et al. 1996) do not obey Redfield stoichiometry. Calculation of primary productivity by multiplying upward transport of N by the Redfield ratio, therefore, will underestimate downward carbon flux (see also Goldman et al. 1992, Richardson and Cullen 1995). The model presented in the present study shows the uncoupling of C and N clearly, both by predicted vertical distributions of POC and PON, and by the predicted fluxes. Using the base model as an example, the predicted gross upward flux of PON (10.4 μmoles N m^{-2} d^{-1}) multiplied by 6.6 (mol:mol) (approximate Redfield proportions) gives an estimate of the downward flux of POC of 68.6 μmoles C m^{-2} d^{-1}. The value returned by the model for the downward flux of POC was 91.7 μmoles C m^{-2} d^{-1}. Thus, multiplying upward N flux by the Redfield ratio would underestimate the downward flux of POC by approximately 20 %.

In summary, this chapter describes a numerical model constructed to estimate the potential contributions of *Rhizosolenia* migrations to nutrient cycling in the open ocean. New production resulting from vertical migrations of *Rhizosolenia* is at most 4% of that resulting from upward fluxes of nitrate due to turbulent diffusion, and may contribute to roughly 1% of export production measured by sediment traps. Although these are small

contributions, the uncoupled nature of carbon and nitrogen cycling during migrations makes them ecologically important, as growth of *Rhizosolenia* at the surface fueled by nitrate acquired below the euphotic zone may result in the net removal of carbon from oceanic surface waters. However, because the abundance of these cells is relatively low, fluxes of carbon and nitrogen due to migrations of *Rhizosolenia* make only minimal contributions to global levels of new and primary production.

Chapter 5

Conclusions

The work presented in this thesis has focused on three main areas: 1) the effects of light and nutrients on the chemical composition of marine planktonic diatoms, 2) the effects of changes in chemical composition on cell buoyancy, and 3) how changes in cell buoyancy affect the cycling of carbon and nitrogen in the ocean.

The chemical composition of *Thalassiosira weissflogii* and *Rhizosolenia formosa* changed significantly in response to variations in light and nutrient regimes. Both of these organisms had large capacities for unbalanced growth, that is, they continued to take up carbon in the absence of nitrate (N) for extended periods of time (2-3 days). In both cases, changes in chemical composition were reversible: high ratios of C:N and carbohydrate:protein induced by N deprivation decreased when cells were re-supplied with N. The reversibility of chemical composition, and the flexible nature of the physiology of these diatoms had not previously been studied in detail, and represents a novel contribution of this work to the overall area of phytoplankton physiology.

Through effects on intracellular density, variations in cellular chemical composition affect cell buoyancy. The relationship between cellular chemical composition and cell buoyancy was examined through both laboratory experiments and modeling. I showed that

increases in carbohydrate:protein ratio could have been responsible for increased sinking of N-depleted *Thalassiosira weissflogii* grown in the experimental tank. Buoyancy experiments using *Rhizosolenia formosa* showed that the sinking rate and the percentage of negatively buoyant cells increased when cells became N-depleted, but that sinking rates and percentages of negatively buoyant cells decreased and the percentage of positively buoyant cells increased after N was re-supplied to culture medium. Increases in the percentage of positively buoyant cells were correlated with observed decreases in cellular C:N ratio; increases in the percentage of negatively buoyant cells and their sinking velocities coincided with increased C:N ratios.

Changes in cell buoyancy affect the vertical movements of diatoms through the water column. For small to medium-sized diatoms, buoyancy changes may be manifested as increases or decreases in cell sinking rates. Work in the experimental water column showed that N-replete *Thalassiosira weissflogii* were near-neutrally buoyant, but that cells sank when they exhausted ambient nitrate. In nature, increased buoyancy upon re-exposure to nitrate will slow the sinking rates of cells as they reach the top of the nutricline. Lande and Wood (1987) showed that slowing of sinking rates at the top of the nutricline may result in increased residence of time of cells in the mixed layer of the ocean, which may result in greater overall levels of primary productivity and growth than if sinking rates did not decrease. For large diatoms such as *Rhizosolenia*, alterations between positive and negative buoyancy allow cells to migrate vertically, giving them access to sources of nitrate found deep within the water column. This is an ecological advantage that may be responsible for the success of these large organisms in oligotrophic regions.

Whether in the form of sinking then resuspension by physical processes, or in the form of vertical migrations, movements of cells between the top of the nutricline and the euphotic zone affect carbon and nitrogen cycling in the ocean. The model of a steady-state *Rhizosolenia* migration cycle showed that new production resulting from transport of N to the surface during migrations is at most 4% of that resulting from the turbulent diffusion of

nitrate into the euphotic zone. This is a small contribution to oceanic new production, but the potential for transport of nitrogen uncoupled from the transport of carbon during migrations means that this form of new production may make disproportionately larger contributions to the net removal of carbon from oceanic surface waters. However, the relatively low abundance of these organisms means that fluxes of carbon and nitrogen due to migrations of *Rhizosolenia* are not important on a global scale.

In summary, the results of Chapter 2 indicate that:

- Under N-replete conditions, *Thalassiosira weissflogii* was near-neutrally buoyant in the experimental water column, but cells sank after depletion of ambient nitrate.
- Increased carbohydrate ballast was sufficient to have caused the increased sinking of N-depleted cells.
- Reversions in chemical composition due to changes in N status can result in detectable changes in cell buoyancy.
- Nutrient-dependent changes in cell buoyancy might result in increased residence time of cells in the mixed layer of the ocean, resulting in enhanced levels of primary productivity and growth.

Work described in Chapter 3 found that the physiological responses of *Rhizosolenia formosa* to changes in nutrient regime were flexible and were thus consistent with the ability to migrate vertically in the open ocean. Specific conclusions are:

- Cells could undergo prolonged periods of unbalanced growth, after which changes in chemical composition and increased buoyancy occurred upon re-introduction of nitrate to culture medium.
- Measurements of nitrate uptake showed that cells could take up nitrate in the dark at rates indicating the potential for luxury consumption of nitrate.
- Photosynthesis-irradiance characteristics of this organism showed that cells may be adapted for growth under a wide range of irradiances.

In Chapter 4, a numerical model was used to estimate the potential contributions of migrations of *Rhizosolenia* to nutrient cycling and new production in the open ocean. The most significant results from the model suggest that:

- New production resulting from the transport of N to the euphotic zone during migrations of *Rhizosolenia* is at most 5 μmoles N m^{-2} d^{-1} though this estimate may vary by as much as an order of magnitude higher or lower because of uncertainties in estimates of the integrated water column abundance of this organism.
- New production resulting from *Rhizosolenia* migrations is at most 4% of that due to turbulent fluxes of nitrate into the euphotic zone, but may make disproportionately higher contributions to the removal of carbon from surface waters because the upward transport of N during migrations is not coupled to the upward transport of carbon.

Calculation of the exact contribution of migrations of *Rhizosolenia* to new and primary production still relies on robust estimates of cell abundance. The geographical coverage of abundance estimates is not yet sufficient to determine their overall biogeochemical importance, although evidence presented here indicates that their contributions to biogeochemical cycling may be negligible.

Bibliography

Alldredge, A.L. & Silver, M.W. 1982. Abundance and production rates of floating diatom mats (*Rhizosolenia castracanei* and *R. imbricata* var. *shrubsolei*) in the Eastern Pacific Ocean. Mar. Biol. 66:83-88.

Altabet, M.A. 1988. Variations in nitrogen isotopic composition between sinking and suspended particles: implications for nitrogen cycling and particle transformations in the open ocean. Deep-Sea Res. 35: 535-554.

Anderson, L.W.J., & Sweeney, B.M. 1977. Diel changes in sedimentation characteristics of *Ditylum brightwellii*: Changes in cellular lipid and effects of respiratory inhibitors and ion-transport modifiers. Limnol. Oceanogr. 22:539-552.

Anderson, L.W.J., & Sweeney, B.M. 1978. Role of inorganic ions in controlling sedimentation rate of a marine centric diatom *Ditylum brightwellii*. J. Phycol. 14:204-214.

Barber, R.T., Murray, J.W, & McCarthy, J.J. 1994. Biogeochemical interactions in the Equatorial Pacific. AMBIO 23:62-66.

Beers, J.R., Reid, F.M.H., & G.L. Stewart. 1975. Microplankton of the North Pacific Central Gyre. Population structure and abundance, June 1973. Int. Rev. ges. Hydrobiol. 60:607-638.

Beklemishev, K. B., Petrikova, M. N. & Semina, G. I. 1961. On the cause of buoyancy of plankton diatoms. Tr. Inst. Okeanol. Akad. Nauk. S. S. S. R. 51:33-36.

Bhovichitra, M., & Swift, E. 1977. Light and dark uptake of nitrate and ammonium by large oceanic dinoflagellates: *Pyrocystis noctiluca, Pyrocystis fusiformis,* and *Dissodinium lunula.* Limnol. Oceanogr. 22:73-83.

Bienfang, P.K. 1981a. SETCOL- A technologically simple and reliable method for measuring phytoplankton sinking rates. Can. J. Fish. Aquat. Sci. 38:1289-1294.

Bienfang, P.K. 1981b. Sinking rates of heterogeneous, temperate phytoplankton populations. J. Plankton Res. 3:235-253.

Bienfang, P.K. 1981c. Sinking rate dynamics of *Cricosphaera carterae* Braarud. II. Senescence response to various limiting substrates in non-steady state populations. J. exp. mar. Biol. Ecol. 49:235-244.

Bienfang, P.K., & Szyper, J.P. 1982. Effects of temperature and salinity on sinking rates of the centric diatom *Ditylum brightwellii.* Biol. Oceanogr. 1:211-223.

Bienfang, P.K., Harrison, P.J., & Quarmby, L.M. 1982. Sinking rate response to depletion of nitrate, phosphate, and silicate in four marine diatoms. Mar. Biol. 67:295-302.

Bienfang, P.K., Szyper, J.P., & Laws, E. 1983. Sinking rate and pigment responses to light-limitation of a marine diatom: implications to dynamics of chlorophyll maximum layers. Oceanol. Acta 6:55-62.

Bienfang, P.K., & Harrison, P.J. 1984. Sinking-rate response of natural assemblages of temperate and subtropical phytoplankton to nutrient depletion. Mar. Biol. 83:293-300.

Bienfang, P.K., Conquest, L., & Antill, E. 1986. Compositional and buoyancy responses to nutrient deficiency in marine phytoplankton. Report of the Oceanic Institute, Makapuu Point, Waimanalo, Hawaii.

Bowman, T.E., & Lancaster, L.J. 1965. A bloom of the planktonic blue-green alga, *Trichodesmium erythraeum*, in the Tonga Islands. Limnol. Oceanogr. 10: 291-292.

Broecker, W.S. 1974. 'NO', a conservative water-mass tracer. Earth Planet. Sci. Lett. 23: 100-107.

Carpenter, E.J. & McCarthy, J.J. 1975. Nitrogen fixation and uptake of combined nitrogenous nutrients by Oscillatoria (Trichodesmium) thiebautii in the western Sargasso Sea. Limnol. Oceanogr. 20: 389-401.

Carpenter, E.J. & Price, C. 1977. Nitrogen fixation, distribution, and production of *Oscillatoria* (*Trichodesmium*) spp. in the western Sargasso and Caribbean Seas. Limnol. Oceanogr. 22: 60-72.

Carpenter, E.J., Harbison, G.R., Madin, L.P., Swanberg, N.R., Biggs, D.C., Hulburt, E.M. McAlister, V.L., & McCarthy, J.J. 1977. *Rhizosolenia* mats. Limnol. Oceanogr. 22:739-741.

Carpenter, E.J., & Romans, K. 1991. Major role of the cyanobacterium *Trichodesmium* in nutrient cycling in the North Atlantic Ocean. Science 254: 1356-1358.

Carr, M-E., Lewis, M.R., Kelley, D., & Jones, B. 1995. A physical estimate of new production in the Equatorial Pacific along 150 W. Limnol. Oceanogr. 40:138-147.

Chisholm, S.W. 1992. Phytoplankton size. *In*: Falkowski, P.G. & Woodhead, A.D. (Eds.) *Primary Productivity and Biogeochemical Cycles in the Sea.* Plenum Press, New York, pp. 299-316.

Cleveland, J.S. & Perry, M.J. 1987. Quantum yield, relative specific-absorption and fluorescence in nitrogen-limited *Chaetoceros gracilis.* Mar. Biol. 94:489-497.

Conover, S.W. 1974. Nitrate, ammonium, and urea as nitrogen sources for marine diatoms in culture and in spring blooms. Ph. D. thesis, Dalhousie University, Halifax, Canada. 175 pp.

Cuhel `.L., Ortner, P.B., & Lean, D.R.S. 1984. Night synthesis of protein by algae. Limnol. Oceanogr. 29: 731-744.

Cullen, J.J., & Horrigan, S.W. 1981. Effects of nitrate on the diurnal vertical migration, carbon to nitrogen ratio, and the photosynthetic capacity of the dinoflagellate *Gymnodinium splendens*. Mar. Biol. 62:81-89.

Cullen, J.J. 1985. Diel vertical migration by dinoflagellates: role of carbohydrate metabolism and behavioral flexibility. *In* Rankin, M.A. (Ed.) *Migration: Mechanisms and Adaptive Significance.* Contr. Mar. Sci. 27 (Suppl.): 135-152.

Cullen, J.J., & Lewis, M.R. 1988. The kinetics of algal photoadaptation in the context of vertical mixing. J. Plankton Res. 10:1039-1063.

de Madariaga, I. 1992. Interspecific differences in the photosynthetic carbon metabolism of marine phytoplankton. Mar. Biol. 114: 509-515.

Dorsey, T.E., MacDonald, P., & Roels, O.A. 1978. Measurement of phytoplankton protein content with the heated biuret folin assay. J. Phycol. 14: 167-171.

Dubois, M., Gilles, K.A., Hamilton, J.K., Rebers, P.A., & Smith, F. 1956. Colorimetric method for determination of sugars and related substances. Anal. Chem. 28:350-356.

Dugdale, R.C., & Goering, J.J. 1967. Uptake of new and regenerated forms of nitrogen in primary productivity. Limnol. Oceanogr. 12:196-206.

Dugdale, R.C., Wilkerson, F.P., Barber, R.T., Blasco, D., & Packard, T.T. 1987. Changes in nutrients, pH, light penetration, and heat budget by migrating

photosynthetic organisms. Oceanol. Acta. Proceedings International Symposium on Equatorial Vertical Motion, Paris, 6-10 May 1985:103-107.

Eppley, R.W. , Holmes, R.W., & Strickland, J. D. H. 1967. Sinking rates of marine phytoplankton measured with a fluorometer. J. exp. mar. Biol. Ecol. 1:191-208

Eppley, R.W., Rogers, J.N., & McCarthy, J.J. 1969. Half-saturation constants for uptake of nitrate and ammonium by marine phytoplankton. Limnol. Oceanogr. 14: 912-920.

Eppley, R.W., & Harrison, W.G. 1975. Physiological ecology of *Gonyaulax polyedra*, a red water dinoflagellate of southern California. *In* LoCicero, V.R. (Ed.) *Toxic Dinoflagellate Blooms*. Science and Technology Foundation, Wakefield MA, pp. 11-22.

Eppley, R.W., & Peterson, B.J. 1979. Particulate organic matter flux and planktonic new production in the deep ocean. Nature 282:677-680.

Eppley, R.W. 1981. Relation between nutrient assimilation and growth in phytoplankton with a brief review of estimates of growth rate in the ocean. *In* Platt, T. (Ed.) *Physiological Bases of Phytoplankton Ecology*. Can. Bull. Fish. Aquat. Sci. 210: 251-263.

Emerson, S. & Hayward, T.L. 1995. Chemical tracers of biological processes in shallow waters of the North Pacific: Preformed nitrate distributions. J. Mar. Res. 53:499-513.

Fasham, M.J.R., Ducklow, H.W., & McKelvie, S.M. 1990. A nitrogen-based model of plankton dynamics in the oceanic mixed layer. J. Mar. Res. 48: 591-639.

Fraga, F., Pérez, F.F., Figueiras, F.G. & Rios, A.F. 1992. Stoichiometric variations of N, P, C, and O_2 during a *Gymnodinium catenatum* red tide and their interpretation. Mar. Ecol. Prog. Ser. 87:123-134.

Geider, R.J. 1984. Light and nutrient effects on microalgal physiology. Ph.D. thesis, Dalhousie University, Halifax. 187 pp.

Geider, R.J., T. Platt, & Raven, J.A. 1986. Size dependence of growth and photosynthesis in diatoms: a synthesis. Mar. Ecol. Prog. Ser. 30:93-104.

Geider, R.J. 1992. Respiration: taxation without representation? *In*: Falkowski, P.G. & Woodhead, A.D. (Eds.) *Primary Productivity and Biogeochemical Cycles in the Sea*. Plenum Press, New York, pp. 299-316.

Glibert, P.M. & Goldman, J.C. 1981. Rapid ammonium uptake by marine phytoplankton. Mar. Biol. Lett. 2:25-31.

Glover, H.E., Prézelin, B.B., Campbell, L., Wyman, M. & Garside, C. 1988. A nitrate-dependent *Synechococcus* bloom in surface Sargasso Sea water. Nature 331:161-163.

Goldman, J.C. 1988. Spatial and temporal discontinuities of biological processes in pelagic surface waters. *In* Rothschild, B.J., (Ed.) *Toward a theory on biological-*

physical interactions in the world ocean. Kluwer Academic, Dordrecht, pp. 273-296.

Goldman, J.C., Hansell, D.A., & Dennett, M.R. 1992. Chemical characterization of three large oceanic diatoms: potential impact on water column chemistry. Mar. Ecol. Prog. Ser. 88: 257-270.

Goldman, J.C. 1993. Potential role of large oceanic diatoms in new primary production. Deep-Sea Res. 40: 159-168.

Goering, J.J., Dugdale, R.C, & Wenzel, D.W. 1966. Estimates of *in situ* rates of nitrogen uptake by *Trichodesmium* sp. in the tropical Atlantic Ocean. Limnol. Oceanogr. 11: 614-521.

Gran, H.H. 1929. Investigation of the production of plankton outside the Romsdalfjord 1926-1927. Rapports et Proces-verbaux des Reunions. Conseil Permanent International des Exploration de la Mer 56: 1-112.

Granata, T. C. 1987. Measurements of phytoplankton sinking and growth under varied light intensities and mixing regimes. Ph. D. thesis, University of California, Berkeley, U. S. A. 169 pp.

Gross, F. & Zeuthen, E. 1948. The buoyancy of plankton diatoms: a problem of cell physiology. Proc. R. Soc. Lond. Ser. B 135:382-389.

Guillard, R. R. L. 1972. Culture of phytoplankton for feeding marine invertebrates. *In* Smith, W. L. & Chanley, M. H. (Eds.) *Culture of marine invertebrate animals.* Plenum Press, New York, pp. 29-60 .

Harrison, W.G. 1976. Nitrate metabolism of the red tide dinoflagellate *Gonyaulax polyedra* Stein. J. Exp. Mar. Biol. Ecol. 21:199-209.

Hayward, T. L. 1991. Primary production in the North Pacific Central Gyre: a controversy with important implications. Trends Ecol. & Evol. 6: 281-284.

Hayward, T.L. 1993. The rise and fall of *Rhizosolenia.* Nature 363: 675-676.

Heaney, S.I. & Eppley, R.W. 1981. Light, temperature, and nitrogen as interacting factors affecting diel vertical migrations of dinoflagellates in cultures. J. Plankton Res. 3: 331-344.

Heaney, S. I. & Butterwick, C. 1985. Comparative mechanisms of algal movement in relation to phytoplankton production. *In* Rankin, M A (Ed.) *Migration: mechanisms and adaptive significance.* Contrib. Mar. Sci. 27 (Suppl):114-134

Heaney, S.I., Davey, M.C., & Brooks, A.S. 1989. Formation of sub-surface maxima of a diatom within a stratified lake and in a laboratory water column. J. Plankton Res. 11:1169-1184.

Henley, W.J. 1993. Measurement and interpretation of photosynthetic light-response curves in algae in the context of photoinhibition and diel changes. J. Phycol. 29: 729-739.

Hensen, V. 1887. Über die Bestimmung des Planktons oder des im Meere treibenden Materials an Pflanzen und Tieren. Ber. Komm. wiss. Unters. dt. Meere 5:1-108.

Horrigan, S.G. & McCarthy, J.J. 1981. Urea uptake by phytoplankton at various stages of nutrient depletion. J. Plankton Res. 3: 403-414.

Horrigan, S.G. & McCarthy, J.J. 1982. Phytoplankton uptake of ammonium and urea during growth on oxidized forms of nitrogen. J. Plankton Res. 4:379-389.

Hurlbert, S.H. 1984. Pseudoreplication and the design of ecological field experiments. Ecol. Monogr. 54:187-211.

Ibelings, B.W., Mur, L.R., & Walsby, A.E. 1991. Diurnal changes in buoyancy and vertical distribution in populations of *Microcystis* in two shallow lakes. J. Plankton Res. 13:419-436.

Iverson, R.L., Bittaker, H.F., & Myers, V.B. 1976. Loss of radiocarbon in direct use of Aquasol for liquid scintillation counting of solutions containing ^{14}C-$NaHCO_3$. Limnol. Oceanogr. 21:756-758.

Jackson, G.A. 1990. A model of the formation of marine algal flocs by physical coagulation processes. Deep-Sea Res. 37:1197-1211.

Jahnke, R.A. 1990. Ocean flux studies:a status report. Rev. Geophys. 28:381-398.

Jenkins, W.J. 1988. Nitrate flux into the euphotic zone near Bermuda. Nature 331: 521-523.

Jitts, H.R., Morel, A. & Saijo, Y. 1976. The relation of oceanic primary production to available photosynthetic irradiance. Aust. J. Mar. Freshwater Res. 27: 441-454.

Kahn, N., & Swift, E. 1978. Positive buoyancy through ionic control in the nonmotile marine dinoflagellate *Pyrocystis noctiluca* Murray ex Schuett. Limnol. Oceanogr. 23:649-658.

Kana, T.M. & Glibert, P.M. 1987a. Effect of irradiances up to 2000 μE m^{-2} s^{-1} on marine *Synechococcus* WH7803- I. Growth, pigmentation, and cell composition. Deep-Sea Res. 34:479-495.

Kana, T.M. & Glibert, P.M. 1987b. Effect of irradiances up to 2000 μE m^{-2} s^{-1} on marine *Synechococcus* WH7803- II. Photosynthetic responses and mechanisms. Deep-Sea Res. 34:497-516.

Karl, D.M. & Knauer, G.A. 1984. Vertical distribution, transport, and exchange of carbon in the northeast Pacific Ocean: evidence for multiple zones of biological activity. Deep-Sea Res. 31: 221-243.

Karl, D.M., Letelier, R., Hebel, D.V., Bird, D.F., & Winn, C.D. 1992. *Trichodesmium* blooms and new nitrogen in the North Pacific Gyre. *In* Carpenter, E.J., Capone, D.G., & Rueter, J.G. (Eds.) *Marine Pelagic Cyanobacteria*: Trichodesmium *and other Diazotrophs*. Kluwer Academic Publishers, Boston, pp. 219-237.

Keller, M. D., Selvin, R. C., Claus, W., & Guillard, R.R.L. 1987. Media for the culture of oceanic ultraphytoplankton. J. Phycol. 23:633-638.

Kiørboe, T., Andersen, K.P., & Dam, H.G. 1990. Coagulation efficiency and aggregate formation in marine phytoplankton. Mar. Biol. 107:235-245.

Kirk, J.T.O. 1994. Light and Photosynthesis in Aquatic Ecosystems, 2nd ed. Cambridge University Press, Cambridge, 509 pp.

Kromkamp, J.& Walsby, A.E. 1990. A computer model of buoyancy and vertical migration in cyanobacteria. J. Plankton Res. 12:161-183.

Lande, R. & Wood, A.M. 1987. Suspension times of particles in the upper ocean. Deep-Sea Res. 34:61-72.

Latasa, M. & Berdalet, E. 1994. Effect of nitrogen or phosphorus starvation on pigment composition of cultured *Heterocapsa* sp. J. Plankton Res. 16: 83-94.

Ledwell, J.R., Watson, A.J., & Law, C.S. 1993. Evidence for slow mixing across the pycnocline from an open-ocean tracer-release experiment. Nature 364: 701-703.

Lewis, M.R. & Smith, J.C. 1983. A small volume, short-incubation-time method for measurement of photosynthesis as a function of incident irradiance. Mar. Ecol. Prog. Ser. 13:99-102.

Lewis, M.R., W.G. Harrison, N.S. Oakey, D. Hebert, T. Platt. 1986. Vertical nitrate fluxes in the oligotrophic ocean. Science 234: 870-873.

Li, W.K.W. & Morris, I. 1982. Temperature adaptation in *Phaeodactylum tricornutum* Bohlin: Photosynthetic rate compensation and capacity. J. Exp. Mar. Biol. Ecol. 58:135-150.

Longhurst, A.R. & Harrison, W.G. 1989. The biological pump: Profiles of plankton production and consumption in the upper ocean. Prog. Oceanog. 22: 47-123.

Martin, J.H., Knauer, G.A., Karl, D.M., and Broenkow, W.W. 1987. VERTEX: Carbon cycling in the northeast Pacific. Deep-Sea Res. 34:267-285.

Martinez, L., Silver, M.W., King, J.M., & Alldredge, A.L. 1983. Nitrogen fixation by floating diatom mats: a source of new nitrogen to oligotrophic ocean waters. Science 221:152-154.

McCarthy, J.J. & Goldman, J.C. 1979. Nitrogenous nutrition of marine phytoplankton in nutrient-depleted waters. Science 203:670-672.

McCarthy, J.J. & Carpenter, E.J. 1983. Nitrogen cycling in near-surface waters of the open ocean. *In* Carpenter, E.J. & Capone, D.G. (Eds.) *Nitrogen in the Marine Environment,* Academic Press, New York, pp. 487-512.

Michaels, A.F. & Silver, M.W. 1988. Primary production, sinking fluxes, and the microbial food web. Deep-Sea Res. 35:473-490.

Michaels, A.F., Bates, N.R., Buesseler, K.O., Carlson, C.A., & Knap, A.H. 1994. Carbon-cycle imbalances in the Sargasso Sea. Nature 372:537-540.

Moore, D.S., McCabe, G.P. 1993. Introduction to the Practice of Statistics. 2nd ed. W.H. Freeman and Company, New York. 854 pp.

Moore, J.K. 1994. Buoyancy and growth characteristics of the marine diatoms *Rhizosolenia formosa* H. Peragallo and *R. acuminata* (H. Per.) H. Peragallo. M.S. thesis, University of Massachusetts, Boston. 98 pp.

Morel, A. 1978. Available, usable, and stored radiant energy in relation to marine photosynthesis. Deep-Sea Res. 25: 673-688.

Munk, W.H. & Riley, G.A. 1952. Absorption of nutrients by aquatic plants. J. Mar. Res. 11: 215-240.

Myklestad, S. 1974. Production of carbohydrates by marine planktonic diatoms. I. Comparison of nine different species in culture. J. exp. mar. Biol. Ecol. 15:261-274.

Neale, P.J. 1987. Algal photoinhibition and photosynthesis in the aquatic environment. *In* Kyle, D.J., Osmond, C.B, & Arntzen, C.J. (Eds.) *Photoinhibition.* Elsevier Science Publishers, Amsterdam, pp.39-65.

Oliver, R.L., & Walsby, A.E. 1984. Direct evidence for the role of light-mediated gas vesicle collapse in the buoyancy regulation of *Anabaena flos-aquae* (cyanobacteria). Limnol. Oceanogr. 29:879-886.

Oliver, R.L. 1994. Floating and sinking in gas-vacuolate cyanobacteria. J. Phycol. 30: 161-173.

O'Neil, J.M. & Roman, M.R. 1992. Grazers and associated organisms of *Trichodesmium.In* Carpenter, E.J., Capone, D.G., & Rueter, J.G. (Eds.) *Marine Pelagic Cyanobacteria:* Trichodesmium *and other Diazotrophs*. Kluwer Academic Publishers, Amsterdam, pp.61-73.

Pasciak, W.J., & Gavis, J. 1974. Transport limitation of nutrient uptake in phytoplankton. Limnol. Oceanogr. 19: 604-617.

Pena, M.A., Lewis, M.R., & Cullen, J.J. 1994. New production in the warm waters of the tropical Pacific Ocean. J. Geophys. Res. 99:14255-14268.

Platt, T., Gallegos, C.L., & Harrison, W.G. 1980. Photoinhibiton of photosynthesis in natural assemblages of marine phytoplankton. J. Mar. Res. 38:687-701.

Prézelin, B.B. & Matlick, H.A. 1983. Nutrient-dependent low-light adaptation in the dinoflagellate *Gonyaulax polyedra*. Mar. Biol. 74:141-150.

Redfield, A.C. 1958. The biological control of chemical factors in the environment. Am. Scientist 46:1-18.

Richardson, T.L., & Cullen, J.J. 1995. Changes in buoyancy and chemical composition during growth of a coastal marine diatom: ecological and biogeochemical consequences. Mar. Ecol. Prog. Ser. 128:77-90.

Richardson, T.L., Ciotti, A.M., Cullen, J.J., and Villareal, T.A. 1996. Physiological and optical properties of *Rhizosolenia formosa* (Bacillariophyceae) in the context of open-ocean vertical migration. Submitted to J. Phycol. 22 December 1995.

Rivkin, R.B., Swift, E., Biggley, W.H., & Voytek, M.A. 1984. Growth and carbon uptake by natural populations of oceanic dinoflagellates *Pyrocystis noctiluca* and *Pyrocystis fusiformis.* Deep-Sea Res. 31:353-367.

Romans, K.M., Carpenter, E.J., & Bergman, B. 1994. Buoyancy regulation in the colonial diazotrophic cyanobacterium *Trichodesmium tenue*: Ultrastructure and storage of carbohydrate, polyphosphate, and nitrogen. J. Phycol. 30:935-942.

Roy, S., & Legendre, L. 1979. DCMU-enhanced fluorescence as an index of photosynthetic activity in phytoplankton. Mar. Biol. 55:93-101.

Sakshaug, E., Demers, S., & Yentsch, C.M. 1987. *Thalassi[illegible]ra oceanica* and *T. pseudonana*: two different photoadaptational responses.

Sambrotto, R.N., Savidge, G., Robinson, C., Boyd, P., Takahashi, T., Karl, D., Langdon, C., Chipman, D., Marra, J., & Codispoti, L. 1993. Elevated consumption of carbon relative to nitrogen in the surface ocean. Nature 363:248-250.

Sancetta, C., Villareal, T.A. & Falkowski, P.G. 1991. Massive fluxes of rhizosolenid diatoms: a common occurrence? Limnol. Oceanogr. 36:1452-1457.

Schöne, H.K. & Schöne, A. 1982. MET 44: A weakly enriched sea-water medium for ecological studies on marine plankton algae, and some examples of its application. Bot. Mar. 25:117-122.

Smayda, T. J. 1970. The suspension and sinking of phytoplankton in the sea. Oceanogr. Mar. Biol. Annu. Rev. 8:353-414.

Smayda, T.J. & Boleyn, B.J. 1966a. Experimental observations on the flotation of marine diatoms. II. *Skeletonema costatum* and *Rhizosolenia setigera*. Limnol. Oceanogr. 11:18-34.

Smayda, T. J. & Boleyn, B.J. 1966b. Experimental observations on the flotation of marine diatoms. III. *Bacteriastrum hyalinum* and *Chaetoceros lauderi*. Limnol. Oceanogr. 11:35-43.

Smetacek, V. S. 1985. Role of sinking in diatom life-history cycles: ecological, evolutionary and geological significance. Mar. Biol. 84:239-251.

Sosik, H.M., & Mitchell, B.G. 1991. Absorption, fluorescence, and quantum yield for growth in nitrogen-limited *Dunaliella tertiolecta*. Limnol. Oceanogr. 36:910-921.

Sokal, R.R. & Rohlf, F.J. 1981. *Biometry*, 2nd. ed. W.H. Freeman & Co., New York, 859 pp.

Steele, J.H., & Yentsch, C.S. 1960. The vertical distribution of chlorophyll. J. mar. biol. Assoc. U. K. 39:217-226.

Strickland, J.D.H., Holm-Hansen, O., Eppley, R.W., & Linn, R.J. 1968. The use of a deep tank in plankton ecology. I. Studies of the growth and composition of phytoplankton crops at low nutrient levels. Limnol. Oceanogr. 14:23-34.

Strickland, J.D.H. & Parsons, T.R. 1972. A practical handbook of seawater analysis, 2nd ed. Bull. Fish. Res. Bd. Can. 167:1-310.

Syrett, P.J. 1981. Nitrogen metabolism of microalgae. *In* Platt, T. (Ed.) *Physiological Bases of Phytoplankton Ecology* Can. Bull. Fish. Aquat. Sci. 210:182-210.

Takahashi, M., & Bienfang, P.K. 1983. Size structure of phytoplankton biomass and photosyr hesis in subtropical Hawaiian waters. Mar. Biol. 76:203-211.

Takahashi, M., Ichimura, S., Kishino, M. & Okami, N. 1989. Shade and chromatic adaptation of phytoplankton photosynthesis in a thermally stratified sea. Mar. Biol. 100: 401-409.

Talling, J.F. 1957. Photosynthetic characteristics of some freshwater plankton diatoms in relation to underwater radiation. New Phytol. 56:29-50.

Terry, K.L. 1982. Nitrate uptake and assimilation in *Thalassiosira weissflogii* and *Phaeodactylum tricornutum*: Interactions with photosynthesis and with the uptake of other ions. Mar. Biol. 69:21-30.

Throndsen, J. 1978. Preservation and storage. In Sournia, A. (Ed.) *UNESCO Phytoplankton Manual.* UNESCO Paris, pp. 69-74.

van Rijn. J., & Shilo, M. 1985. Carbohydrate fluctuations gas vacuolation and vertical migration of scum-forming cyanobacteria in fishponds. Limnol. Oceanogr. 30:1219-1228.

Venrick, E.L. 1974. The distribution and significance of *Richelia intracellularis* Schmidt in the North Pacific Central Gyre. Limnol. Oceanogr. 19:437-435.

Venrick, E.L., McGowan, J.A., & Mantyla, A.W. 1973. Deep maxima of photosynthetic chlorophyll in the Pacific Ocean. Fish. Bull.71: 41-52.

Villareal, T.A. 1987. Evaluation of nitrogen fixation in the diatom genus *Rhizosolenia* Ehr. in the absence of its cyanobacterial symbiont *Richelia intracellularis* Schmidt. J. Plankton Res. 9:965-971.

Villareal, T. A. 1988. Positive buoyancy in the oceanic diatom *Rhizosolenia debyana* H. Peragallo. Deep-Sea Res 35:1037-1045.

Villareal, T.A. & Carpenter, E.J. 1989. Nitrogen fixation, suspension characteristics, and chemical composition of *Rhizosolenia* mats in the Central North Pacific Gyre. Biol. Oceanogr. 6: 327-345.

Villareal, T.A., & Carpenter, E. J. 1990. Diel buoyancy regulation in the marine diazotrophic cyanobacterium *Trichodesmium thiebautii*. Limnol. Oceanogr. 35:1832-1837.

Villareal, T.A. 1992. Buoyancy properties of the giant diatom *Ethmodiscus*. J. Plankton Res. 14:459-463.

Villareal, T.A., Altabet, M.A. & Culver-Rymsza, K. 1993. Nitrogen transport by vertically migrating diatom mats in the North Pacific Ocean. Nature 363:709-712.

Villareal, T.A. & Carpenter, E.J. 1994. Chemical composition and photosynthetic characteristics of *Ethmodiscus rex* (Bacillariophyceae): Evidence for vertical migration. J. Phycol. 30:1-8.

Villareal, T.A. & Lipschultz, F. 1995. Internal nitrate concentrations in single cells of large phytoplankton from the Sargasso Sea. J.Phycol. 31:689-696.

Villareal, T.A., Woods, S., Moore, J.K. & Culver-Rymsza, K. 1996. *Rhizosolenia* mat vertical migration cycles and their significance to NO_3^- fluxes in the central North Pacific gyre. J. Plankton Res. In press.

Vincent, W.F. 1980. Mechanisms of rapid photosynthetic adaptation in natural phytoplankton communities. I. Changes in photochemical capacity as measured by DCMU-induced chlorophyll fluorescence. J. Phycol. 16:568-577.

Vogel, S. 1981. *Life in moving fluids: The physical biology of flow.* Princeton University Press, Princeton, N.J. 352 pp.

Waite, A., Bienfang, P.K., & Harrison, P.J. 1992a. Spring bloom sedimentation in a subarctic ecosystem. I. Nutrient sensitivity. Mar. Biol. 114:119-129.

Waite, A., Bienfang, P.K., Harrison, P.J. 1992b. Spring bloom sedimentation in a subarctic ecosystem. II. Succession and sedimentation. Mar. Biol. 114:131-138.

Waite, A., Thompson, P.A., & Harrison, P.J. 1992c. Does energy control the sinking rates of marine diatoms? Limnol. Oceanogr. 37:468-477.

Walsby, A.E. 1978. The properties and buoyancy-providing role of gas vacuoles in *Trichodesmium* Ehrenberg. Br. phycol. J. 13:103-116.

Walsby, A.E., & Reynolds, C.S. 1980. Sinking and floating. *In* Morris, I. (Ed.) *The physiological ecology of phytoplankton.* Univ. of California Press, Los Angeles, pp. 371-412.

Walsby, A.E., Reynolds, C.S., Oliver, R.L., & Kromkamp, J. 1989. The role of gas vacuoles and carbohydrate content in the buoyancy and vertical distribution of *Anabaena minutissima* in Lake Rotongaio New Zealand. Ergebn. Limnol. 32:1-25.

Walsby, A.E., & Xypolyta, A. 1977. The form resistance of chitin fibres attached to the cells of *Thalassiosira fluviatilis* Hustedt. Br. phycol. J. 12:215-223.

Watanabe, M., Kohata, K. & Kimura, T. 1991. Diel vertical migration and nocturnal uptake of nutrients by *Chatonella antiqua* under stable stratification. Limnol. Oceanogr. 36:593-602.

Welschmeyer, N.A. & Lorenzen, C.J. 1981. Chlorophyll-specific photosynthesis and quantum efficiency at subsaturating light intensities. J. Phycol. 17: 283-293.

West, E. S. & Todd, W. R. 1963. *Textbook of Biochemistry*. 3rd ed. The MacMillan Company, New York.

Yentsch, C.S. & Lee, R.W. 1966. A study of photosynthetic light reactions, and a new interpretation of sun and shade phytoplankton. J. Mar. Res. 24:319-337.

Yoder, J.A., Ackleson, S.G., Barber, R.T., Flament, P., & Balch, W.M. 1994. A line in the sea. Nature 371:689-692.

Zevenboom, W. 1986. Ecophysiology of nutrient uptake, photosynthesis, and growth. *In* Platt, T. & Li, W. (Eds.) *Photosynthetic Picoplankton*. Can. Bull. Fish. Aquat. Sci. 214:391-422.